ANALYSIS, SHAPE SENSITIVITIES AND APPROXIMATIONS OF MODAL RESPONSE OF GENERALLY LAMINATED TAPERED SKEW PLATES

by

Sarvesh Singhvi

Thesis submitted to the Faculty of the
Virginia Polytechnic Institute and State University
in partial fulfillment of the requirements for the degree of

MASTER OF SCIENCE

in

Aerospace Engineering

APPROVED:

Rakesh K. Kapania, Chairman

Eric R. Johnson

Efstratios Nikolaidis

September, 1991

Blacksburg, Virginia

ANALYSIS, SHAPE SENSITIVITIES AND APPROXIMATIONS OF MODAL RESPONSE OF GENERALLY LAMINATED TAPERED SKEW PLATES

by

Sarvesh Singhvi

Committee Chairman: Rakesh K. Kapania

Aerospace Engineering

(ABSTRACT)

A method is developed for the static, free vibration and shape sensitivity analyses of generally laminated tapered skew plates having arbitrary edge conditions such as clamped, simply supported or free. The procedure consists of the application of the Rayleigh-Ritz method with Chebyshev polynomials in the displacement function. An approximate approach that uses artificial, stiff springs is used to satisfy the geometric boundary conditions. This method enables one to analyze plates of various geometric shapes defined by natural coordinates. Before using it for a plate, the method is first applied to the one-dimensional problem of free torsional vibrations of doubly symmetric thin walled beams of open section, subjected to an axial compressive static load and resting on a continuous elastic foundation. Accurate numerical results for natural frequencies for various values of warping and elastic foundation parameters are presented. The method is then extended to laminated plates and accurate frequencies and mode shapes are obtained for various plate geometries and lamination sequences. The sensitivity of the natural frequencies and the mode shapes with respect to various shape parameters is also determined. These derivatives are then used to approximate the natural frequencies and mode shapes and the approximations are found to be in good agreement with those obtained from reanalysis over the range of the particular shape parameter.

ACKNOWLEDGEMENTS

This thesis is dedicated to my family and friends for their support over the past few years. I would also like to thank Dr. Rakesh K. Kapania whose advice and assistance made this research possible. Thanks are also due to Dr. E. R. Johnson and Dr. E. Nikolaidis for serving on my committee. Finally, portions of the research presented here were sponsored by NASA, Langley Research Center under contract NAS1-18471 to VPI&SU.

TABLE OF CONTENTS

LIST OF FIGURES

LIST OF TABLES

1. Introduction

1.1 Laminated Plates

Laminated composite plates are currently used widely because of their substantial advantages. Fiber/resin composite laminates are being used or proposed for use in structural components such as wings, horizontal and vertical stabilizers for airplanes, helicopter and wind-mill blades, and fan blades for aircraft turbine engines. The modern aircraft wing panel is composed of high-strength composite laminates to reduce structural weight and to increase the aircraft's performance. A knowledge of the fundamental coupling mechanisms involved and of the vibration characteristics of a composite wing is essential to the aeroelastic tailoring and design of a wing. Vibration analysis is an important design factor because stresses can be induced by the vibration in the structural components which are sufficiently high to cause instability and even failure.

Laminated composite plates are typically comprised of orthotropic layers (or plies or laminas) which are stacked upon each other and bonded together so as to deform as a single plate. The layers are often made of straight parallel fibers (or filaments) such as glass, boron or graphite, imbedded in a matrix material, such as epoxy resin or a metal. Each lamina can be considered as a homogeneous, orthotropic material having a value of Young's modulus considerably greater in the longitudinal direction than in the transverse direction. Adjacent laminae will have longitudinal axes generally not parallel. Cross-ply laminated plates arise in the special case when the longitudinal axes of adjacent laminae are perpendicular, whereas angle-ply laminates occur when adjacent layers are alternately oriented at angles of $+\theta$ and $-\theta$ with respect to the coordinates of the plate.

If the fibers (and therefore the orthotropic axes) of the layers are all parallel, then the plate may be considered orthotropic. If the fibers of adjacent layers are not all parallel, but the layers are stacked so that they are arranged symmetrically with respect to the plate midplane, then the problem may be treated by either orthotropic or anisotropic plate theory, depending upon the details of the stacking orientation with respect to the plate coordinate system. However, if the layers are not symmetrically arranged, then coupling exists between bending and stretching and this tends to reduce the effective stiffness, thus lowering the natural frequencies.

1.2 Past Research

There are many kinds of theories with varying sophistication available for the analysis of plates. First, there are linear and nonlinear theories. Within each of these theories, there are three distinct levels: 1) Thin plate analysis; 2) Moderately thick plate analysis (including thickness-shear-deformation, and sometimes thickness-normal deformation); and 3) Classical elasticity (non-homogeneous in the case of a laminated plate).

The thin plate analysis has been the most popular, probably due to its simplicity. However, even this type of analysis has two subclasses: a) simplified, correctly applicable only to a plate laminated symmetrically with respect to its middle plane, and b) complete analysis, including laminate bending-stretching coupling and thus applicable to arbitrarily laminated plates.

Leissa [1969] completed a monograph which summarized the world literature dealing with free vibrations of plates. Although composite plates were clearly in use at the time, it is clear that the best analyses available treated them as orthotropic, homogeneous plates for purposes of vibration analysis. Since 1969 literally scores of published papers have appeared dealing with vibrations of composite plates. Many

of these references have been described in the outstanding literature surveys of Bert [1982], by himself, and together with Francis [1974]. Since then, a significant number of investigations have been conducted on the linear vibrations of laminated plates. Both analytical (closed form, Galerkin, Rayleigh-Ritz method) and numerical methods have been used. A review of the technical literature on the vibration response of anisotropic plates was given by Leissa [1981] and on dynamic behavior of laminated composites by Bert [1985]. Kapania and Raciti [1989] provided a comprehensive survey of the more recent studies on the vibration of laminated plates.

1.2.1 Symmetric Laminates

For symmetrically laminated plates which can be represented as orthotropic or anisotropic homogeneous plates, thereby permitting uncoupling of the flexural equations from the inplane stretching equations, the classical types of boundary conditions which can exist on each edge can yield a total of 21 independent problems for rectangular shapes. For symmetric laminates, the classical lamination theory (CLT) has been used successfully in most cases. CLT assumes that the Kirchhoff's hypothesis is valid for the laminate and that the through the thickness effects and geometric nonlinearities are negligible. The CLT assumptions and the integration of the laminae constitutive equations lead to the well-known A, B and D matrices. For symmetric laminates, the B matrix is identically zero and therefore the inplane and out-of-plane effects are uncoupled.

Crawley [1979] investigated the resonant frequencies and mode shapes of a series of clamped rectangular plates of graphite/epoxy and hybrid graphite/epoxy/aluminum alloy which were laminated in various symmetric lamination schemes. The experimental results were compared with those of a mixed finite element and the agreement for mode shapes was excellent. Agreement for frequencies was reasonable;

discrepancies were attributed to differences between dynamic flexural and static in-plane moduli.

Crawley and Dugundji [1980] made a Kantorovich (partial Ritz) variational analysis of symmetrically laminated cantilever plates. In this technique, a mode shape is assumed only in the chordwise direction and the problem is reduced to a set of uncoupled ordinary differential equations. The solution of these equations gave both the eigenvalues of free vibration and the proper forms of the non-dimensional frequency which can be used to estimate the natural frequencies of laminated plates. Jensen and Crawley [1984] used three approximate methods (Ritz, Kantorovich and finite element) to study the vibrations of cantilevered plates having bending-twisting coupling, and compared results with experimental data.

1.2.2 Unsymmetric Laminates

Most of the research done on laminated composite plates is restricted to the special case of symmetric laminates. These are simpler to analyze since they do not exhibit bending-stretching coupling that is characteristic of unsymmetric laminates. But, as suggested by Minich and Chamis [1975], it may be possible to select coupling in laminates that will provide built-in self-damping mechanisms when subjected to dynamic excitations. Also, structural components fabricated from fiber composite laminates are occasionally found to be warped and it is believed that the warpage is largely due to coupling responses that result from fabrication errors in orienting the various plies. In addition, cross-coupling parameters that describe the degree of coupling between bending curvature and twist rate for a laminated composite are used in aeroelastic tailoring to control mode shapes and frequencies of high aspect ratio lifting surfaces [Jensen and Crawley, 1984]. Another example of an application of unsymmetric laminates concerns minimizing or avoiding flutter in airfoil designs.

Because of the bending-stretching coupling, it would be impossible to pull on unsymmetric laminates without at the same time bend and/or twist the laminate. Although the bending-stretching is present only in unsymmetric laminates, the stretching-shearing and the bending-twisting coupling may characterize both symmetric and unsymmetric laminates. The effect of the stretching-shearing coupling is to induce shear when a stretching force is applied to the laminate and vice versa. The effect of bending-twisting coupling is to induce twisting when a bending moment is applied to the laminate and vice versa. Due to the coupling between bending and stretching for unsymmetrical laminates, their exact analytical solutions are difficult to obtain. Approximate methods may be the only tools available to study the large number of problems which do not have exact solutions. The Rayleigh-Ritz method is one example of such an approach. Finite-element methods, which can handle all cases of mixed boundary conditions, usually require long computing times if one is interested in obtaining the natural frequencies including those for the higher modes. Apparently the first published results of the vibrational analysis of plates with bending-stretching coupling is due to Ashton and Waddoups [1969] who used beam eigenfunctions as admissible functions in the Rayleigh-Ritz method to analyze rectangular plates. They compared reasonably well with experimental results for the completely free and cantilever cases. The case of clamped boundary conditions is more complicated analytically, but perhaps more representative of practical structures. One of the first linear analyses for the free vibration of unsymmetrically laminated plates with clamped edges was presented by Bert and Mayberry [1969]. Using Kirchhoff's hypothesis, and minimizing the Lagrangian, in Hamilton's principle, by the Rayleigh-Ritz method, the analysis was reduced to the solution of a standard eigenvalue problem.

For the case of arbitrarily laminated angle-ply plates with simple support boundary conditions, Whitney and Leissa [1970], using the classical Kirchhoff plate theory in conjunction with the nonlinear terms in von Karman's theory, presented closed-form solutions for the natural frequencies. As would be expected, their results show a strong effect of bending-stretching coupling in lowering the frequencies as compared with uncoupled orthotropic plate theory. The results for unsymmetrically laminated, simply supported, cross-ply plates were subsequently further extended by Jones [1973] who showed that even though the coupling effects rapidly die out in antisymmetric laminates as the number of layers is increased, they decrease very slowly for unsymmetric laminates. Still another extension was made by Lin and King [1974] to show how exact solutions can be obtained for classes of unsymmetrically laminated plates having two opposite sides simply supported, with arbitrary edge conditions on the other two sides. For other boundary conditions the eigenvalues were estimated using Bolotin's method.

For unsymmmetric laminates the classical types of boundary conditions can yield 16 different possibilities for each edge. Approximate methods have been used to treat a few of these cases. Minich and Chamis [1975] used a finite element method to obtain frequencies and nodal patterns for cantilevered plates.

Experimental and analytical data for the vibration characteristics of cantilevered, unsymmetrically laminated, boron-epoxy panels were presented by Thornton [1976]. The application of the NASTRAN CQDPLT element to rectangular-planform cantilever plates gave excellent agreement with experimental results. For this set of boundary conditions the reduced stiffness simplification was shown to be adequate. In this approach the direct bending-stretching coupling terms are omitted, but the actual bending stiffness matrix $[D_{ij}]$ is replaced by the reduced one $[D_{ij}{}^{*}]$ defined as

$$[D_{ij}{}^*] = [D_{ij}] - [B_{ij}][A_{ij}]^{-1}[B_{ij}]$$

The effect of the panel asymmetry was to decrease the frequency of vibration. Laura and Grossi [1978] considered rectangular homogeneous anisotropic plates with simply supported edges having elastic rotational constraints. However, the latter conditions are satisfied only approximately. Solution was obtained by the Rayleigh-Ritz method with low-degree polynomial modal functions. For cases in which comparisons with previous solutions were possible, sufficiently good agreement for engineering purposes was obtained.

The recent study by Kamal and Durvasula [1986] uses a shear deformation plate theory, incorporating all possible laminate boundary conditions, to determine the free vibrations of unsymmetrically laminated plates. Vibrations of generally laminated rectangular plates with arbitrary edge conditions were studied by Baharlou and Leissa [1987]. The edge conditions were considered to be clamped, simply supported or free. A strain-energy functional containing both bending and stretching effects and accommodating arbitrary ply stacking sequences was used in an extension of the Ritz method. The displacement functions were taken to be simple non-dimensionalized algebraic polynomials. The main advantage of this method is that one avoids choosing the displacement functions a priori. It should, however, be kept in mind that the use of very high-order polynomials in the test functions may result in unconditional matrices. This is due to the fact that as the order of the polynomials is increased, the terms become numerically linearly dependent [Fletcher, 1984].

Finally, Khdeir [1988] studied the free vibrations of antisymmetrically angle-ply laminated plates with various boundary conditions. The solution was applicable only to those plates for which the two opposite edges are simply-supported.

1.2.3 Skew Plates

Generally orthotropic skew plates have been analyzed using the Ritz method for various combinations of simply supported, clamped and free edges by Nair and Durvasula [1974]. For each combination of skew angle and side ratio, it was found that one unique orientation of the major material-symmetry axis resulted in a maximum frequency. B-spline functions were proposed by Mizusawa *et al.* [1979] to study the free vibration of skew plates.

In recent years, considerable effort is being spent on accurately and efficiently analyzing the wings that have skin panels made of composite materials. The emphasis is on representing a wing by an equivalent plate. Lakshminarayana *et al.* [1985] obtained the natural frequencies of a swept symmetrically laminated wing panel by the finite element method, using a three-node triangular element with 15 degrees of freedom at each node. Giles [1986] presented an equivalent plate model for analyzing aircraft wing structures with general planform such as cranked wing boxes. Multiple trapezoidal segments were used to represent such planforms. A Ritz-solution technique that employs global displacement functions that span all the segments was used. Terms from a power series were selected for the displacement functions. The formulation was initially restricted to symmetrically laminated wings but this restriction was later removed [Giles, 1987].

Lee and Lee [1990] used an eight-node quadrilateral finite element based on the shear deformable theory to evaluate the vibration characteristics for various shaped symmetrically laminated wings. Recently, McGee and Leissa [1991] performed the first known three dimensional free vibrational study of skewed cantilever thick isotropic plates using the Ritz method. The assumed displacement functions are in the form of algebraic polynomials which satisfy the fixed face exactly and are mathematically complete. Results were compared with those obtained by three-dimensional finite elements.

1.2.4 Orthogonal Polynomials

The use of beam characteristic orthogonal polynomials in the Rayleigh-Ritz method was initially introduced by Bhat [1985, 1987] for the flexural vibration analysis of isotropic rectangular and triangular plates. He chose the first polynomial in the orthogonal set as the simplest polynomial which satisfied at least the geometrical boundary conditions and, if possible, all the boundary conditions. The higher members of the set were constructed by the Gram-Schmidt orthogonalization process. Dickinson and Blasio [1986] have modified the set of orthogonal polynomials to generate results for vibration and buckling analyses of orthotropic rectangular plates.

Recently, Lam, Liew and Chow [1989] used a set of two-dimensional plate functions to obtain free vibration solutions for rectangular composite plates for various edge conditions. This method was further extended by Liew and Lam [1990] who used a set of two-dimensional orthogonal plate functions as an admissible deflection function in the Rayleigh-Ritz method. From a prescribed starting function satisfying the boundary conditions, the higher terms in the plate functions were generated by using the Gram-Schmidt orthogonalization process. The method was applied to obtain results for the free vibrations of isotropic skew plates with different support conditions.

1.2.5 Sensitivity Analysis

Recently, a number of studies have been conducted on the sensitivity of various static and dynamic aeroelastic responses (e.g. flutter, divergence, etc.) to four wing shape variables namely surface area, taper ratio, aspect ratio and sweep angle (see for example, Kapania, Eldred and Barthelemy [1991]; Bergen and Kapania [1984]). All these studies required the derivatives of the stiffness and mass matrices with

respect to the previously mentioned four shape design variables. These derivatives were obtained using a finite difference approach. Such an approach, though very easy to implement, suffers from one major drawback: the results may be extremely sensitive to the step size. A larger step size leads to significant truncation errors and a too small step size may lead to round-off errors. To avoid these problems, it is desired that the derivatives be obtained analytically as far as possible.

In addition to the sensitivity of the stiffness and mass matrices, the sensitivity of the modal response (free vibrations and mode shapes) is also of interest. Haftka and Kapania [1986], for example, represented the modelling errors in large space strucutures in terms of the errors (or perturbations) in the modal response. Sheena and Karpel [1985] performed the static aeroelastic analysis of wings using free vibration modes. Recently, Karpel [1990] also obtained the sensitivity derivatives of flutter characteristics and stability margins for aeroservoelastic design of wings by representing the wing in terms of its modal coordinates. The sensitivity analysis of aeroelastic responses thus needs the sensitivity of the modal response.

It is highly desirable in optimization to be able to calculate the effect of design variable changes without having to perform a full analysis for each design iteration. This need has led to an increased interest in accurate and efficient approximation techniques. Many optimization procedures use first-order Taylor series approximations of the objective function and constraints for this purpose. Pritchard and Adelman [1991] recognized that the formulas for the sensitivity derivatives of system behavior variables can be interpreted as differential equations that may be solved to obtain closed form exponential approximations. On this basis, they developed the Differential Equation Based method, which they demonstrated for frequency and mode shape approximations. They also extended the method to multiple design variables.

Methods for first-order design sensitivities have been developed by Fox and Kapoor [1968], who presented exact expresssions for the rates of change of eigenvalues and eigenvectors with respect to the design parameters of the actual structure and indicated that the derivatives could be used successfully to approximate the analysis of new designs. Wang [1991] presented two improved approximate methods to compute eigenvector derivatives.

1.3 Present Work

The work described in this thesis covers the initial process of learning a method to some new results. Work started on a reasonably complex one dimensional problem before proceeding to the plate problem and then on to the sensitivity analysis of the plate problem. The extension from one dimension to two dimensions was non-trivial. To the best of the author's knowledge, no published results exist for the vibrations of generally laminated tapered skew plates. The purpose of this study is to fill this gap and to demonstrate the possible advantages of Chebyshev polynomials over simple polynomials.

The present work develops a method to find frequencies and mode shapes for all the possible combinations of boundary conditions that generally exist for an arbitrarily laminated composite tapered skew plate. The term 'composite plate' has various meanings in the literature. It is occasionally used in connection with plates having step-wise thickness variation. It is often used also to denote layerered plates, where each layer is made of an isotropic material. 'Sandwich plate' typically is used to describe a plate having a core material which separates two relatively thin face sheets of higher modulus material. In the present study a 'composite plate' will be made up of layers (or laminae), each lamina being composed of straight, parallel fibers imbedded in an epoxy resin. Each lamina can be considered as a homogeneous,

orthotropic material having a value of Young's modulus considerably greater in the longitudinal direction than in the transverse direction. Adjacent laminae will have longitudinal axes generally not parallel. A point to be noted is that 'tapered' implies that the root chord and the tip chord lengths of the trapezoidal plate are unequal. Finally, it should be noted that a plate is considered perfectly flat.

Within the limitations of the classical lamination theory, the Rayleigh-Ritz method is used with Chebyshev polynomials as displacement functions. Appropriate springs with large stiffness coefficients are used to simulate the effect of the geometric boundary conditions. Displacement functions are taken in the form of Chebyshev polynomials in combination with natural coordinates. This method enables one to analyze plates of various geometric shapes. Additionally this method will avoid using the computationally costly finite element method whenever this method suffices. The use of global displacement functions also facilitates the calculation of the higher-order derivatives of the displacements. These higher-order (upto 4th) derivatives are needed in a postprocessor that was developed by Bonanni *et al.* [1988] for calculating the interlaminar stresses by integrating the elasticity equilibrium equations. The comparison of the present work with existing theoretical results has been carried out and it is demonstrated that accurate results are obtained by this method. New results are presented for some previously unsolved problems. The present analysis gives the influence of the sweep angle, the fiber orientation, the aspect ratio, the plate area and the taper ratio of a composite plate on the vibration characteristics and the mode shapes.

The present study also presents first order shape sensitivities of the natural frequencies and mode shapes of the generally laminated tapered skew plates. The derivatives of the eigenvalues and eigenvectors with respect to various shape variables are computed analytically and the results are compared with those obtained

using the finite difference method in order to confirm their accuracy. Extensive numerical results are presented for both symmetrically and unsymmetrically laminated plates. The four independent shape parameters considered are: (i) the plate surface area, (ii) the aspect ratio, (iii) the taper ratio and (iv) the sweep angle. To the best of the authors' knowledge, no such study has been performed for generally laminated skew plates. Once their first-order derivatives are obtained, the eigenvalues and eigenvectors are then approximated over the range of the variable using linear, exponential and pseudo-exponential approximation schemes and compared with the values obtained from reanalysis. The approximate results are compared with those obtained by actual reanalysis and found to be in good agreement.

2. Beam Problem using Orthogonal Polynomials

2.0 Overview

Before extending it to two dimensions, the Rayleigh-Ritz method is first applied to a one dimensional problem. Thus, the objective of this chapter is to demonstrate the efficacy of using orthogonal polynomials in the Rayleigh-Ritz method and for purposes of illustration, the problem of free torsional vibration and buckling of doubly symmetric thin walled beams of open section, subjected to an axial compressive static load and resting on a continuous elastic foundation is considered. Both simple polynomials as well as orthogonal functions are used as displacement functions in order to demonstrate the advantages of the latter over the former. Two sets of boundary conditions are treated: (i) fixed-fixed and (ii) fixed-simply supported. Wherever possible, the functions are so chosen such that the essential boundary conditions are satisfied. In the cases where the functions do not satisfy all the essential boundary conditions, the penalty type approach is adopted. In that, appropriate springs with large stiffness coefficients are provided to simulate the essential boundary conditions. Numerical results for natural frequencies and buckling loads for various values of warping and elastic foundation parameters are obtained and compared with those obtained by other researchers. A good agreement is observed.

2.1 Introduction

The vibrations and buckling of continuously-supported finite and infinite beams resting on elastic foundation have applications in the design of aircraft structures, base frames for rotating machinery, highway pavements, railroad tracks etc. While there are a number of publications on flexural vibrations of rectangular beams and

plates on an elastic foundation, the literature on torsional vibrations and buckling of beams on elastic foundation is rather limited. Christiano and Salmela [1971] investigated the free torsional vibrations and stability of doubly-symmetric long thin-walled beams of open sections resting on elastic foundations. Kameswara Rao et al. [1974] used a finite element method to study the problem of torsional vibration of long, thin-walled beams of open sections resting on elastic foundations. Kameswara Rao and Appala Satyam [1975] developed approximate expressions for torsional frequency and buckling loads for thin-walled beams resting on Winkler-type elastic foundation and subjected to a time-invariant axial compressive force. Kameswara Rao and Mirza [1989] developed an improved analytical method based on the dynamic stiffness matrix approach and included the effects of Winkler-type elastic foundation and warping torsion in their study of the same problem.

It is known that higher mode frequencies predicted by approximate methods are generally in considerable error. In order to improve this situation, a large number of elements or terms in the series expansion have to be included in the computations to get values with acceptable accuracy. Increasing the number of elements in the finite element method makes it computationally costly. A viable alternative is the Rayleigh-Ritz method. Simple polynomials have been successfully used in the Rayleigh-Ritz method to determine the lower modes of vibration of beams and plates. But when the order of the simple polynomials is increased i.e. when the number of terms in the series is increased they become numerically linearly dependent [Fletcher, 1984], as Fig. 2.1 illustrates, and the mass and stiffness matrices become computationally singular. Thus this method fails for higher modes when ordinary algebraic polynomials are used. However, this problem can be avoided by using a set of orthogonal polynomials as the assumed displacement function. In this chapter three different types of displacement functions are used: (i) simple

polynomials, (ii) orthogonal functions and (iii) Chebyshev polynomials which are a particular type of orthogonal functions. Two sets of boundary conditions are treated, but as the Rayleigh-Ritz method requires that only the essential boundary conditions be satisfied, the displacement functions are accordingly chosen. However, in those cases where the assumed displacement functions cannot satisfy even the geometric boundary conditions, e.g. when Chebyshev polynomials are used, a penalty type approach is employed. Springs of sufficiently large stiffness constants are used to simulate the fixed or simply supported edges. It is demonstrated that this method yields satisfactorily accurate results. Extensive numerical results for torsional natural frequencies and buckling loads for some typical values of warping and foundation parameters are presented. The results clearly illustrate the motivation for preferring orthogonal polynomials over simple polynomials.

2.2 Formulation and Analysis

Consider a long doubly-symmetric thin-walled beam of open section of length L and resting on a Winkler-type elastic foundation of torsional stiffness K_s. The beam is subjected to a constant static axial compressive force P and is undergoing free torsional vibrations. As given by Kameswara Rao and Appala Satyam [1975], the corresponding differential equation of motion can be written as

$$EC_w\frac{\partial^4\phi}{\partial z^4} - (GC_s - \frac{P}{A}I_p)\frac{\partial^2\phi}{\partial z^2} + K_s\phi + \rho I_p\frac{\partial^2\phi}{\partial t^2} = 0 \qquad (2.1)$$

in which E is the modulus of elasticity; C_w the warping constant; G the shear modulus; C_s the torsion constant; I_p the polar moment of inertia; A the area of cross-section; ρ the mass density of the material of the beam; ϕ the angle of twist; z the distance along the length of the beam and t the time.

Neglecting the effects of longitudinal inertia and shear deformation, the total potential energy of the beam V, consisting of the strain energy of deformation of the beam, the work done by the external compressive load and the reaction by the elastic foundation, is given by Appala Satyam [1974] as

$$V = \frac{1}{2}\int_0^L [EC_w(\phi'')^2 + (GC_s - \frac{P}{A}I_p)(\phi')^2 + K_s(\phi)^2]\mathrm{d}z \tag{2.2}$$

where the prime denotes differentiation with respect to z. The kinetic energy can be written as

$$T = \frac{1}{2}\int_0^L \rho I_p(\dot{\phi})^2\mathrm{d}z \tag{2.3}$$

where the dot denotes differentiation with respect to time t. For free torsional vibrations, in order to derive approximate but satisfactory expressions for the natural frequencies and buckling loads, the angle of twist $\phi(z,t)$ can be expressed in the form

$$\phi(z,t) = \sum_{i=1}^{n} \psi_i(z)q_i(t) \tag{2.4}$$

where $q(t)$ are time dependent generalized displacements and $\psi(z)$ are a complete set of linearly independent displacement functions which satisfy the structure's essential boundary conditions but not necessarily the natural boundary conditions.

Now, in terms of the assumed functions the kinetic energy of the beam is written as

$$T = \frac{1}{2}\sum_{i=1}^{n}\sum_{j=1}^{n}\bar{m}_{ij}\dot{q}_i\dot{q}_j \tag{2.5}$$

where the generalized masses are defined by

$$\bar{m}_{ij} = \int_0^L \rho I_p \psi_i \psi_j \mathrm{d}z \qquad (i,j = 1,2...n) \tag{2.6}$$

This can be written in matrix form as

$$T = \frac{1}{2}(\dot{q})^T[\bar{m}](\dot{q}) \tag{2.7}$$

where $[\bar{m}]$ is known as the mass matrix. Similarly, the potential energy can be written as

$$V = \frac{1}{2}\sum_{i=1}^{n}\sum_{j=1}^{n}\bar{k}_{ij}q_i q_j \tag{2.8}$$

where the generalized stiffness coefficients are defined by

$$\bar{k}_{ij} = \int_0^L [EC_w(\psi_i'')(\psi_j'') + (GC_s - \frac{P}{A}I_p)(\psi_i')(\psi_i') + K_s(\psi_i)(\psi_j)]\mathrm{d}z \tag{2.9}$$

The strain energy expression can be written in the matrix form as

$$V = \frac{1}{2}(q)^T[\bar{k}](q) \tag{2.10}$$

The equations of motion are obtained by substituting Eq. 2.7 and Eq. 2.10 into Lagrange's equations, which are given by

$$\frac{d}{dt}\left(\frac{\partial L}{\partial \dot{q}_i}\right) - \frac{\partial L}{\partial q_i} = 0 \tag{2.11}$$

where the Lagrangian $L = T - V$. In terms of the generalized coordinates the matrix equation governing the free vibration is found to be

$$[\bar{m}](\ddot{q}) + [\bar{k}](q) = 0 \tag{2.12}$$

For sinusoidal vibrations we take

$$q_i(t) = e^{i\omega_n t} \tag{2.13}$$

where ω_n is the torsional natural frequency in rad/sec. Thus we have to solve the eigenvalue problem

$$[\bar{k}](q) = \omega_n^2[\bar{m}](q) \tag{2.14}$$

in order to determine the principal frequencies of vibration and hence the mode shapes. We now form the following non-dimensional parameters

$$\begin{aligned} \text{Warping Parameter } K \text{ where } K^2 &= \frac{L^2 G C_s}{E C_w} \\ \text{Load Parameter } \Delta \text{ where } \Delta^2 &= \frac{L^2 P I_p}{A E C_w} \\ \text{Foundation Parameter } \gamma \text{ where } \gamma^2 &= \frac{L^4 K_s}{4 E C_w} \\ \text{Frequency Parameter } \lambda \text{ where } \lambda^2 &= \frac{L^4 \rho I_p \omega_n^2}{E C_w} \end{aligned} \tag{2.15}$$

The double precision IMSL subroutine DGVCSP is used to solve the eigenvalue problem. The domain is first transformed from [0 to L] to [-1 to +1], in order to facilitate the use of Chebyshev Polynomials which are defined over this range. The integrals are evaluated analytically and also checked numerically using the IMSL subroutine DQDAG.

2.3 Boundary Conditions

The Rayleigh-Ritz method requires that the set of trial functions must be linearly independent, must satisfy the essential boundary conditions and must be complete. They need not satisfy the natural boundary conditions. The two sets of boundary conditions considered here are fixed-fixed and fixed-simply supported.

For the fixed-fixed boundary conditions the boundary conditions to be satisfied are the same at both ends i.e.

$$\phi = \phi' = 0 \quad \text{at } z = 0 \text{ and } z = L \tag{2.16}$$

We assume the following trigonometric function which satisfies all the essential boundary conditions

$$\psi_i(z) = (1 - \cos 2i\pi \frac{z}{L}) \qquad (i = 1, ...n) \tag{2.17}$$

For the beam fixed at one end and simply supported at the other end the essential boundary conditions at the fixed end are

$$\phi = \phi' = 0 \quad \text{at } z = 0 \tag{2.18}$$

and at the simply supported end we have

$$\phi = 0 \quad \text{at } z = L \tag{2.19}$$

We choose four distinct displacement functions to solve this problem and compare the results obtained by each. The assumed functions are shown below.

(i) Simple polynomials satisfying all the essential boundary conditions

$$\psi_i(z) = \left(1 - \frac{z}{L}\right)\left(\frac{z}{L}\right)^{i+1} \qquad (i = 1, ...n) \tag{2.20}$$

(ii) Orthogonal functions consisting of a combination of algebraic and trigonometric terms. These satisfy all the essential boundary conditions also.

$$\psi_i(z) = \frac{z}{L} \sin \frac{\pi i z}{L} \qquad (i = 1, ...n) \tag{2.21}$$

(iii) Power series of simple polynomials not satisfying all the essential boundary conditions

$$\psi_i(z) = \left(\frac{z}{L}\right)^{i-1} \qquad (i = 1, ...n) \tag{2.22}$$

(iv) Chebyshev polynomials. These do not satisfy all the essential boundary conditions. The Chebyshev Polynomial of degree i, $T_i(z)$ is defined as

$$T_i = \cos\left(i \ \cos^{-1}\frac{z}{L}\right) \qquad (i = 1, ...n) \tag{2.23}$$

Further, each term in the series is orthogonal to all other terms in the series, making them ideal for our purpose. The polynomials satisfy the orthogonality relation

$$\int_{-1}^{1} T_i(z)T_j(z)(1-z^2)^{-1/2}dz = \frac{\pi}{2}c_i\delta_{ij} \tag{2.24}$$

where

$$c_0 = 2 \tag{2.25}$$

$$c_i = 1 \qquad i > 0 \tag{2.26}$$

For the last two cases, where all the essential boundary conditions are not satisfied explicitly, the penalty type approach is used. The fixed and simply supported ends are simulated by adding springs of sufficiently large stiffnesses K_i. We add the following spring energy terms to the potential energy of the beam

$$\frac{1}{2}K_1[\phi(0)]^2 + \frac{1}{2}K_2[\phi(L)]^2 + \frac{1}{2}K_3[\phi'(0)]^2 + \frac{1}{2}K_4[\phi'(L)]^2 \tag{2.27}$$

Furthermore, these spring energy terms are non-dimensionalized using the following parameters

$$
\begin{aligned}
K_1 &= \alpha_1 \frac{EC_w}{L^3} \\
K_2 &= \alpha_2 \frac{EC_w}{L^3} \\
K_3 &= \alpha_3 \frac{EC_w}{L} \\
K_4 &= \alpha_4 \frac{EC_w}{L}
\end{aligned}
\tag{2.28}
$$

Any essential boundary condition can be simulated by picking appropriate positive values for α_i's. For example, a fixed end at $z = 0$ requires that both α_1 as well as α_3 be given appropriately large values whereas a simply supported end at $z = L$ can be simulated by specifying α_3 to be non-zero and sufficiently large while α_4 is forced to be zero. Likewise, fixed-fixed and simply supported beams can be studied using this method. A free edge implies no restraints (no springs) at all. Thus all possible combinations of boundary conditions can be treated.

2.4 Results and Discussion

The approach developed in the preceding section can be applied to the calculation of natural torsional frequencies of multi-span doubly symmetric thin-walled beams of open section such as beams of I-section. All classical and non-classical (elastic restraints) boundary conditions can be incorporated in the present model without any difficulty. To demonstrate the effectiveness of the present approach, a single-span, thin-walled I-beam is chosen. Unless specified otherwise, the numerical values obtained for the frequency parameter λ are for the first mode of vibration. For the fixed-simply supported cases which involve the spring energy terms i.e. the ones using displacement functions not satisfying all the essential boundary conditions, the non-dimensionalized spring constants $\alpha_1 = \alpha_2 = \alpha_3$ were initially given the successive values of $10^4, 10^5, 10^6$ while $\alpha_4 = 0$. In each case λ^2 stabilized at approximately the same value. The numerical results shown in the following sections

are all generated using a value of 10^5 for the non-zero non-dimensionalized spring constants.

2.4.1 Convergence Analysis

The convergence of the non-dimensionalized eigenvalue λ^2 is studied as a function of the number of terms n in the displacement function. In particular, a comparison between the results obtained by using simple polynomials and those obtained with orthogonal functions is presented for higher modes of vibration.

First, the Fixed-Fixed (F-F) case is studied, as shown in Fig. 2.2. An orthogonal trigonometric function is used as the assumed displacement function, with the warping parameter $K = 1$, the foundation parameter $\gamma = 12$ and the load parameter $\Delta = 2$. It can be seen that the convergence of the fundamental frequency parameter is quite rapid initially before leveling out at $n = 8$.

Next, the Fixed-Simply Supported (F-SS) beam is treated. The convergence of the frequency parameter for the first mode of vibration with $K = 1$, $\gamma = 4$ and $\Delta = 0$ is illustrated in Fig. 2.3. Chebyshev polynomials are used. Here, it is seen that the eigenvalue drops steeply by just increasing the number of terms in the displacement function from four to five, before quickly stabilizing.

Next, Fig. [2.4-2.7] compare the convergence of the first four frequency parameters for a Free-Simply Supported beam using simple polynomials and orthogonal functions. It is noted that the simple polynomials *fail* when more than nine terms are used in the displacement function. This is because the mass and stiffnes matrices become *computationally singular* for higher order simple polynomials. Orthogonal functions do not pose this problem and therefore yield more accurate results, especially for higher modes.

2.4.2 Frequencies and Buckling Loads

Next, Eq. 2.14 is solved for values of warping parameter $K = 1$ and $K = 10$ and for various values of foundation parameter γ in the range 0-12. Results are obtained for the Fixed-Simply Supported case. These are compared with results obtained using approximate methods such as Galerkin's technique [Kameswara Rao and Appala Satyam, 1975] and also with exact values [Kameswara Rao and Mirza, 1989], as shown in Tables [2.1-2.3]. It is seen that the values of the fundamental frequency parameter obtained in this study are consistently higher than the exact values, as expected. Tables 2.1 and 2.2 present results obtained by using Chebyshev polynomials and Table 2.3 shows frequency values obtained with simple polynomials.

The variation of the fundamental frequency and buckling load parameters for values of K equal to 1 and 10 are shown in the characteristic curves of Fig. 2.8 and Fig. 2.9 respectively. A close look at the results clearly reveals that the effect of an increase in axial compressive load parameter Δ is to drastically decrease the fundamental frequency parameter λ. One can easily read the values of buckling load parameter Δ_{cr} from these figures for $\lambda^2 = 0$. When the axial load is not present the values of λ^2 for various values of γ can be obtained for values of $\Delta = 0$. As can be expected, the effect of the elastic foundation is found to increase the frequency of vibration especially for the first few modes. However, this influence seems to be quite negligible on higher modes. Thus, the combined influence of the foundation parameter and the load parameter can be observed to be opposing each other. Hence the combined influence is the superimposition of the individual effects on the frequency of vibration.

Table 2.1. Exact and approximate values of λ^2 ($\gamma = 4.0$) for the first mode of vibration of a fixed, simply supported beam (Chebyshev polynomials).

K	Δ	Exact	Approximate	Present Study
1.0	0.0	314.265	325.950	320.186
	2.0	268.632	276.602	272.403
	4.0	132.226	128.557	134.673
10.0	0.0	1439.672	1547.319	1458.763
	4.0	1257.879	1349.926	1285.546
	8.0	712.010	757.747	743.673

Table 2.2. Exact and approximate values of λ^2 ($\gamma = 8.0$) for the first mode of vibration of a fixed, simply supported beam (Chebyshev polynomials).

K	Δ	Exact	Approximate	Present Study
1.0	0.0	506.302	517.894	510.784
	2.0	460.548	468.596	467.763
	4.0	324.676	320.624	325.873
10.0	0.0	1631.753	1739.526	1728.648
	4.0	1449.536	1541.898	1536.982
	8.0	904.893	949.692	938.975

Table 2.3. Comparison between exact and approximate values of λ^2 ($\gamma = 12.0$) for the first mode of vibration of a fixed, simply supported beam (simple polynomial not satisfying essential boundary conditions).

K	Δ	Exact	Approximate	Present Study
1.0	0.0	826.253	837.892	835.742
	2.0	780.735	788.735	786.963
	4.0	644.378	640.655	643.981
10.0	0.0	1951.865	2059.296	2017.841.
	4.0	1769.758	1861.886	1804.731
	8.0	1224.926	1269.686	1253.980

2.5 Concluding Remarks

A method has been developed for computing the natural torsion frequencies and buckling loads of long, thin-walled beams of open section resting on continuous Winkler-type elastic foundation and subjected to an axial time-invariant compressive load. The approach presented in the preceding sections is quite general and can easily be extended to isotropic and laminated, rectangular and skew plates. A computer program has been developed to accurately determine the torsional buckling loads, frequencies and corresponding modal shapes. Results have been presented for a beam with two different sets of boundary conditions, showing the effect of increasing the number of terms in the displacement function. The influence of elastic foundation, axial compressive load and warping is clearly demonstrated. While an increase in the values of the elastic foundation parameter resulted in an increase in frequency, the effect of an increase in axial load parameter is found to be to drastically decrease the frequency to zero at the limit when the axial load equals the buckling load for the beam.

When a simple polynomial was used as the displacement function the mass and stiffness matrices became *computationally singular* when the order of the matrix $n = 6$ with single precision and $n = 10$ with double precision, irrespective of the manner in which the essential boundary conditions were satisfied. On the other hand, when orthogonal functions were used the matrices remained positive definite. The penalty type approach gave accurate results compared to the cases where the boundary conditions were satisfied explicitly. Thus, in conclusion we note that orthogonal functions yield more accurate results for higher modes of vibration than simple polynomials.

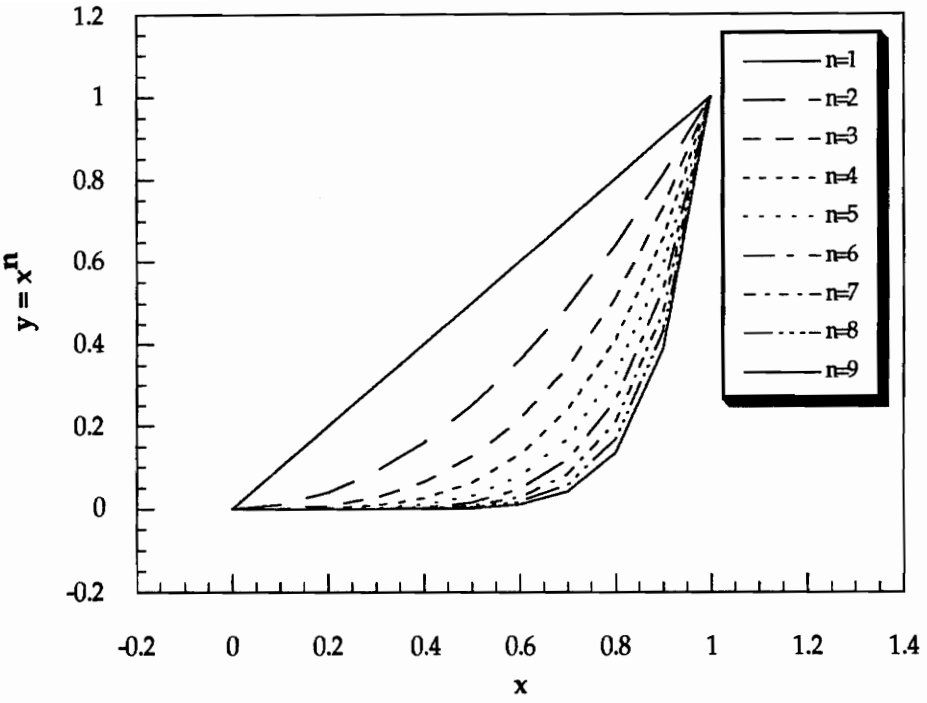

Fig. 2.1. Numerical Linear Dependence of Higher Order Simple Polynomials.

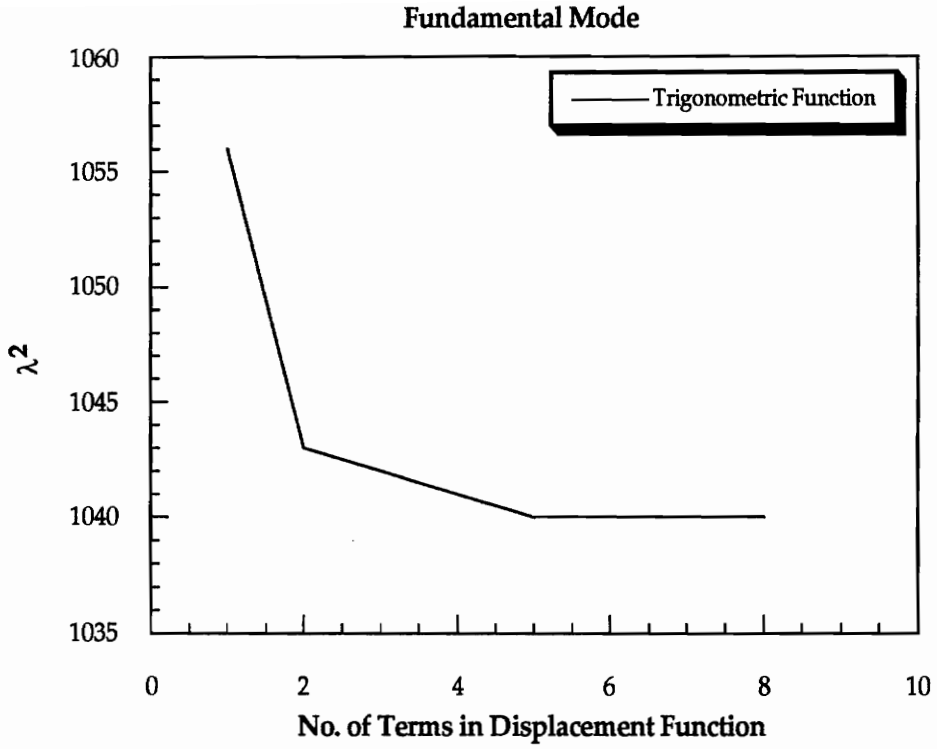

Fig. 2.2. Convergence Analysis of Frequency Parameter for F-F Beam.

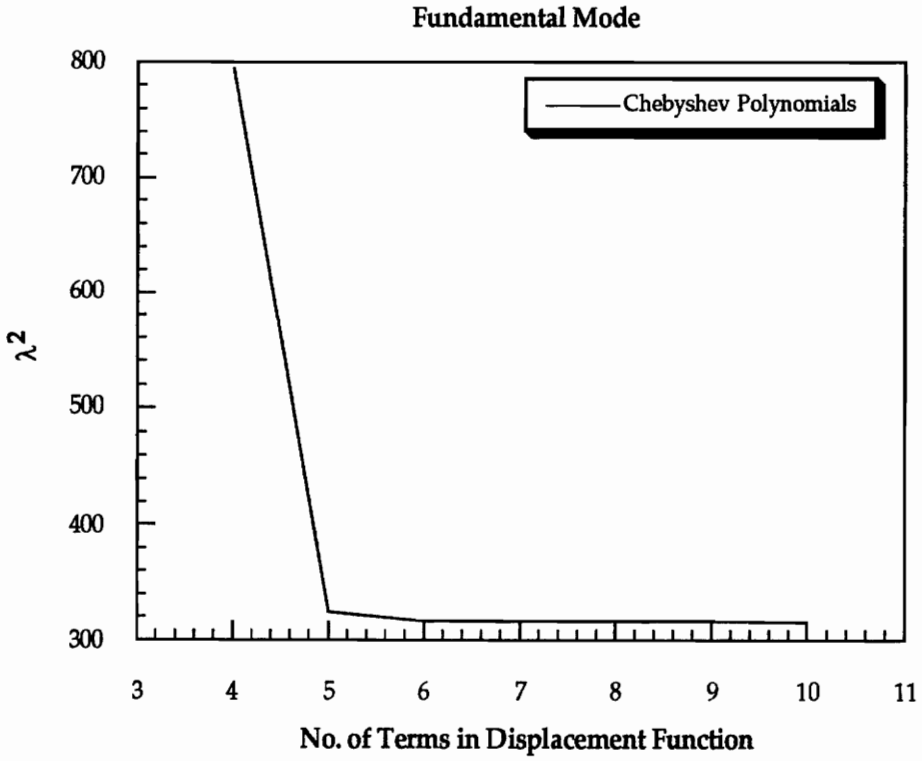

Fig. 2.3. Convergence Analysis using Chebyshev Polynomials for F-SS Beam.

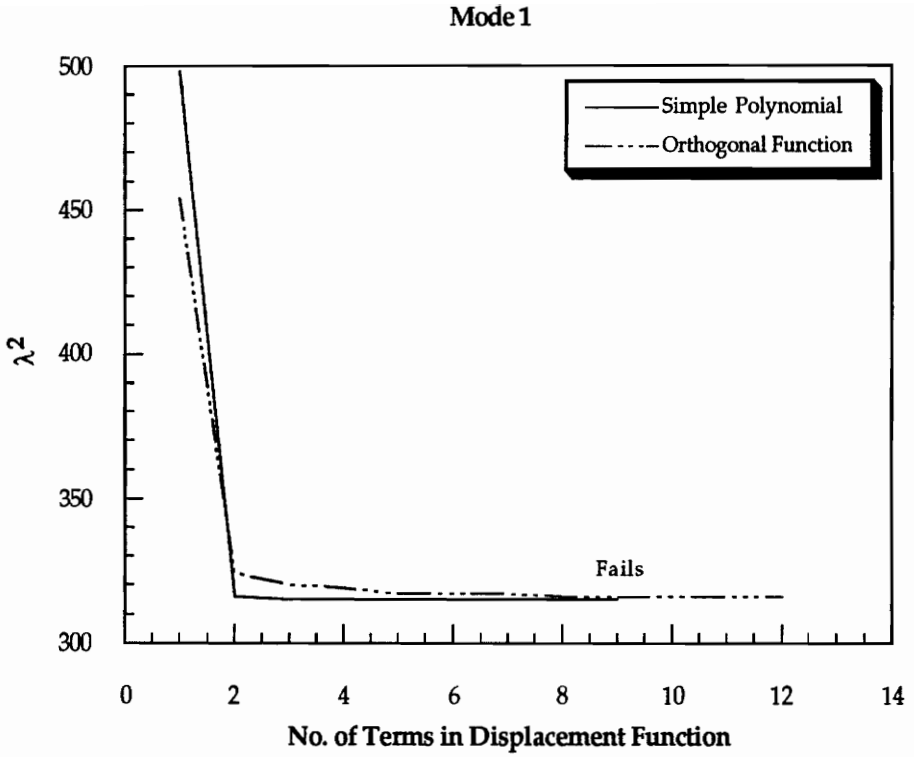

Fig. 2.4. Convergence Analysis of 1st Mode for F-SS Beam with B.C. Satisfied.

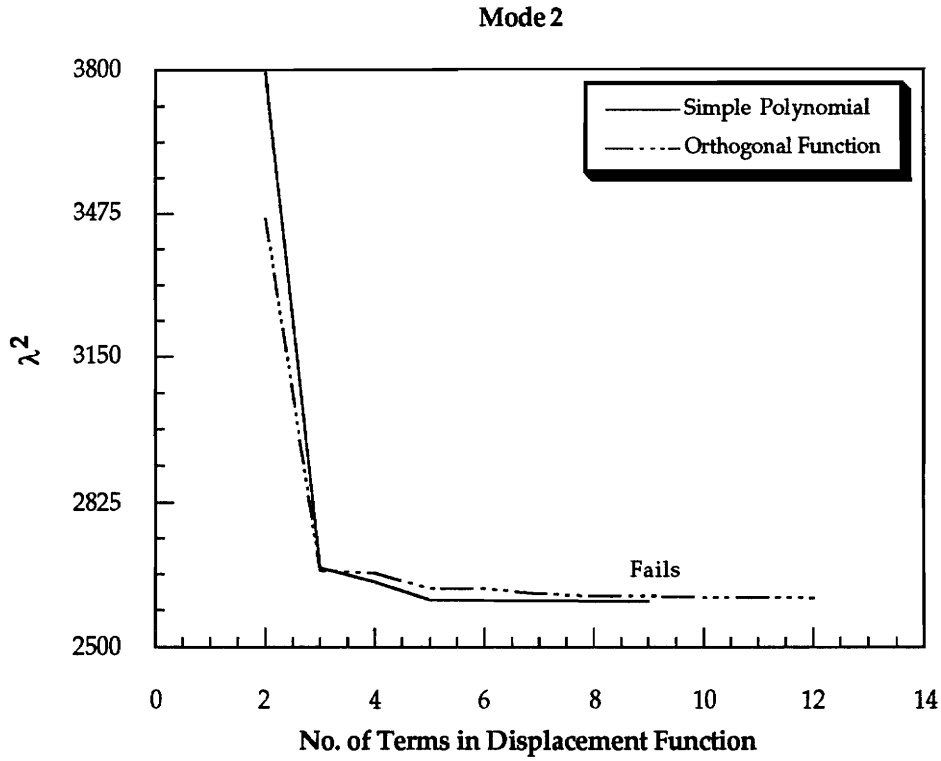

Fig. 2.5. Convergence Analysis of 2nd Mode for F-SS Beam with B.C. Satisfied.

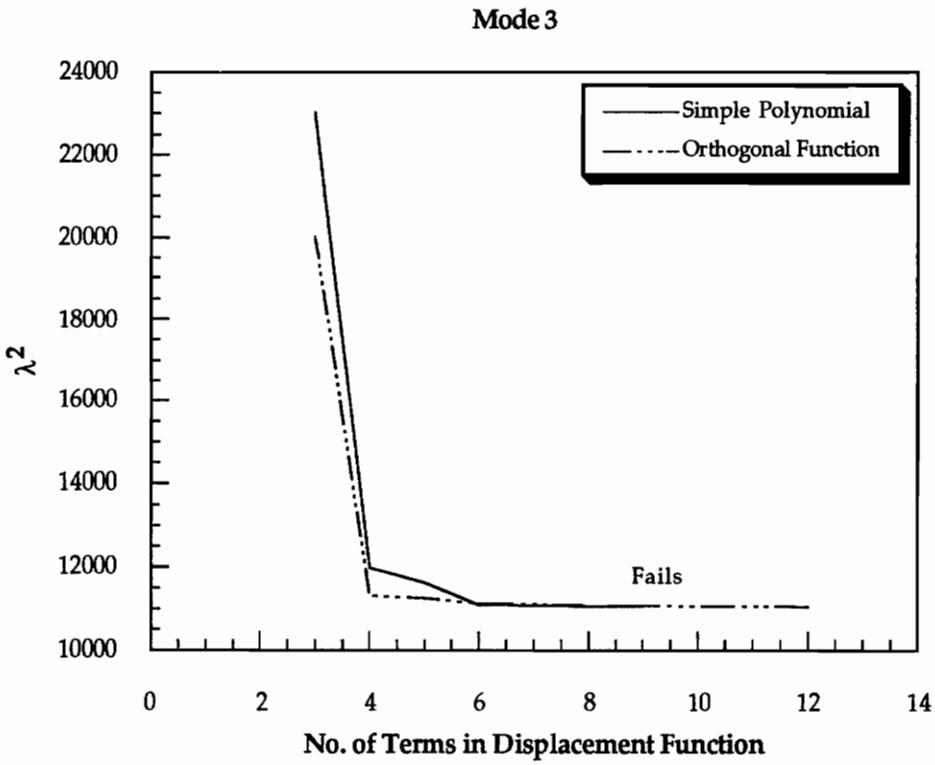

Fig. 2.6. Convergence Analysis of 3rd Mode for F-SS Beam with B.C. Satisfied.

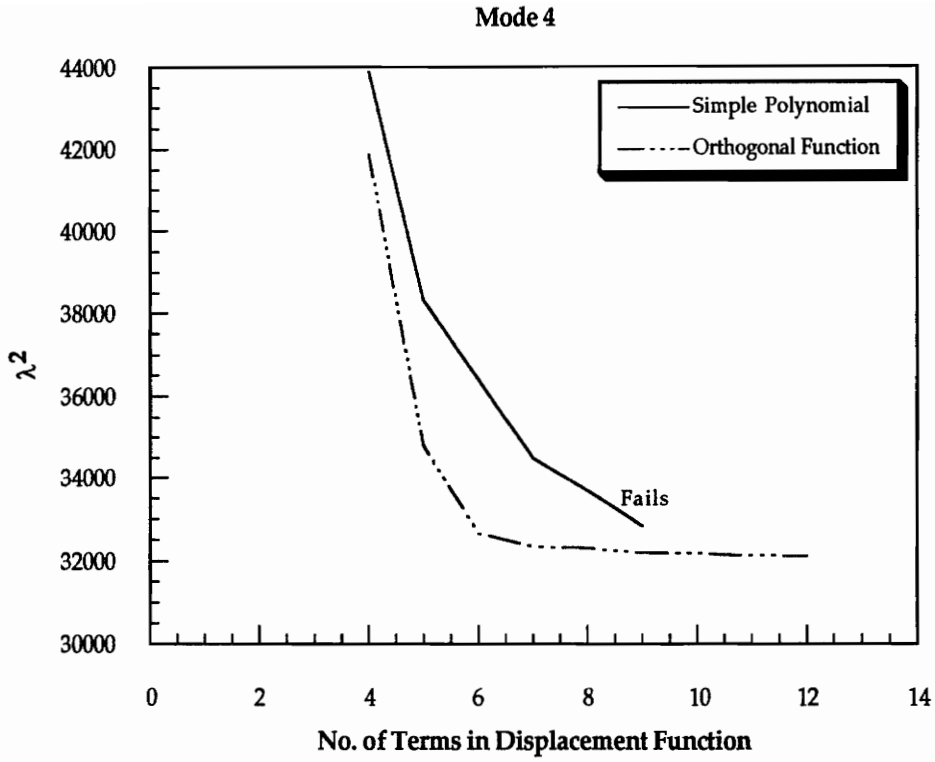

Fig. 2.7. Convergence Analysis of 4th Mode of F-SS Beam with B.C. Satisfied.

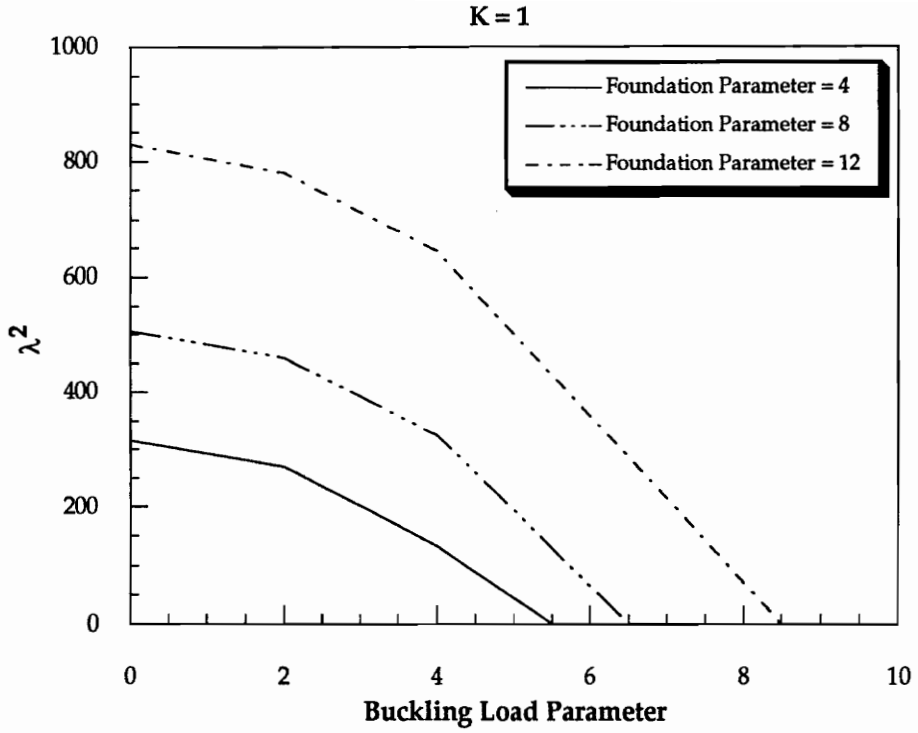

Fig. 2.8. Effect of Elastic Foundation on Frequency Parameter for K = 1.

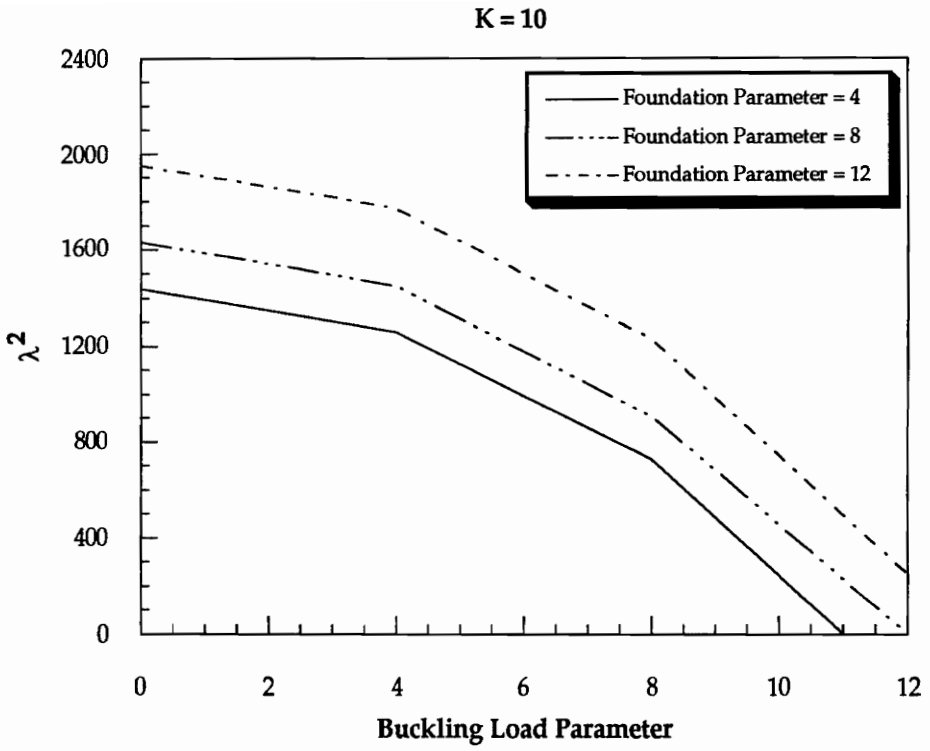

Fig. 2.9. Effect of Elastic Foundation on Frequency Parameter for K = 10.

3. Formulation and Analysis For Skew Plates

3.0 Overview

The approach developed in the previous chapter is now extended to two dimensions. The method of analysis is explained in this chapter. After explaining the coordinate systems, the derivation of the energy expressions is summarized for an arbitrarily laminated plate. Then the application of the Rayleigh-Ritz method with Chebyshev polynomials as the displacement function is demonstrated for the free vibration and static analyses of a plate with arbitrary boundary conditions. Finally, expressions for the first order derivatives of the stiffness and mass matrices, eigenvalues (frequencies) and eigenvectors (mode shapes) are presented, followed by methods to approximate the eigenvalues and eigenvectors.

3.1 Coordinate Systems

The original rectangular (x, y) coordinate system and the transformed (η, ξ) coordinate system of the plate are shown in Fig. 3.1. The $x - y$ plane is the mid-plane of the plate and the z axis is normal to the plate. For an unswept plate the fiber angle is measured counterclockwise from the positive y axis. As the wing is swept the fiber angle is also rotated correspondingly. The (x, y) coordinate system, though useful in describing the physical domain of the plate, is not conducive to the use of Chebyshev polynomials as these are defined for $-1 \leq \eta, \xi \leq 1$. We therefore transform the domain to a non-dimensionalised one. This also facilitates the use of Gaussian quadrature to evaluate the integrals described in this chapter.

3.2 Energy Expressions

The displacements of the middle surface of the plate in the x, y and z directions are denoted by u, v and w, respectively.

The strains in terms of the displacements of the mid-plane are

$$\begin{pmatrix} \epsilon_x \\ \epsilon_y \\ \gamma_{xy} \end{pmatrix} = \begin{pmatrix} u_{,x} \\ v_{,y} \\ u_{,y} + v_{,x} \end{pmatrix} - z \begin{pmatrix} w_{,xx} \\ w_{,yy} \\ 2w_{,xy} \end{pmatrix} \tag{3.1}$$

The stress-strain relationships can be written in the following form

$$\begin{pmatrix} \sigma_x \\ \sigma_y \\ \sigma_{xy} \end{pmatrix} = \begin{bmatrix} Q_{11} & Q_{12} & Q_{16} \\ Q_{12} & Q_{22} & Q_{26} \\ Q_{16} & Q_{26} & Q_{66} \end{bmatrix} \begin{pmatrix} \epsilon_x \\ \epsilon_y \\ \gamma_{xy} \end{pmatrix} \tag{3.2}$$

where Q_{ij} are well known transformed reduced stiffnesses.

The potential energy of deformation for a thin plate (neglecting transverse normal and shear strains) is

$$V_1 = 1/2 \int_V (\sigma_x \epsilon_x + \sigma_y \epsilon_y + \sigma_{xy} \gamma_{xy}) \mathrm{d}V \tag{3.3}$$

where V is the volume of the plate. The expression for the strain energy of the plate due to its deformation can be written in terms of the middle surface of the plate by using Eq. 3.1 and Eq. 3.2 in Eq. 3.3, resulting in

$$V_1 = 1/2 \int \int_S \begin{pmatrix} \epsilon \\ \kappa \end{pmatrix}^T \begin{bmatrix} A & B \\ B & D \end{bmatrix} \begin{pmatrix} \epsilon \\ \kappa \end{pmatrix} \mathrm{d}S \tag{3.4}$$

where A_{ij}, B_{ij}, D_{ij} are the stretching (in-plane), coupling and bending stiffnesses, respectively given by

$$(A_{ij}, B_{ij}, D_{ij}) = \int_{-h/2}^{h/2} Q_{ij}(1, z, z^2) \mathrm{d}z \tag{3.5}$$

and S is the plate surface area. The strain and curvature vectors ϵ and κ, respectively are given as

$$\begin{pmatrix} \epsilon \\ \kappa \end{pmatrix}^T = (u_x \;\; v_y \;\; u_y + v_x \;\; w_{xx} \;\; w_{yy} \;\; 2w_{xy}) \tag{3.6}$$

where the subscripts denote partial derivatives. The kinetic energy, neglecting rotary inertia and tangential inertia [Baharlou and Leissa, 1987], is

$$T = 1/2 \int_S \rho w_{,t}^2 \, \mathrm{d}S \tag{3.7}$$

where ρ is the mass per unit area of the plate and t is the time. The corresponding expression for the strain energy in the transformed co-ordinate system is

$$V_1 = 1/2 \int_{-1}^{1} \int_{-1}^{1} \begin{pmatrix} \epsilon' \\ \kappa' \end{pmatrix}^T [T]^T \begin{bmatrix} A & B \\ B & D \end{bmatrix} [T] \begin{pmatrix} \epsilon' \\ \kappa' \end{pmatrix} |J| \mathrm{d}\eta \mathrm{d}\xi \tag{3.8}$$

where J is the Jacobian of the transformation and $[T]$ is the transformation matrix that relates the strain and the curvature vectors in the (x, y) coordinate system to the pseudo strain and curvature vectors in the natural coordinate system as shown below

$$\begin{pmatrix} \epsilon \\ \kappa \end{pmatrix} = [T] \begin{pmatrix} \epsilon' \\ \kappa' \end{pmatrix}$$

where

$$\begin{pmatrix} \epsilon' \\ \kappa' \end{pmatrix}^T = (u_\eta \;\; u_\xi \;\; v_\eta \;\; v_\xi \;\; w_\eta \;\; w_{\eta\eta} \;\; w_{\xi\xi} \;\; w_{\eta\xi}) \tag{3.9}$$

The details of the $[T]$ matrix, which is related to the matrix of the co-ordinate transformation, are given in the Appendix.

The essential boundary conditions are taken care of by adding springs on the specified edges; linear springs for simply supported edges, linear and rotational springs for clamped edges and no springs for free edges. A typical spring energy term for a linear spring would be

$$1/2 \int K g(n,s)^2 \mathrm{d}\gamma$$

and a typical rotational spring energy term looks like

$$1/2 \int K' g(n,s)_{,h}^2 \mathrm{d}\gamma$$

where

$$g = u, v \text{ or } w$$

$$h = n \text{ or } s$$

$$\gamma = s \text{ or } s$$

and where K and K' are the spring constants for linear and rotational type of springs, respectively and s and n are the tangential and the normal coordinates to the edge. The potential energy of these springs V_2 is added to the energy of deformation of the plate to give the total potential energy

$$V = V_1 + V_2 \tag{3.10}$$

3.3 Rayleigh-Ritz Method

For the small oscillation, free vibration problem the displacements of the mid-surface of the plate u, v and w, which are harmonic functions of time, can be written as

$$u\ (\eta, \xi, t) = U\ (\eta, \xi) e^{i\omega t}$$

$$v\ (\eta, \xi, t) = V\ (\eta, \xi) e^{i\omega t} \tag{3.11}$$

$$w\ (\eta, \xi, t) = W\ (\eta, \xi) e^{i\omega t}$$

where ω is the angular frequency of vibration in rad/sec. The amplitudes of vibration U, V and W, are expressed in terms of the Chebyshev polynomials T_i as shown

$$U(\eta, \xi) = \sum_{i=0}^{I} \sum_{j=0}^{J} R_{ij} T_i(\eta) T_j(\xi)$$

$$V(\eta, \xi) = \sum_{k=0}^{K} \sum_{l=0}^{L} S_{kl} T_k(\eta) T_l(\xi) \tag{3.12}$$

$$W(\eta, \xi) = \sum_{m=0}^{M} \sum_{n=0}^{N} P_{ij} T_m(\eta) T_n(\xi)$$

where the Chebyshev polynomials are given by

$$\begin{aligned} T_0\ (\psi) &= 1 \\ T_1\ (\psi) &= \psi \\ T_i\ (\psi) &= 2\psi T_{i-1} - T_{i-2} \qquad -1 \leq \psi \leq 1 \end{aligned} \tag{3.13}$$

The Lagrange equations for the case of free vibrations are

$$\begin{aligned} \frac{d}{dt}\left(\frac{\partial L}{\partial \dot{R}_{ij}}\right) - \frac{\partial L}{\partial R_{ij}} &= 0 \\ \frac{d}{dt}\left(\frac{\partial L}{\partial \dot{S}_{kl}}\right) - \frac{\partial L}{\partial S_{kl}} &= 0 \\ \frac{d}{dt}\left(\frac{\partial L}{\partial \dot{P}_{mn}}\right) - \frac{\partial L}{\partial P_{mn}} &= 0 \end{aligned} \tag{3.14}$$

where L is the Lagrangian defined by $L = T - V$ and the dots denote differentiation with respect to time. Upon substitution of Eq. 12 into Eq. 7 and Eq. 10 and further substitution of these into Eq. 14, we get

$$([K] - \lambda[M])\{q\} = 0 \tag{3.15}$$

Equation 3.15 is a linear eigenvalue problem where [K] and [M] are the stiffness and mass matrices resulting from Eq. 3.10 and Eq. 3.7, respectively and λ is a frequency parameter. The eigenvector $\{q\}$ is defined as

$$q = (R_{00}, R_{01}, \ldots R_{ij};\ S_{00}, S_{01}, \ldots S_{kl};\ P_{00}, P_{01}, \ldots P_{mn})^T \tag{3.16}$$

The coefficients R_{ij}, S_{kl} corresponding to the inplane displacements are condensed out using static condensation to reduce the size of the matrices. We can write Eq. 3.15 as follows

$$\begin{bmatrix} K_{11} & K_{12} & K_{13} \\ K_{12} & K_{22} & K_{23} \\ K_{13} & K_{23} & K_{33} \end{bmatrix} \begin{pmatrix} R_{ij} \\ S_{kl} \\ P_{mn} \end{pmatrix} = \lambda \begin{bmatrix} 0 & 0 & 0 \\ 0 & 0 & 0 \\ 0 & 0 & M_{33} \end{bmatrix} \begin{pmatrix} R_{ij} \\ S_{kl} \\ P_{mn} \end{pmatrix} \tag{3.17}$$

Eliminating R_{ij} and S_{kl} we get the following condensed set of equations

$$([K_{33}]' - \lambda[M_{33}])\{P_{mn}\} = 0 \tag{3.18}$$

The resulting condensed set of equations are solved for the eigenvalues using IMSL subroutine DEVCRG and mode shapes obtained from the corresponding eigenvectors. It is noted that since the inplane inertias are neglected in this study, no further approximations result using this condensation. The transformed coordinate system facilitates the use of Gaussian quadrature to evaluate the integrals. Both ten and sixteen Gauss points are used depending upon the order of the polynomials to be integrated.

The deflections under static, transverse loading can also be determined. Using the proper energy functionals corresponding to a uniformly distributed force or moment would result in a set of linear algebraic equations

$$[K]\{q\} = \{F\} \tag{3.19}$$

where $\{F\}$ is the load vector. Thus the polynomial coefficients of Eq. 3.12, rather than the eigenvalue determinant of Eq. 3.18, can be determined using Eq. 3.19. These equations are solved using IMSL subroutine DLSLRG.

3.4 Sensitivity Analysis

The derivatives of the stiffness and mass matrices with respect to the shape parameters are computed analytically and also by the finite difference method. The stiffness matrix for the plate alone i.e. excluding the springs is

$$[K] = \int_{-1}^{1}\int_{-1}^{1} [B]^T[T]^T \begin{bmatrix} A & B \\ B & D \end{bmatrix} [T]\,[B]|J|\mathrm{d}\eta\mathrm{d}\xi \tag{3.20}$$

where $[B]$ is the matrix whose elements consist of the partial derivatives of the Chebyshev polynomials with respect to the natural coordinates η and ξ and is defined by

$$\begin{pmatrix} \epsilon' \\ \kappa' \end{pmatrix} = [B]\{q\} \tag{3.21}$$

Now, in Eq. 3.20, only the matrix $[T]$ and the Jacobian $|J|$, both of which are related to the co-ordinate transformation from the (x, y) to the (η, ξ) systems, are dependent upon the shape parameter ν. Applying the chain rule of differentiation to Eq. 3.20, we get

$$\frac{\partial[K]}{\partial\nu} = \int_{-1}^{1}\int_{-1}^{1}\{\,[B]^T\left[\frac{\partial T}{\partial\nu}\right]^T\begin{bmatrix}A & B\\ B & D\end{bmatrix}[T][B]|J| + [B]^T[T]^T\begin{bmatrix}A & B\\ B & D\end{bmatrix}\left[\frac{\partial T}{\partial\nu}\right][B]|J| + [B]^T[T]^T\begin{bmatrix}A & B\\ B & D\end{bmatrix}[T][B]\frac{\partial|J|}{\partial\nu}\,\}\mathrm{d}\eta\mathrm{d}\xi \tag{3.22}$$

The mass matrix is dependent upon the shape parameters only through the Jacobian $|J|$. A typical element of the mass matrix of order n would be

$$M_{ij} = \int_{-1}^{1}\int_{-1}^{1} T_k(\eta)T_l(\xi)T_o(\eta)T_p(\xi)|J|\mathrm{d}\eta\mathrm{d}\xi \tag{3.23}$$

where

$$\begin{aligned} k &= 0,1,2...K\\ l &= 0,1,2...L\\ o &= 0,1,2...K\\ p &= 0,1,2...L \end{aligned} \tag{3.24}$$

and

$$(K+1)(L+1) = n \tag{3.25}$$

Thus, the partial derivative of a typical element of the mass matrix with respect to the shape parameters is

$$\frac{\partial M_{ij}}{\partial\nu} = \int_{-1}^{1}\int_{-1}^{1} T_k(\eta)T_l(\xi)T_o(\eta)T_p(\xi)\frac{\partial|J|}{\partial\nu}\mathrm{d}\eta\mathrm{d}\xi \tag{3.26}$$

The derivatives of the spring energy terms with respect to the shape parameters are straightforward and will not be discussed in detail. The sensitivity of the ith eigenvalue λ_i and the ith eigenvector $\{\phi_i\}$ with respect to various shape parameters

(area, aspect ratio, taper ratio and sweep angle) is determined both analytically as well as by the finite difference (central-difference) method. The analytical formulation is explained in detail in the following sections.

3.4.1 Eigenvalue Sensitivities

The self-adjoint eigenvalue problem for undamped systems in structural dynamics is given by

$$[K]\{\phi_i\} = \lambda_i[M]\{\phi_i\} \tag{3.27}$$

where the scalar quantities λ_i (eigenvalues) and the corresponding nontrivial vectors $\{\phi_i\}$ are to be determined. In the common structural application, the n x n matrices $[K]$ and $[M]$ are, respectively, the stiffness and mass matrices of the actual structure. Their order n corresponds to the number of elastic degrees of freedom of the system. Consider a change in the design variable ν, which may be a combination of elements of $[K]$ and $[M]$ (corresponding to the realistic physical context where it is not, in general, possible to make a modification of stiffness that has no implications for the mass distribution and vice versa). As given by Wang [1991], the eigenvalue derivative is

$$\frac{\partial \lambda_i}{\partial \nu} = \{\phi_i\}^T \left(\frac{\partial [K]}{\partial \nu} - \frac{\partial [M]}{\partial \nu} \lambda_i \right) \{\phi_i\} \tag{3.28}$$

Here $\{\phi_i\}$, the ith eigenvector, is normalized with respect to the mass matrix such that

$$\{\phi_i\}^T [M] \{\phi_i\} = 1 \tag{3.29}$$

Note that the expression of Eq. 3.28 involves only the eigenvalue and eigenvector under consideration, and thus a complete solution of the eigenproblem is not needed to obtain these derivatives.

3.4.2 Eigenvector Sensitivities

As given by Fox and Kapoor [1968], the eigenvector derivative is

$$\frac{\partial\{\phi_i\}}{\partial\nu} = \sum_{j=1}^{n} \alpha_{ij}\{\phi_j\} \tag{3.30}$$

where

$$\alpha_{ij} = \frac{\{\phi_j\}^T \left(\frac{\partial[K]}{\partial\nu} - \lambda_i \frac{\partial[M]}{\partial\nu}\right)\{\phi_i\}}{(\lambda_i - \lambda_j)} \qquad j \neq i \tag{3.31}$$

and

$$\alpha_{ii} = -1/2 \left(\{\phi_i\}^T \frac{\partial[M]}{\partial\nu}\{\phi_i\}\right) \tag{3.32}$$

Since the denominator of Eq. 3.31 contains the term $(\lambda_i - \lambda_j)$, the eigenvector sensitivity cannot be computed for modes with coincident natural frequencies.

3.4.3 Approximation of Frequencies

As given by Pritchard and Adelman [1991], the equation for the derivative of the ith vibration eigenvalue λ_i with respect to a design variable ν can also be written as

$$\frac{\mathrm{d}\lambda_i}{\mathrm{d}\nu} = b - a\lambda_i \tag{3.33}$$

where

$$a = \{\phi_i\}^T \frac{\partial[M]}{\partial\nu}\{\phi_i\} \tag{3.34}$$

and

$$b = \{\phi_i\}^T \frac{\partial[K]}{\partial \nu} \{\phi_i\} \tag{3.35}$$

Here, the eigenvector is normalized as in Eq. 3.29.

Eq. 3.33 may be interpreted as a first-order differential equation in λ_i with variable coefficients. However if a and b do not vary extensively with ν, then they may be evaluated at the nominal design and considered constant. After applying the nominal condition that $\lambda = \lambda_0$ when $\nu = \nu_0$, the general solution to Eq. 3.33, provided a is nonzero, is

$$\lambda_i = (\lambda_{i0} - b/a)\, e^{-a(\nu - \nu_0)} + b/a \tag{3.36}$$

For the case where $a = 0$, the method produces the linear Taylor series approximation. The exponential term can be approximated by expanding it upto three terms and neglecting higher order terms as shown

$$e^x = 1 + \frac{x}{1!} + \frac{x^2}{2!} \tag{3.37}$$

Later, it is seen that this approximation is sufficiently accurate.

3.4.4 Approximation of Mode Shapes

As given by Pritchard and Adelman [1991], the equation for the derivative of the mode shape $\{\phi_i\}$, with respect to a design variable can also be written as

$$\frac{\mathrm{d}\{\phi_i\}}{\mathrm{d}\nu} = \{Q\} + D\{\phi_i\} \tag{3.38}$$

where the vector $\{Q\}$ and the scalar D can be determined by comparing Eq. 3.30 with Eq. 3.38. On doing so, it is apparent that

$$D = \alpha_{ii} \tag{3.39}$$

and

$$\{Q\} = \sum_{j=1}^{n} \alpha_{ij}\{\phi_j\} \qquad j \neq i \tag{3.40}$$

Eq. 3.38 is a nonlinear first-order vector differential equation with variable coefficients. In order to solve this equation, D and $\{Q\}$ are evaluated at the nominal design and held constant. After applying the nominal condition that $\{\phi_i\} = \{\phi_i\}_0$ when $\nu = \nu_0$, the solution to Eq. 3.38 is

$$\{\phi_i\} = \left(\{\phi_i\}_0 + \frac{1}{D}\{Q\}\right) e^{D(\nu-\nu_0)} - \frac{1}{D}\{Q\} \tag{3.41}$$

Eq. 3.41 is a vector equation; it is uncoupled in the sense that each component of $\{\phi_i\}$ varies independently with the design variable ν. The difference between components is reflected in the corresponding components of $\{\phi_i\}_0$ and $\{Q\}$. Note that the exponential expansion of Eq. 3.37 may be applied to Eq. 3.41 also. Also, note that Eq. 3.41 is invalid for the case when $D = 0$, i.e. when the mass matrix is independent of the particular parameter under consideration.

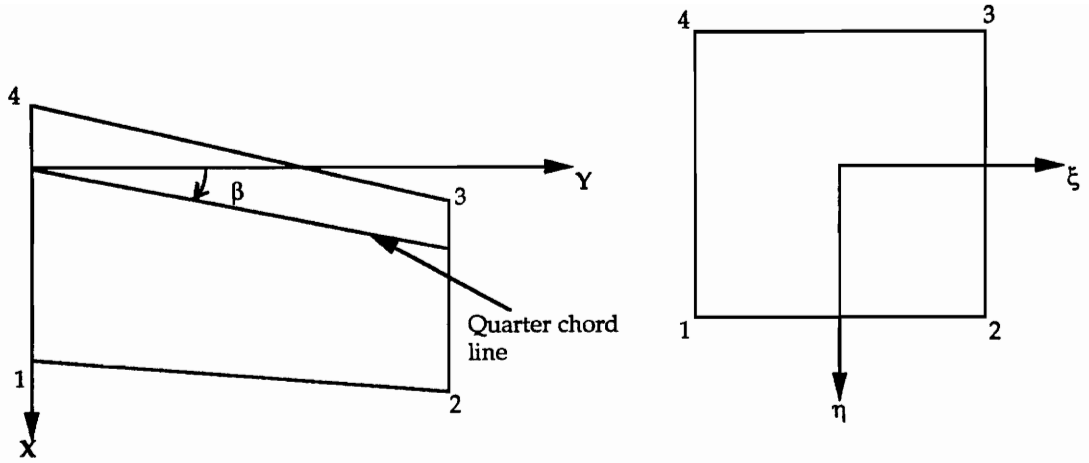

Fig. 3.1. The Original and Transformed Co-ordinate Systems for Skew Plates.

4. Results

4.0 Overview

The method developed in the previous chapter has the capability of handling free vibration and static analyses for various possible combinations of the geometric boundary conditions of generally laminated skew plates. Convergence studies are first performed in order to establish the optimum number of terms to be used in the deflection function. The effect of the spring constants on the vibration frequencies is also studied before deciding on an acceptable value to be used consistently for all the remaining results. Numerical results obtained for various lamination sequences and plate geometries are compared with those found in the literature. Some new results are also presented. Finally, an extensive sensitivity analysis of the free vibration response is performed. All numerical results are computed on the IBM 3090 supercomputer. An important point to be noted is that the aspect ratio is defined as (span^2/area) and *not* as (span/root chord) as may be found in some studies.

4.1 Static Analysis

Initially, the static analysis of a 6 in by 3 in, 0.08 in thick, $[0/90]_{4s}$, specially orthotropic rectangular plate subjected to a uniform moment per unit length M_x of 10 in-lb/in is performed. Three of the edges are simply supported while one of the 6 in edges is free as shown in Fig. 4.1. The deflection of the free edge is determined and compared satisfactorily with that obtained by a finite element code developed by Kapania and Yang [1987] as shown in Table 4.1. The material properties used

Table 4.1. Displacement (in) along the free edge of rectangular plate described in Fig. 4.1 using 2nd, 6th and 8th order Chebyshev polynomials.

x	FEM	2nd Order	6th Order	8th Order
-1.5	0.00000	0.00000	0.00000	0.00000
0.0	0.07262	0.07609	0.07263	0.07263
1.5	0.09677	0.10145	0.09679	0.09680
3.0	0.07262	0.07609	0.07263	0.07263
4.5	0.00000	0.00000	0.00000	0.00000

are: E_1 = 18.5 x 10^6 psi (128 GPa); E_2 = 1.64 x 10^6 psi (11.275 GPa); G_{12} = 0.87 x 10^6 psi (5.99 GPa) and $\nu_{12} = 0.30$.

4.2 Free Vibration Analyses

The free vibration analyses of isotropic, symmetrically laminated and unsymmetrically laminated plates are next considered. Initially, rectangular plates are analysed before progressing to tapered, skew plates. Mode shapes are plotted for representative cases and the frequencies are compared, whenever possible, with those obtained by other researchers. Unless otherwise mentioned, the results presented in the following sections are for cantilever plates. A point to be noted is that as the Rayleigh-Ritz method is being used in this study, all the results obtained are upper bounds to the exact values.

4.2.1 Effect of Spring Stiffness on Convergence Analysis

First, an analysis is performed to study the convergence of the natural frequencies, for various spring stiffnesses, as the number of terms in the polynomial series for the transverse displacement is increased. An isotropic plate, swept back 15 degrees at the quarter chord point, is considered for illustration purposes. It is seen from Figs. [4.2-4.4] that the four lowest natural frequency parameters all converge when upto

eighth order Chebyshev polynomials are used in the displacement function series. In addition, it is observed that the frequency parameters converge to approximately the same value when spring stiffnesses of different orders of magnitude are used. In order to preserve consistency, the spring stiffnesses used to obtain all subsequent results in this study have the non-dimensionalized value of 10^5. The actual numerical values depicting the convergence history of the first five natural frequencies of vibration of the isotropic rhombic plate are also shown in Table 4.2. In the present study, to ensure that satisfactorily converged results are obtained, ninth order Chebyshev polynomials are used throughout.

Table 4.2. Convergence analysis of five lowest frequency parameters of an isotropic rhombic cantilever plate with a skew angle of 15 deg.

Degree of Polynomial	Mode 1	Mode 2	Mode 3	Mode 4	Mode 5
3	0.369	0.932	3.027	3.645	5.159
4	0.364	0.891	2.287	2.725	3.566
5	0.363	0.883	2.272	2.693	3.481
6	0.363	0.882	2.254	2.669	3.435
7	0.363	0.881	2.253	2.668	3.432
8	0.363	0.881	2.253	2.668	3.432

4.2.2 Isotropic Rhombic Plate

Next, the influence of the skew angle on the free vibration of an isotropic rhombic plate is studied. The non-dimensional frequency parameter

$$\sqrt{\lambda'} = (\omega a^2/\pi^2)\sqrt{\rho h/D}$$

is computed. Here the flexural rigidity $D = Eh^3/(1-\nu^2)$, ω is the natural frequency of vibration of the plate, a the length of an edge of the plate, h the thickness of the

plate and ρ and E the mass density per unit area and Young's modulus of elasticity of the material, respectively. A Poisson's ratio of $\nu = 0.3$ has been used in the calculations. The results compare very well with those obtained by Liew and Lam [1990], who used orthogonal polynomials in the Rayleigh-Ritz method, as shown in Table 4.3. It is noted that these orthogonal polynomials were developed using Gram-Schmidt orthogonalization technique. The present method avoids using such a technique. We see that as the skew angle increases the frequency parameter also increases. This is expected since, when the skew angle increases, it reduces the flexibility of the plate in the y direction. The nodal patterns of modes 2, 3, 4 and 5 for rhombic plates with a skew angle of 15 degrees are shown in Fig. 4.5. The symmetry and antisymmetry of the modes about the longer diagonal of the rhombic plate can be seen from the nodal patterns.

4.2.3 Symmetrically Laminated Plate

The program is then tested for symmetrically laminated plates. Since mid-plane symmetrically laminated plates do not have any coupling between bending and stretching (all B_{ij} are zero), this simplifies the problem. Table 4.4 shows the five lowest frequencies of vibration of both square and rectangular plates for various stacking sequences. The results compare well with those obtained by Baharlou and Leissa [1987] who used the Ritz method, Crawley and Dugundji [1980] who used an 8 node general quadrilateral shallow shell finite element (RS40) and Crawley [1979] who determined the frequencies both experimentally and by the FEM (RS40). The three different laminate configurations considered are the $[0_2/\pm 30]_s$ (bending stiff), $[0/\pm 45/90]_s$ (quasi-isotropic) and $[\pm 45/\mp 45]_s$ (torsionally stiff). The nominal ply thickness is 0.0052 in (0.13 mm). It is noted that the modal ranking can be changed by choice of laminate. The material properties of the Hercules AS1/3501-6

Table 4.3. Four lowest frequency parameters of an isotropic rhombic cantilever plate for various sweep angles.

Skew Angle (Degrees)	Liew and Lam [1990]	Present Study
0.0	0.35	0.35
	0.86	0.86
	2.17	2.16
	2.77	2.76
15.0	0.36	0.36
	0.88	0.88
	2.25	2.25
	2.64	2.63
30.0	0.40	0.40
	0.96	0.95
	2.54	2.56
	2.64	2.63
45.0	0.47	0.46
	1.14	1.14
	2.76	2.75
	3.22	3.21

graphite/epoxy used are as follows: E_1 = 18.5 x 10^6 psi (128 GPa); E_2 = 1.6 x 10^6 psi (11 GPa); G_{12} = 0.65 x 10^6 psi (4.48 GPa); ν_{12} = 0.25 and density = 0.055 lb/in^3 (1500 Kg/m ^{3}).

Next, the effect of the taper ratio on the free vibration frequencies of a symmetrically laminated rectangular plate is studied as shown in Table 4.5. Wherever possible the results are compared with those obtained by Jensen and Crawley [1984] who used the FEM (RS40). It is seen that as the taper ratio increases, the frequencies decrease. The material properties of the Hercules AS1/3501-6 graphite/epoxy used are: E_1 = 98.0 GPa; E_2 = 7.9 GPa; G_{12} = 5.6 GPa; ν_{12} = 0.28 and density = 1520 Kg/m^3.

Table 4.4. Five lowest frequencies (Hz) of eight-ply (0.0416 in thick) symmetrically laminated graphite/epoxy cantilever plates.

Stacking Sequence	Plate Dimensions	Crawley [1979] (Observed)	Baharlou and Leissa [1987]	Crawley and Dugundji [1980]	Present Study
$[0_2/\pm 30]_s$	3 in by 3 in	234.2	262.10	261.90	262.89
		362.0	363.70	363.50	365.79
		728.3	771.40	761.80	765.58
		1449.0	1642.00	1662.00	1613.16
		1503.0	1653.00	1709.00	1645.93
$[0_2/\pm 30]_s$	6 in by 3 in	58.3	65.39	65.37	65.62
		148.0	137.90	137.50	138.38
		362.7	408.70	408.30	410.05
		508.0	527.10	525.60	528.49
		546.0	589.40	588.30	586.23
$[0/\pm 45/90]_s$	3 in by 3 in	196.4	-	224.30	225.14
		418.0	-	421.80	425.63
		960.0	-	1012.00	1020.21
		1215.0	-	1426.00	1418.18
		1550.0	-	1722.00	1721.59
$[\pm 45/\mp 45]_s$	3 in by 3 in	131.2	-	138.90	139.98
		472.0	-	499.50	505.39
		790.5	-	805.00	808.92
		1168.0	-	1326.00	1332.61
		1486.0	-	1648.00	1657.51
$[0/\pm 45/90]_s$	6 in by 3 in	48.6	-	55.58	55.83
		169.0	-	175.40	176.92
		303.0	-	345.30	347.05
		554.0	-	591.80	597.29
		739.0	-	820.10	817.65
$[\pm 45/\mp 45]_s$	6 in by 3 in	31.3	-	31.90	32.43
		185.8	-	191.30	194.06
		214.0	-	228.20	231.36
		533.0	-	565.30	571.60
		653.0	-	708.30	716.96

Table 4.5. Variation with taper ratio of the five lowest frequencies (Hz) of a six ply (305 mm by 76.25 mm) symmetrically laminated $[30_2/0]_s$ graphite/epoxy cantilevered plate of thickness 0.804 mm.

Taper Ratio	Jenson and Crawley [1984]	Present Study
	6.30	6.27
	37.30	36.51
1.00	56.90	56.72
	-	97.38
	-	170.44
	-	7.04
	-	38.95
0.75	-	63.49
	-	101.18
	-	177.79
	-	8.21
	-	42.26
0.50	-	72.86
	-	106.83
	-	182.33

The nodal lines (lines of zero displacement) corresponding to the 2nd, 3rd, 4th and 5th modes of vibration are of a $[0_2/\pm 30]_s$ rectangular glass/epoxy panel of aspect ratio 2 are shown in Fig. 4.6. The mode shapes corresponding to the 2nd and 3rd modes are either pure torsion or highly coupled to bending. The area of the plate is 63.0 in^2. The thickness of each layer is 0.02333 in. The material properties of the glass/epoxy material are as follows: $E_1 = 5.6$ x 10^6 psi (38.61 GPa); $E_2 = 1.2$ x 10^6 psi (8.27 GPa); $G_{12} = 0.6$ x 10^6 psi (4.14 GPa); $\nu_{12} = 0.26$ and density = 0.092 lb/in^3 (2546.54 Kg/m^3).

4.2.4 Unsymmetrically Laminated Plate

Next the case of unsymmetrically laminated unswept plates is studied. The six lowest frequencies of plates of increasing asymmetry are compared with those obtained by Thornton [1977], who used a coupled rectangular plate bending element incorporated into NASTRAN for his analysis. The results are shown in Table 4.6. Of course, inplane stretching effects are most important for plates having only two plies. In general, the frequencies decrease as the asymmetry increases, though there are notable exceptions e.g. the third mode. This is further illustrated in Figs. [4.8-4.10] for the three lowest frequencies of a square $[0/\theta]_T$ laminate of area 64.0 in^2, with θ ranging from 0 to 90. The maximum reduction in frequency occurred in the first mode. Nodal lines for modes 2, 3, 4 and 5 are plotted (Fig. 4.7) for the [0/22.5] case. The material properties of the boron/epoxy used are: E_1 = 23.3 x 10^6 psi (161.21 GPa); E_2 = 1.81 x 10^6 psi (12.52 GPa); G_{12} = 0.976 x 10^6 psi (6.75 GPa); ν_{12} = 0.22 and density = 0.069 lb/in^3 (1881.81 Kg/m^3).

4.2.5 Symmetrically Laminated Tapered Skew Plates

Next, some results are obtained for symmetrically laminated skew plates. The three lowest frequencies of a six ply glass/epoxy $[\theta_2/0]_s$ symmetrically laminated swept wing panel are shown in Table 4.7. For an unswept plate the fiber angle θ is measured counterclockwise from the positive y axis. As the wing is swept, the fiber angle is also rotated correspondingly. As the angle of the outer plies increases from (0-90) degrees, the lowest mode, which can always be characterized as 1st bending, decreases monotonically due to the decrease in spanwise stiffness. The effect of ply orientation is more pronounced on the natural frequencies corresponding to the three lowest modes. This is attributed to the bending-torsion coupling present in the laminate. This is further illustrated in Figs. [4.11-4.13] for a 30 degree swept

Table 4.6. Six lowest frequencies (Hz) of two-ply (8 in by 8 in) unsymmetrically laminated boron/epoxy cantilevered plates.

Thickness of Panel (in.)	Stacking Sequence	Thornton [1977]	Present Study
0.0492	$[0/22.5]_T$	34.4	34.26
		56.1	56.34
		119.0	123.40
		214.0	216.17
		235.0	246.57
		253.0	263.48
0.0460	$[0/45.0]_T$	24.3	24.16
		24.3	24.16
		48.5	48.61
		118.0	121.89
		151.0	152.25
		193.0	195.69
		242.0	255.83
0.0470	$[0/67.5]_T$	21.8	21.69
		43.4	43.59
		130.0	132.86
		138.0	139.63
		177.0	180.19
		254.0	267.15

wing panel of aspect ratio 3.111, taper ratio 0.5, area 63 in^2 and thickness 0.14 in. The results compare well with those obtained experimentally and by a TRIPLT finite element by Lakshminarayana *et al.* [1985]. They also agree satisfactorily with the frequencies obtained by Lee and Lee [1990] who used a four-node quadrilateral element. Note that the 1st torsional frequency is approximately equal for $\theta = 0$ and $\theta = 90$ as would be expected from CLT.

Next, some new results are generated. The five lowest frequencies of vibration of a

Table 4.7. Natural frequencies (Hz) of a symmetrically laminated glass/epoxy swept ($\beta = 30$) panel of thickness 0.14 in, aspect ratio 3.111, taper ratio 0.5 and area 63 in^2.

Stacking Sequence	Mode No.	Lee and Lee [1990] [F.E.M.]	Lakshminarayana *et al.* [1985] [F.E.M]	Lakshminarayana *et al.* [1985] [Observed]	Present Study
$[0_2/0]_s$	1	16.80	16.67	17.55	17.30
	2	81.03	80.40	83.80	84.44
	3	100.08	99.52	98.65	98.29
$[15_2/0]_s$	1	16.00	15.90	15.70	16.96
	2	75.08	73.50	73.60	77.28
	3	111.98	114.56	108.15	111.40
$[30_2/0]_s$	1	13.18	13.15	13.90	13.94
	2	67.61	66.67	65.70	69.65
	3	116.65	120.86	110.80	116.59
$[45_2/0]_s$	1	10.45	11.05	11.05	11.48
	2	59.01	59.13	57.01	60.13
	3	112.55	117.37	116.10	114.46
$[60_2/0]_s$	1	9.33	9.82	10.10	10.04
	2	52.98	53.50	52.75	53.48
	3	100.65	105.60	105.25	103.36
$[75_2/0]_s$	1	9.24	9.16	9.60	9.31
	2	52.98	49.84	50.30	49.78
	3	88.99	93.38	91.35	90.79
$[90_2/0]_s$	1	8.60	8.82	8.45	9.00
	2	47.43	47.41	45.45	48.01
	3	82.64	86.58	89.15	83.25

symmetrically laminated $[30_2/0]_s$ skew cantilevered glass/epoxy plate of fixed taper ratio and area are shown in Table 4.8 for various quarter chord sweep angles and aspect ratios. It is seen that as the aspect ratio or the absolute value of the sweep angle is increased, in general the frequencies decrease. The material properties of

Table 4.8. Five lowest natural frequencies (Hz) of a symmetrically laminated glass/epoxy skew cantilevered plate of thickness 0.14 in, area 63 in^2 and taper ratio 0.5 for various values of sweep.

	Sweep in Degrees						
Aspect Ratio	-45	-30	-15	0	15	30	45
	24.55	34.37	44.13	53.36	59.42	58.86	47.30
	102.55	123.02	130.55	131.41	129.29	122.64	108.78
1.0	156.13	189.31	235.46	281.33	296.06	284.42	259.31
	255.23	322.66	360.12	356.54	357.68	353.91	299.90
	408.53	434.13	398.32	408.59	437.44	462.66	433.82
	7.42	10.98	14.01	16.01	16.19	13.94	9.52
	40.17	59.48	75.76	83.23	80.38	69.65	49.83
3.111111	103.51	106.43	107.98	113.05	118.34	116.59	109.00
	109.78	160.59	204.80	221.29	210.12	181.59	133.54
	209.03	270.80	280.28	300.27	314.71	294.88	239.86
	4.55	6.78	8.60	9.62	9.44	7.89	5.33
	24.77	36.88	46.70	51.89	50.55	42.35	28.87
5.0	66.57	99.29	103.69	104.67	105.21	103.06	76.79
	102.24	103.07	126.15	139.85	135.89	115.60	104.11
	130.17	194.01	245.96	260.66	252.11	216.28	152.34

the glass/epoxy used are: E_1 = 5.6 x 10^6 psi (38.61 GPa); E_2 = 1.2 x 10^6 psi (8.27 GPa); G_{12} = 0.6 x 10^6 psi (4.14 GPa); ν_{12} = 0.26 and density = 0.092 lb/in^3 (2546.54 Kg/m^3).

The effect of the sweep angle on the first four natural frequencies of a $[30_2/0]_s$ skew plate of taper ratio 0.75 is illustrated for various aspect ratios in Figs. [4.14-4.19]. The area of the plate is 23256.25 mm^2 and its thickness is 0.804 mm. It is observed that the frequencies reach a peak somewhere near the unswept configuration and decrease for both forward as well as backward sweep angles. The material properties of the Hercules AS1/3501-6 graphite/epoxy used are: E_1 = 98.0 GPa; E_2 = 7.9 GPa; G_{12} = 5.6 GPa; ν_{12} = 0.28 and density = 1520 Kg/m^3.

4.2.6 Unysmmetrically Laminated Tapered Skew Plate

The five lowest frequencies of vibration of an unsymmetrically laminated skew cantilever boron/epoxy plate of constant taper ratio and area are shown in Table 4.9 for various quarter chord sweep angles.

Table 4.9. Five lowest frequencies (Hz) of an unsymmetrically laminated $[0/22.5]_T$ boron/epoxy skew cantilevered plate of thickness 0.0492 in, area 64 in^2 and taper ratio 1.0 for various values of sweep.

	Sweep in Degrees						
Aspect ratio	-45	-30	-15	0	15	30	45
	16.94	24.78	31.09	34.26	28.57	33.45	20.42
	47.75	52.27	55.17	56.34	51.34	55.18	45.09
1.0	105.04	137.48	129.82	123.40	121.36	120.71	115.75
	142.07	157.75	194.89	216.17	185.06	212.78	144.76
	207.27	204.49	229.00	246.57	239.73	246.32	219.94

Table 4.10 demonstrates the variation of the natural frequencies with aspect ratio and sweep angle for a boron/epoxy plate of taper ratio 0.75 and stacking sequence $[0/22.5]_T$ and $[0/-22.5]_T$ (given in parantheses). Here too it is seen that as the aspect ratio or the absolute value of the sweep angle is increased, in general the frequencies decrease.

The effect of the sweep angle on the five lowest frequencies of a $[0/\theta]_T$ skew laminate of taper ratio 0.75 and aspect ratio 3.0 is depicted in Figs. [4.20-4.24] for both positive as well as negative fiber angle θ. The two obvious trends illustrated in these graphs are: i) the curves for negative and positive fiber angles are almost mirror images of each other and ii) the frequencies reach a maximum near the $\theta = 0$ point and taper off on either side. The area of the plate is 64 in^2 and its thickness is 0.0492 in. The material properties of the boron/epoxy used are: $E_1 = 23.3 \times 10^6$

Table 4.10. Five lowest frequencies (Hz) of an unsymmetrically laminated $[0/22.5]_T$ boron/epoxy skew cantilevered plate of thickness 0.0492 in, area 64 in^2 and taper ratio 0.75 for various values of sweep.

Aspect ratio	-45	-30	-15	0	15	30	45
	18.19	26.77	33.91	38.03	38.28	34.18	25.41
	(22.14)	(30.87)	(35.82)	(36.52)	(33.23)	(26.81)	(18.79)
	54.24	60.28	64.65	67.20	66.64	61.82	53.06
	(50.62)	(58.26)	(63.25)	(65.21)	(64.78)	(62.55)	(57.45)
1.0	107.47	149.09	151.71	145.42	142.16	141.53	138.39
	(128.83)	(138.06)	(139.95)	(144.64)	(152.48)	(150.09)	(109.58)
	152.15	170.77	202.45	227.30	231.09	210.35	161.55
	(149.80)	(195.52)	(222.06)	(222.59)	(200.50)	(175.11)	(162.96)
	234.14	220.05	241.28	260.77	263.26	252.34	241.51
	(229.32)	(249.15)	(257.19)	(256.18)	(238.99)	(215.43)	(224.05)
	5.84	8.75	11.08	12.26	11.92	9.99	6.82
	(6.38)	(9.38)	(11.33)	(11.84)	(10.88)	(8.74)	(5.92)
	33.98	46.28	46.84	46.38	44.61	41.11	33.95
	(32.51)	(40.24)	(44.13)	(46.37)	(47.34)	(47.19)	(34.59)
3.0	45.28	51.36	65.94	74.53	74.81	66.34	53.05
	(52.63)	(64.78)	(73.31)	(73.63)	(65.71)	(51.63)	(46.10)
	93.16	135.58	141.15	140.61	132.06	115.84	90.90
	(86.69)	(111.23)	(127.43)	(137.44)	(140.66)	(137.43)	(95.03)
	128.74	142.00	183.04	208.14	210.92	190.18	151.87
	(148.66)	(185.99)	(208.45)	(207.54)	(183.99)	(143.54)	(130.95)
	3.46	5.19	6.55	7.18	6.88	5.67	3.82
	(3.66)	(5.43)	(6.64)	(6.99)	(6.46)	(5.19)	(3.49)
	20.34	30.56	37.73	38.99	36.63	31.07	21.79
	(20.93)	(29.90)	(35.56)	(38.11)	(37.07)	(30.49)	(20.54)
5.0	43.06	43.67	45.19	48.20	48.94	46.87	44.27
	(44.67)	(47.34)	(49.45)	(48.98)	(46.27)	(44.49)	(43.61)
	55.95	84.31	104.39	108.20	100.54	84.15	59.15
	(56.83)	(80.89)	(97.10)	(105.12)	(102.43)	(84.19)	(56.52)
	109.53	123.47	129.72	138.88	141.46	134.27	113.75
	(109.78)	(134.83)	(142.79)	(141.27)	(132.64)	(125.67)	(110.72)

psi (161.21 GPa); E_2 = 1.81 x 10^6 psi (12.52 GPa); G_{12} = 0.976 x 10^6 psi (6.75 GPa); ν_{12} = 0.22 and density = 0.069 lb/in^3 (1881.81 Kg/m^3).

4.3 Shape Sensitivity Results

Derivatives of the mass and stiffness matrices, eigenvalues and eigenvectors are computed using three different step-sizes in the central-difference method. These are compared with those obtained analytically. Approximations to the frequencies and mode shapes are implemented and tested. Both symmetric $[0/25/25/0]_T$ as well as unsymmetric $[0/25]_T$ laminate configurations are treated. The test cases involve perturbations of the surface area, aspect ratio, taper ratio and sweep angle. A laminated cantilevered plate is the subject of this study. The thickness of each lamina is 0.0246 in (0.00062484 m). The nominal surface area of the plate is 64 in^2 (0.0412902 m^2) with a nominal taper ratio (root chord/tip chord) of 0.75. The nominal aspect ratio, defined as (span^2/area) and not as (span/root chord), is taken to be 3. The plate is swept back at an angle of 15 degrees at the quarter chord point. As per the standard convention, the fibers are assumed to be swept along with the plate. The material properties of the boron/epoxy used are: E_1 = 23.3 x 10^6 psi (161.21 GPa); E_2 = 1.81 x 10^6 psi (12.52 GPa); G_{12}= 0.976 x 10^6 psi (6.75 GPa); ν_{12} = 0.22; density = 0.069 lb/in^3 (1881.81 Kg/m^3).

4.3.1 Derivatives of Stiffness and Mass Matrices

As a ninth order Chebyshev polynomial is used in the displacement function to ensure stable convergence of the eigenvalues, this translates into mass and stiffness matrices of size 100 x 100. As it is not possible to present the derivatives of all the elements of these matrices, only a few representative non-zero values are shown. The accuracy of the remaining values is of the same order. The values of the

corresponding elements of the stiffness and mass matrices at the nominal design are also shown to give a better persective on the derivatives.

Table 4.11 compares the analytical and finite difference derivatives of some representative terms of the condensed stiffness matrix with respect to the four shape parameters. Both symmetric as well as unsymmetric stacking sequences are considered. Step-sizes of 0.01%, 0.1% and 1.0% are chosen in the central-difference method. This means that the shape variable is perturbed by $\pm 0.005\%$, $\pm 0.05\%$ and $\pm 0.5\%$ respectively, from the nominal value. There is good agreement between the values obtained using the two methods as well as among the results obtained by using different stepsizes. Other than that, no conclusive trend in the results is obvious. Some of the elements decrease and others increase in value due to the same perturbation.

A similar comparison is made of the derivatives of some representative terms of the mass matrix with respect to the area and taper ratio for a symmetric laminate. As can be seen in Table 4.12, the same step-sizes are chosen as those taken for the stiffness matrix. It must be noted that the derivative of the mass matrix with respect to the aspect ratio or sweep angle is identically zero as the mass matrix is a function of the shape parameters only through the Jacobian, which is independent of both the aspect ratio as well as the sweep angle. Here, too, it is seen that the agreement between the finite difference and analytical methods is acceptable. Also, in general there is better agreement between the values obtained using a step-size of 0.1% and 1.0% than there is between these values and those obtained with a step-size of 0.01%. This may mean that the mass matrix is too sensitive to very small perturbations.

Table 4.11. Comparison of analytical and central difference shape sensitivities of some representative elements of the stiffness matrix for both symmetric and unsymmetric laminates.

	Central Difference			
Nominal Value	0.01%	0.1%	1.0%	Analytical
Area $[0/25]_s$				
0.52786e+06	0.41250e+04	0.41234e+04	0.41239e+04	0.41231e+04
-0.17595e+06	-0.13750e+04	-0.13734e+04	-0.13747e+04	-0.13741e+04
-0.35191e+05	-0.27500e+03	-0.27500e+03	-0.27494e+03	-0.27498e+03
-0.15082e+05	-0.11719e+03	-0.11781e+03	-0.11783e+03	-0.11765e+03
Taper Ratio $[0/25]_s$				
0.52786e+06	-0.30133e+06	-0.30173e+06	-0.30164e+06	-0.30148e+06
-0.17595e+06	0.10000e+06	0.10053e+06	0.10055e+06	0.10059e+06
-0.35191e+05	0.20133e+05	0.20107e+05	0.20109e+05	0.20125e+05
-0.15082e+05	0.86667e+04	0.86267e+04	0.86173e+04	0.86457e+04
Aspect Ratio $[0/25]_T$				
0.52786e+06	-0.88000e+05	-0.88000e+05	-0.87980e+05	-0.87996e+05
-0.17595e+06	0.29333e+05	0.29333e+05	0.29327e+05	0.29331e+05
-0.35191e+05	0.58667e+04	0.58667e+04	0.58653e+04	0.58662e+04
-0.15082e+05	0.25000e+04	0.25133e+04	0.25137e+04	0.25004e+04
Sweep $[0/25]_T$				
-0.70477e+04	-0.54000e+03	-0.54000e+03	-0.54000e+03	-0.54041e+03
0.28188e+05	0.21600e+04	0.21600e+04	0.21598e+04	0.21612e+04
-0.28212e+05	-0.21667e+04	-0.21620e+04	-0.21618e+04	-0.21645e+04
-0.40824e+05	0.13333e+02	0.18000e+02	0.17933e+02	0.16523e+02

4.3.2 Derivatives of Eigenvalues and Eigenvectors

Table 4.13 compares the analytical and finite difference first order sensitivities of the first four eigenvalues $\lambda = \omega^2$ where ω is the natural frequency in rad/sec. Once again, in general greater consistency is observed between values obtained for step-sizes of 0.1% and 1.0% than for one of 0.01%. The analytical derivatives are found to be in satisfactory agreement with the central-difference ones. It is not possible to

Table 4.12. Comparison of analytical and central difference shape sensitivities of some representative elements of the mass matrix for a symmetric laminate.

	Central Difference			
Nominal Value	0.01%	0.1%	1.0%	Analytical
Area $[0/25]_s$				
0.11161e-02	0.17344e-04	0.17437e-04	0.17439e-04	0.17381e-04
-0.53148e-04	-0.82969e-06	-0.83046e-06	-0.83042e-06	-0.83116e-06
-0.37203e-03	-0.58125e-05	-0.58125e-05	-0.58129e-05	-0.58127e-05
0.31888e-04	0.49844e-06	0.49828e-06	0.49826e-06	0.49837e-06
Taper Ratio $[0/25]_s$				
-0.53148e-04	0.24307e-03	0.24296e-03	0.24296e-03	0.24312e-03
0.31888e-04	-0.14573e-03	-0.14577e-03	-0.14578e-03	-0.14575e-03
0.75925e-05	-0.34720e-04	-0.34709e-04	-0.34709e-04	-0.34719e-04
0.35432e-05	-0.16200e-04	-0.16197e-04	-0.16198e-04	-0.16191e-04

draw any conclusions regarding the effect of the stacking sequence on the derivatives. To give an idea of the magnitude of the original eigenvalues computed at the base design, they are listed alongside their corresponding derivatives.

As it isn't feasible to present the derivatives of all the elements of the eigenvector (as a ninth order Chebyshev polynomial is being used, the eigenvector has one hundred elements), only a few representative non-zero derivatives of the dominant coefficients are shown here. The accuracy of the derivatives of the remaining coefficients is of the same order. Table 4.14 shows the derivative of the first eigenvector with respect to the four shape parameters perturbed about the nominal value. Here we see a notable discrepancy in between the 0.01% step-size results and the others, in particular for the area perturbations. The values obtained analytically are in closer agreement with those obtained using step-sizes of 0.1% or 1.0%. Thus, we see that a step-size of 0.01% may be too small to give reliable finite difference sensitivities of the modal response considered in this study.

Table 4.13. Comparison of analytical and central difference shape sensitivities of the four lowest eigenvalues for both symmetric and unsymmetric laminates.

	Central Difference			
Nominal Value	0.01%	0.1%	1.0%	Analytical
Area $[0/25]_s$				
0.36565e+05	-0.11411e+04	-0.11411e+04	-0.11412e+04	-0.11313e+04
0.35835e+06	-0.11172e+05	-0.11175e+05	-0.11176e+05	-0.11174e+05
0.12841e+07	-0.40000e+05	-0.40062e+05	-0.40056e+05	-0.40060e+05
0.35792e+07	-0.11156e+06	-0.11159e+06	-0.11159e+06	-0.11162e+06
Taper Ratio $[0/25]_s$				
0.36565e+05	-0.31333e+05	-0.31413e+05	-0.31409e+05	-0.31420e+05
0.35835e+06	-0.50267e+06	-0.50293e+06	-0.50297e+06	-0.50287e+06
0.12841e+07	-0.34667e+06	-0.34667e+06	-0.34733e+06	-0.34691e+06
0.35792e+07	-0.26133e+07	-0.26147e+07	-0.26149e+07	-0.26141e+07
Aspect Ratio $[0/25]_T$				
0.51717e+04	-0.37300e+04	-0.37293e+04	-0.37295e+04	-0.37216e+04
0.79016e+05	-0.14600e+05	-0.14600e+05	-0.14598e+05	-0.14604e+05
0.20628e+06	-0.13467e+06	-0.13470e+06	-0.13471e+06	-0.13457e+06
0.67505e+06	-0.19700e+06	-0.19717e+06	-0.19717e+06	-0.19699e+06
Sweep $[0/25]_T$				
0.51717e+04	-0.18733e+03	-0.18693e+03	-0.18691e+03	-0.18794e+03
0.79016e+05	-0.77333e+03	-0.77333e+03	-0.77367e+03	-0.77352e+03
0.20628e+06	-0.28667e+04	-0.28600e+04	-0.28593e+04	-0.28657e+04
0.67505e+06	-0.19067e+05	-0.19080e+05	-0.19082e+05	-0.19084e+05

4.3.3 Approximations to Eigenvalues and Eigenvectors

The eigenvalues and eigenvectors are approximated using three different methods and compared with the true values obtained by reanalysis. Once the slope is determined, a linear approximation to the frequencies can be immediately plotted. Using the method developed by Pritchard and Adelman [1991], an exponential approximation to the eigenvalues and eigenvectors can be obtained. And finally, a

Table 4.14. Comparison of analytical and central difference shape sensitivities of some representative coefficients of the 1st eigenvector for both symmetric and unsymmetric laminates.

	Central Difference			
Nominal Value	0.01%	0.1%	1.0%	Analytical
Area $[0/25]_s$				
0.79848e+00	0.00000e+00	-0.93750e-05	-0.84375e-05	-0.89675e-05
0.16277e+00	0.15625e-04	0.46875e-05	0.60937e-05	0.57475e-05
-0.38080e-01	0.00000e+00	-0.15625e-05	-0.14062e-05	-0.15346e-05
0.54476e-01	0.00000e+00	-0.31250e-05	-0.32812e-05	-0.31840e-05
Taper Ratio $[0/25]_s$				
0.79848e+00	0.16000e-01	0.15067e-01	0.15093e-01	0.15973e-01
0.14992e-02	-0.20000e-01	-0.19600e-01	-0.19613e-01	-0.19611e-01
-0.24439e-04	-0.66667e-03	-0.65333e-03	-0.64667e-03	-0.65347e-03
-0.15509e-04	0.32667e-02	0.32707e-02	-0.32704e-02	0.32698e-02
Aspect Ratio $[0/25]_T$				
0.78683e+00	-0.66667e-03	-0.53333e-03	-0.52333e-03	-0.59863e-03
-0.55556e-03	-0.33333e-03	-0.46667e-03	-0.46000e-03	-0.40847e-03
0.17016e-04	-0.15667e-02	-0.15433e-02	-0.15460e-02	-0.15513e-02
-0.94927e-05	-0.23667e-03	-0.23653e-03	-0.23653e-03	-0.23659e-03
Sweep $[0/25]_T$				
0.78683e+00	-0.18000e-02	-0.17667e-02	-0.17693e-02	-0.17683e-02
-0.55556e-03	0.26000e-02	0.26000e-02	0.25987e-02	0.25993e-02
0.17016e-04	0.42000e-03	0.42467e-03	0.42473e-03	0.42201e-03
-0.94927e-05	-0.36120e-03	-0.36115e-03	-0.36114e-03	-0.36198e-03

pseudo-exponential scheme is adopted wherein the exponential is expanded upto three terms and higher order terms are neglected. These approximations are plotted alongside the true eigenvalues.

First the eigenvalues are plotted as a function of area. It is found that the exponential and the three term expansion of the exponential yield either identical or almost identical curves. The linear approximation, as expected, is not as accurate

as the exponential approximations. As can be seen from Figs. [4.25-4.28], the 1st and 2nd eigenvalues decrease smoothly with an increase in the plate area for both symmetrically and unsymmetrically laminated plates. Aside from the magnitudes of the eigenvalues, there is remarkable similarity between the plots obtained for the first and second modes of vibration.

For the case of taper ratio perturbations the exponential approximation to the fundamental eigenvalue coincides with the three term expansion to the exponential approximation and is very accurate. In general all three schemes give a better approximation to the true eigenvalues than they did for area perturbations. Even the linear approximation is acceptable over a fairly wide range of taper ratio. Here also, as shown in Figs. [4.29-4.30], the natural frequencies for both symmetric and unsymmetric laminates decrease with an increase in taper ratio. It is interesting to note that the plots for symmetric and unsymmetric laminate configurations are remarkably similar for the same parameter. Though the numerical values of the eigenvalues obtained for a symmetric laminate are higher than those for an unsymmetric laminate, the trend is the same.

Regarding the sensitivities of the eigenvalues with respect to the aspect ratio and sweep angle, it must be recalled that as the mass matrix is independent of these parameters the exponential approximation is invalid. Therefore only a linear approximation to the fundamental frequency of vibration is performed. An increase in the aspect ratio yields a negative slope for the true eigenvalue curve for both symmetric and unsymmetric stacking sequences (see Figs. [4.31-4.32]), as was the case with the area and taper ratio. An increase in any of these three parameters resulted in similar smoothly decreasing trends in the vibration frequencies. The effect of the sweep angle on the fundamental natural frequency does not follow the same trends as those of the other parameters. As can be seen in Figs. [4.33-4.34],

the decreasing trend of the eigenvalue with the sweep angle, though smooth, is opposite that of the trends exhibited by the other shape parameters. Also, the linear approximation is satisfactory for a comparatively narrower range of the variable.

Next, the dominant coefficient of the eigenvector corresponding to the first mode of vibration is approximated over the range of each shape variable using three different methods. The first is a linear approximation similar to the one used for the eigenvalues i.e. once the slope of the curve at the nominal value is determined, a straight line is drawn through that point with this slope. The second approximation is the exponential one, which is similar to the one used in the eigenvalue approximation. The last method is the pseudo-exponential scheme resulting from applying a three term expansion to the exponential term of the previous method.

The effect of area perturbations on the dominant coefficient of the first eigenvector for the case of a symmetrically laminated plate is first considered. As seen in Fig. 4.35, the coefficient decreases smoothly with an increase in the plate area, a fact which is approximated reasonably accurately by the exponential and pseudo-exponential schemes. The linear approximation is not as accurate as the other two, which is to be expected.

Next, we see from Fig. 4.36 that the taper ratio has the opposite effect on the dominant coeffcient than the sweep did. The coefficient increases smoothly with taper ratio. Also, the two exponential schemes yield identical curves which approximate the actual curve very accurately while the linear approximation is also reasonably accurate over most of the range of the variable. The approximations in general are more accurate than they were for area perturbations. It may be recalled that this was true for the eigenvalue sensitivities, too.

As mentioned previoulsy, the exponential approximation is invalid when the mass matrix is independent of a particular shape variable. This is so for the aspect ratio

and sweep angle. Thus, as for the case of the corresponding eigenvalues, only the linear approximation is performed for these cases. The effect of the aspect ratio on the dominant coefficient of the first eigenvector is illustrated in Fig. 4.37. It is interesting to note that the curve, though smoothly decreasing before the nominal aspect ratio, begins to increase soon thereafter. The linear approximation is seen to be accurate for a rather narrow range of aspect ratio in this case.

Finally, we see from Fig. 4.38 that the sweep angle has a similar effect on the eigenvector as it does on the eigenvalue i.e. though the coefficient decreases as smoothly as it did with the area, the trend is markedly different. The linear approximation is seen to be more accurate in this case than it was for the aspect ratio sensitivity.

To summarize, the linear approximations are, in general, valid only within a limited range of the design variable whereas the exponential approximation, wherever possible, gives far closer agreement with the true eigenvalues and eigenvectors over a considerably wider range.

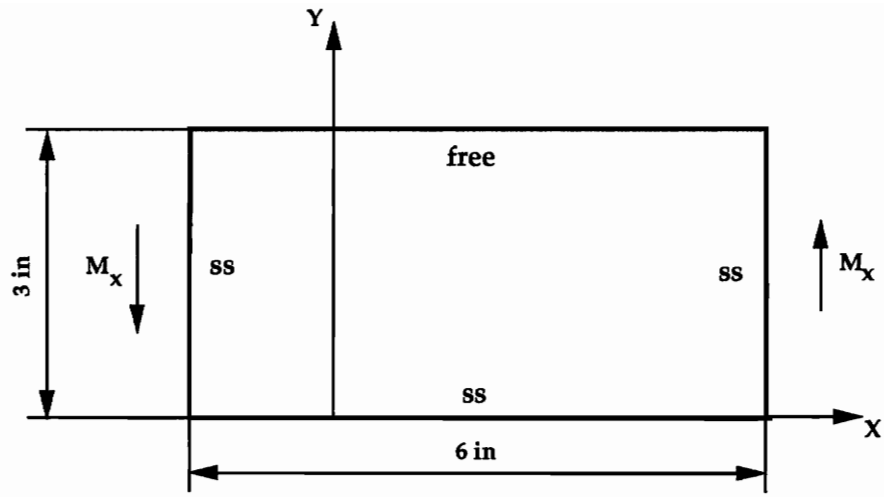

Fig. 4.1. Static Analysis of a Specially Orthotropic Rectangular Plate.

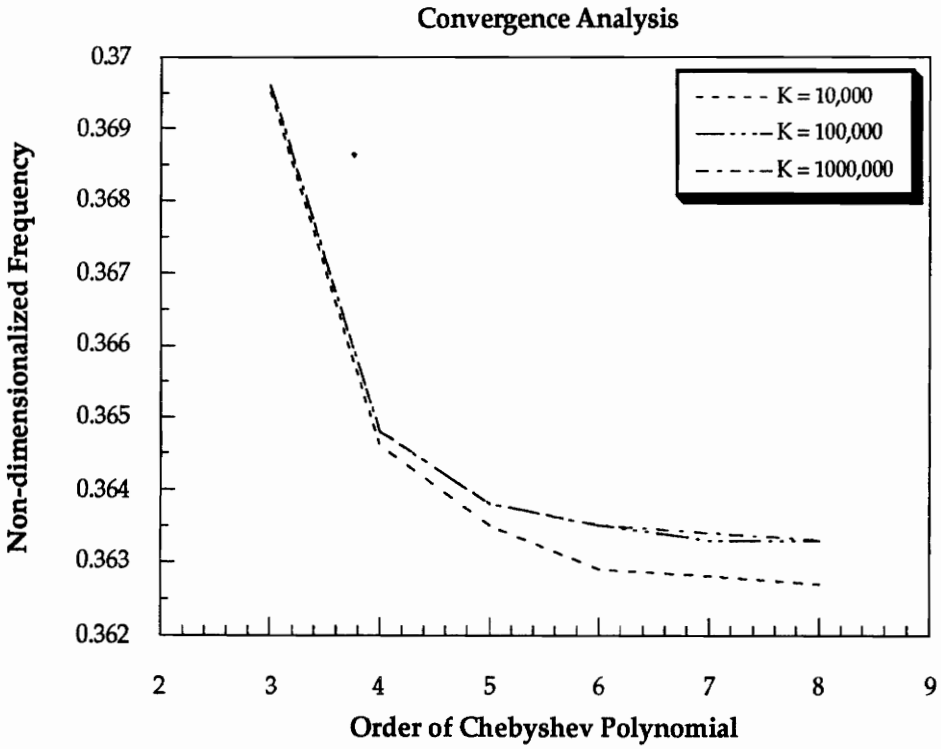

Fig. 4.2 Effect of Spring Stiffness K on 1st Natural Frequency of Isotropic Skew Plate.

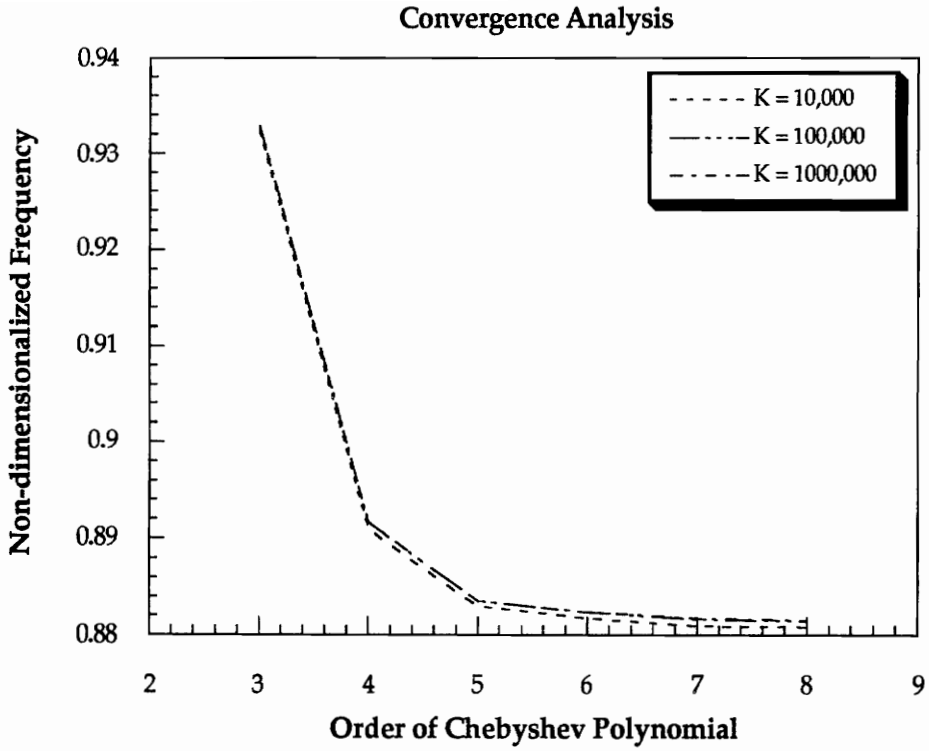

Fig. 4.3 Effect of Spring Stiffness K on 2nd Natural Frequency of Isotropic Skew Plate.

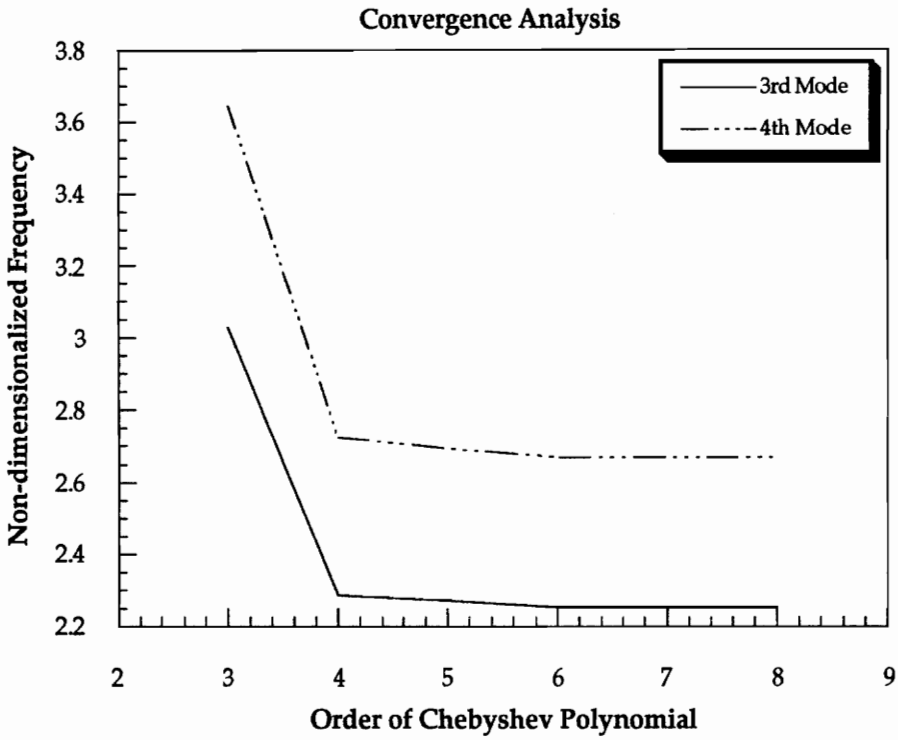

Fig. 4.4 Convergence of 3rd and 4th Frequency Parameters of Isotropic Skew Plate.

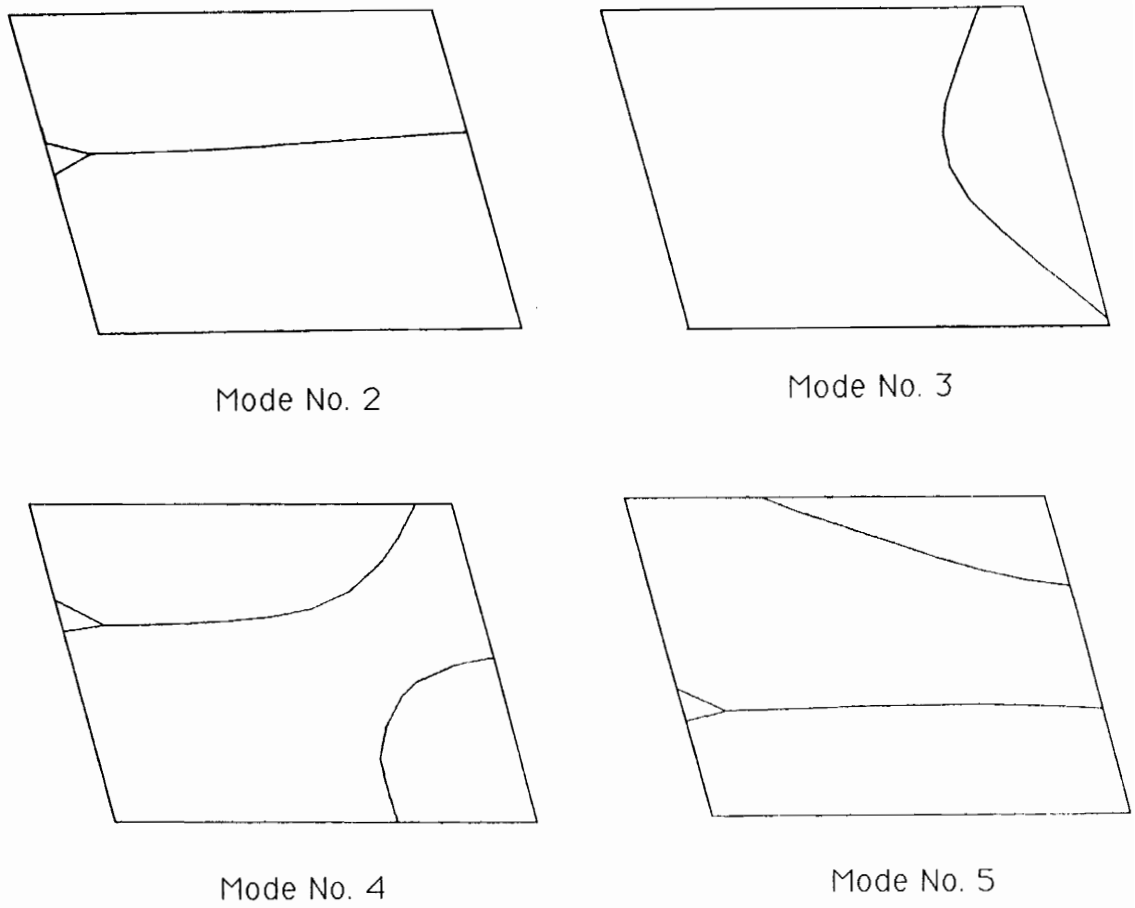

Fig. 4.5. 2nd, 3rd, 4th and 5th Mode Shapes for an Isotropic Skew Plate.

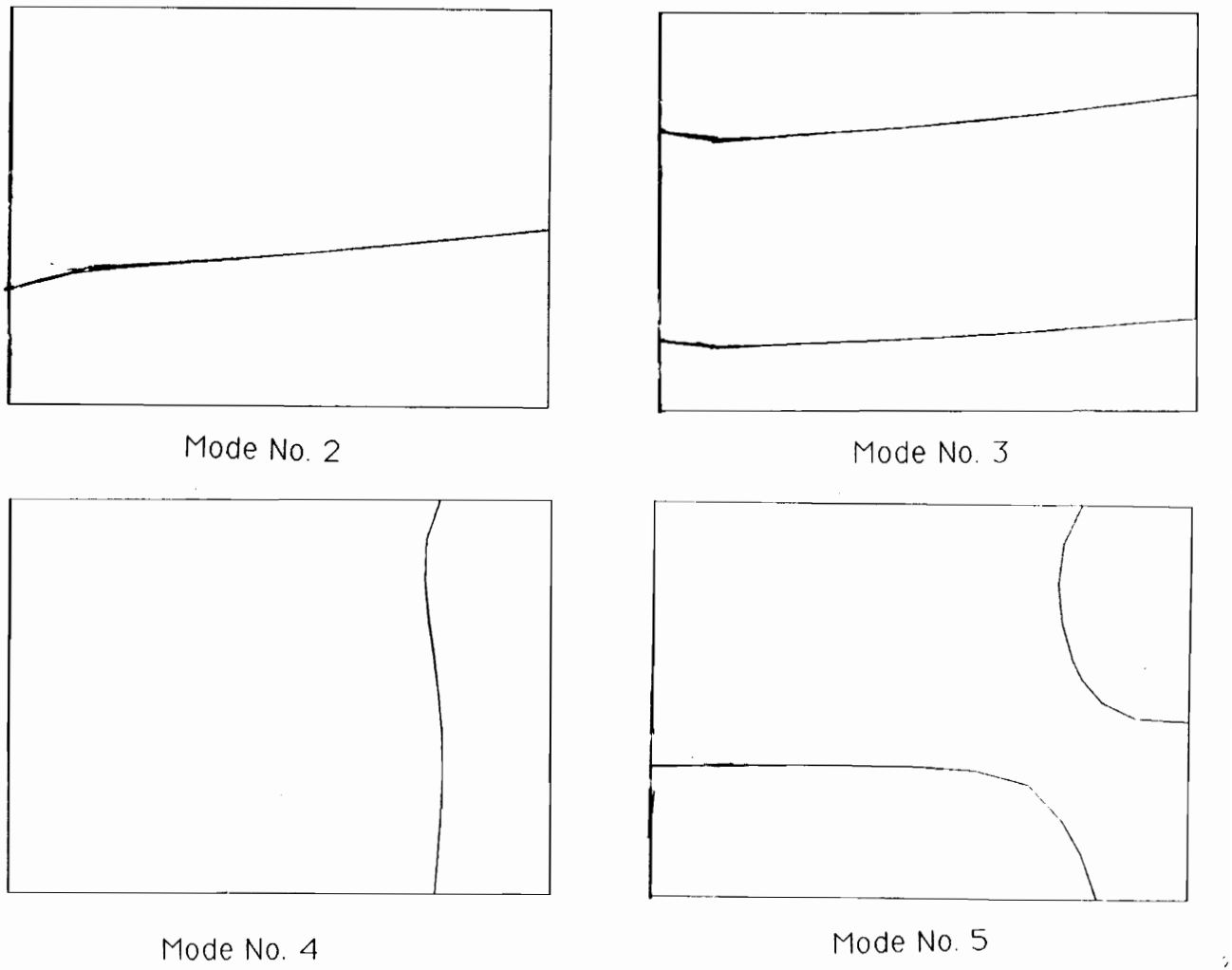

Fig. 4.7. Nodal Lines for 2nd, 3rd, 4th and 5th Modes of an Unsymmetric Laminate.

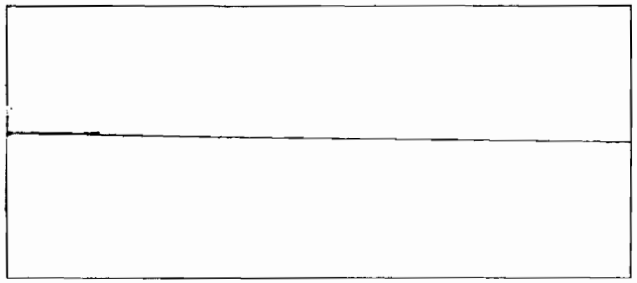

Mode No. 2

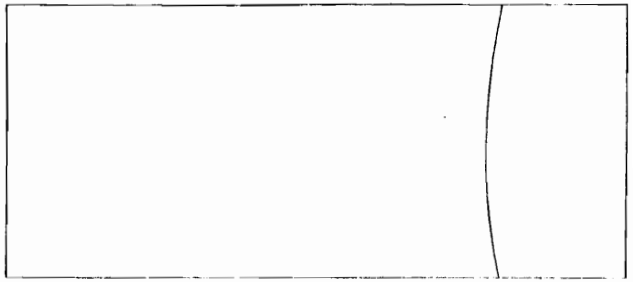

Mode No. 3

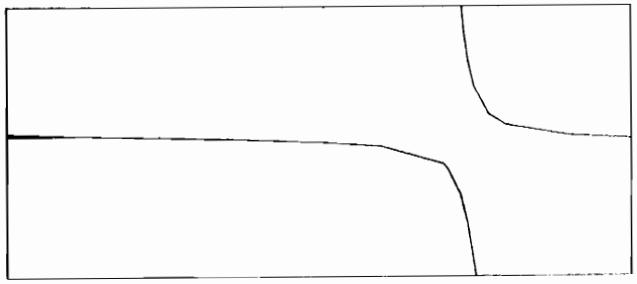

Mode No. 4

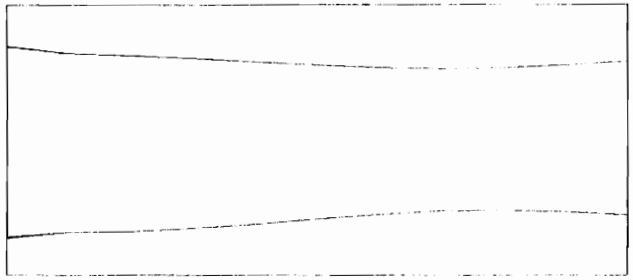

Mode No. 5

Fig. 4.6. Nodal Lines for 2nd, 3rd, 4th and 5th Modes of a Symmetric Laminate.

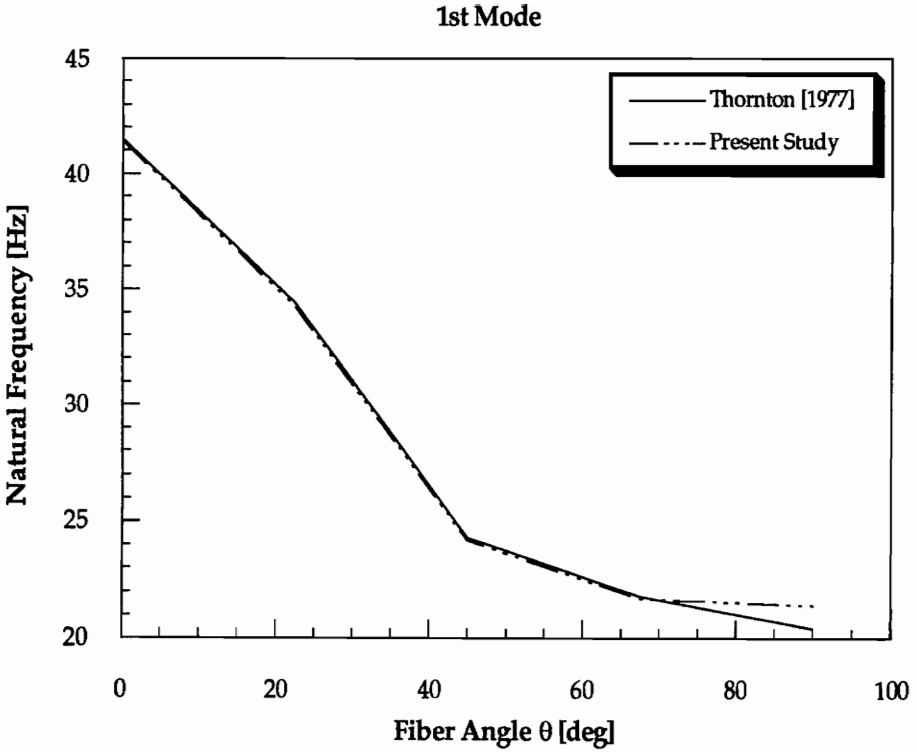

Fig. 4.8 Variation of 1st Frequency of Vibration with Fiber Angle θ for [0/θ] Laminate.

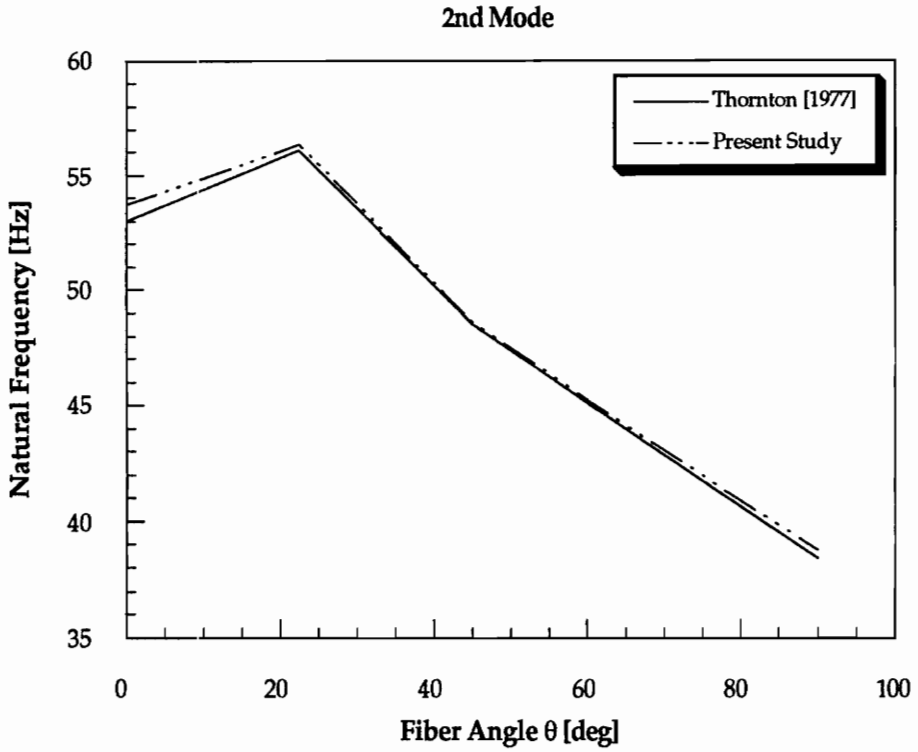

Fig. 4.9 Variation of 2nd Frequency of Vibration with Fiber Angle θ for [0/θ] Laminate.

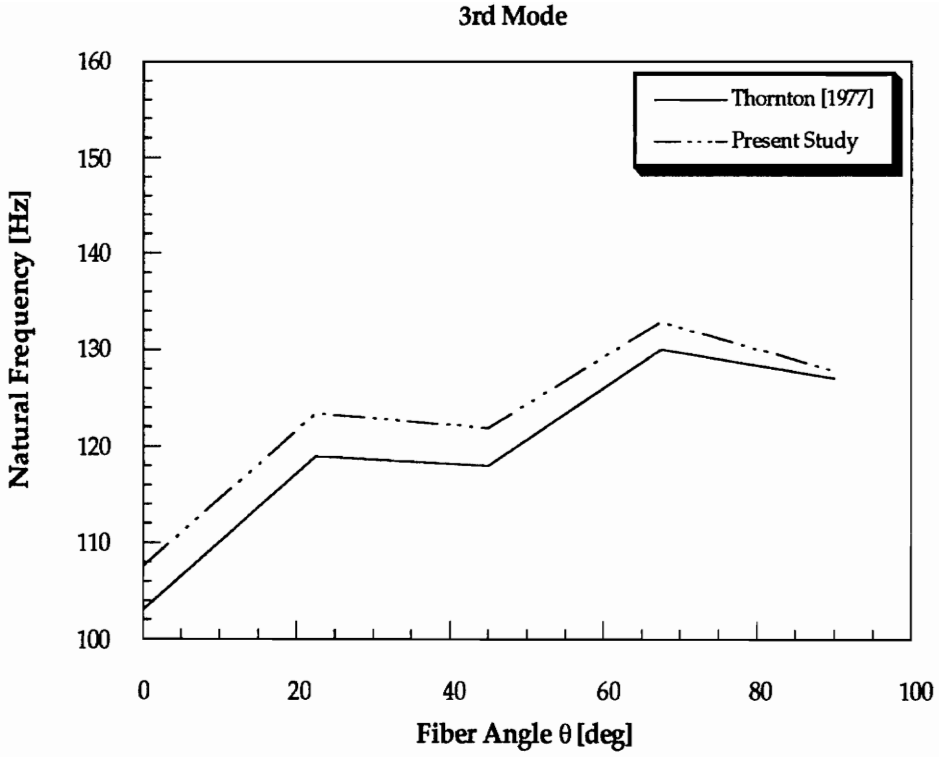

Fig. 4.10 Variation of 3rd Frequency of Vibration with Fiber Angle θ for [0/θ] Laminate.

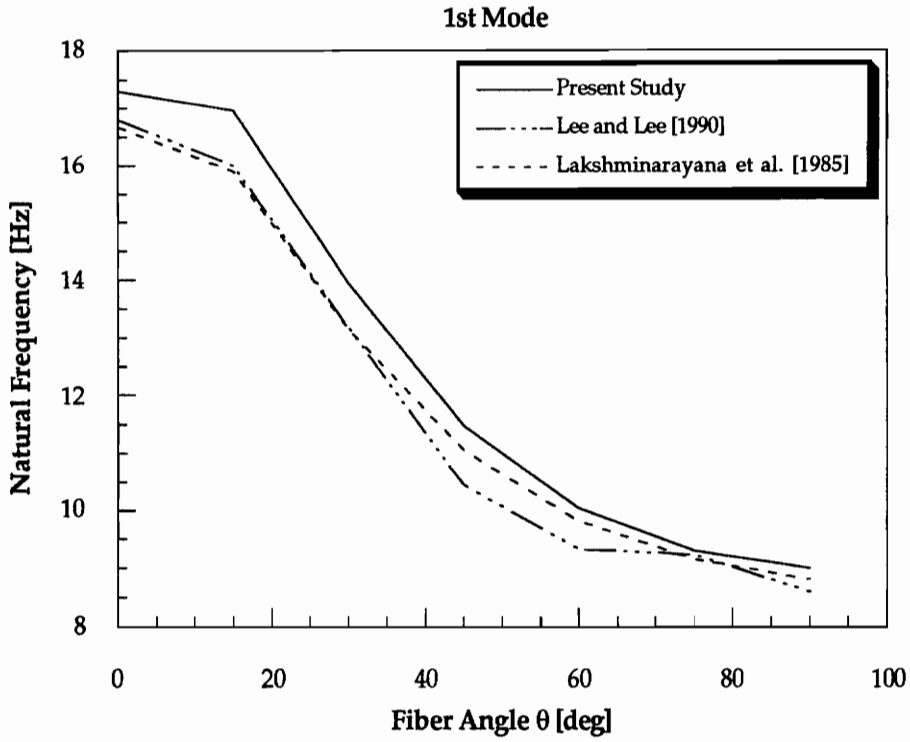

Fig. 4.11 Variation of 1st Vibration Frequency with Fiber Angle θ for $[\theta_2/0]_s$ Laminate.

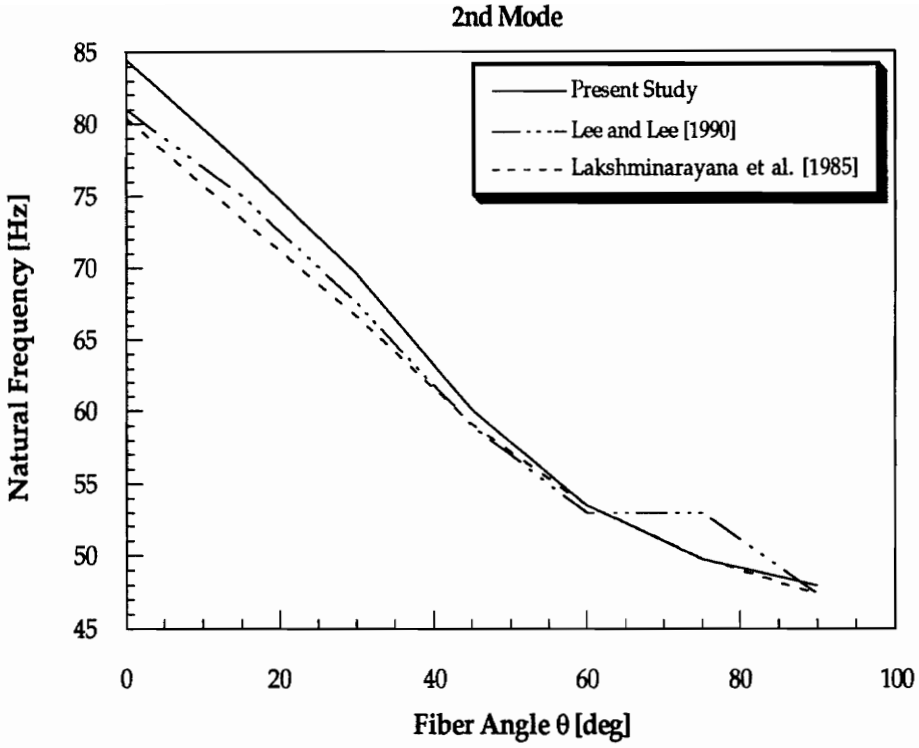

4.12 Variation of 2nd Vibration Frequency with Fiber Angle θ for $[\theta_2/0]_s$ Laminate.

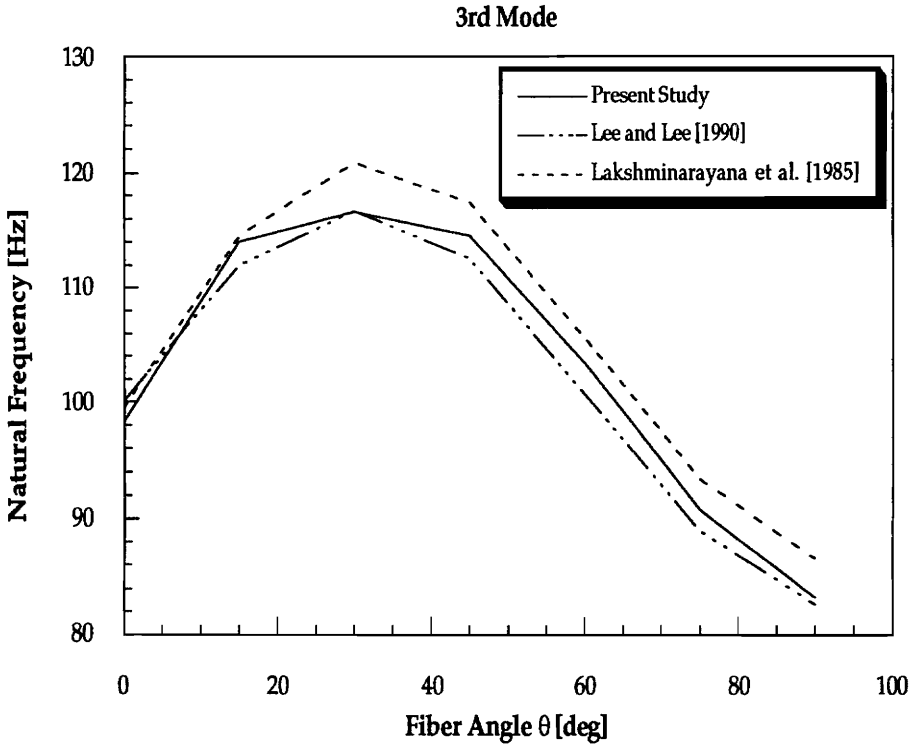

Fig. 4.13 Variation of 3rd Vibration Frequency with Fiber Angle θ for $[\theta_2/0]_s$ Laminate.

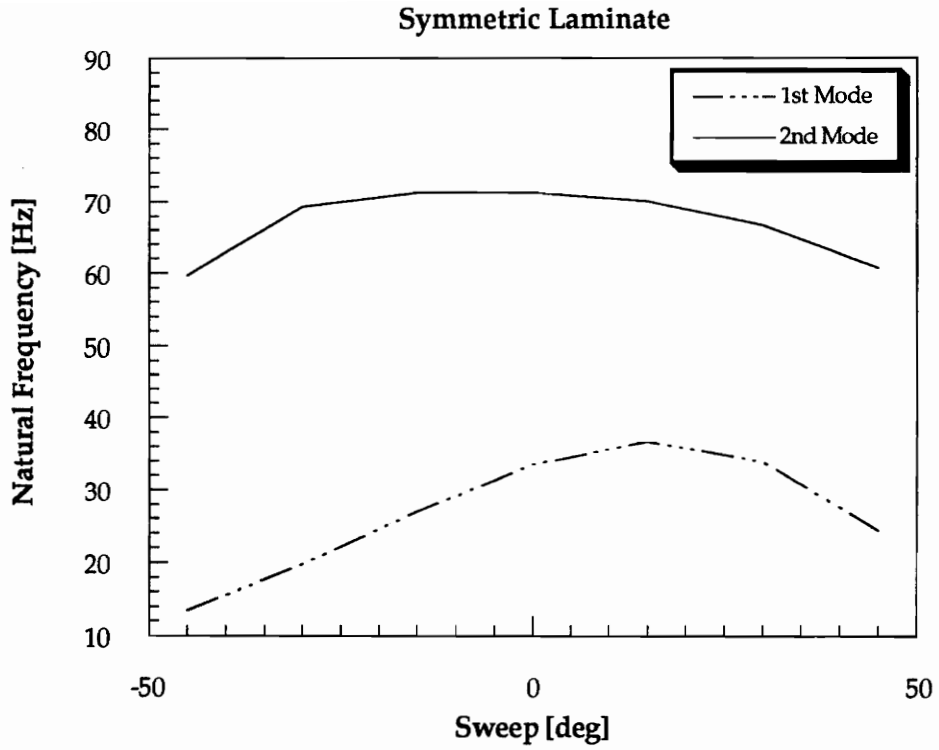

Fig. 4.14 Variation with Sweep of 1st and 2nd Vibration Frequencies for Aspect Ratio 1.

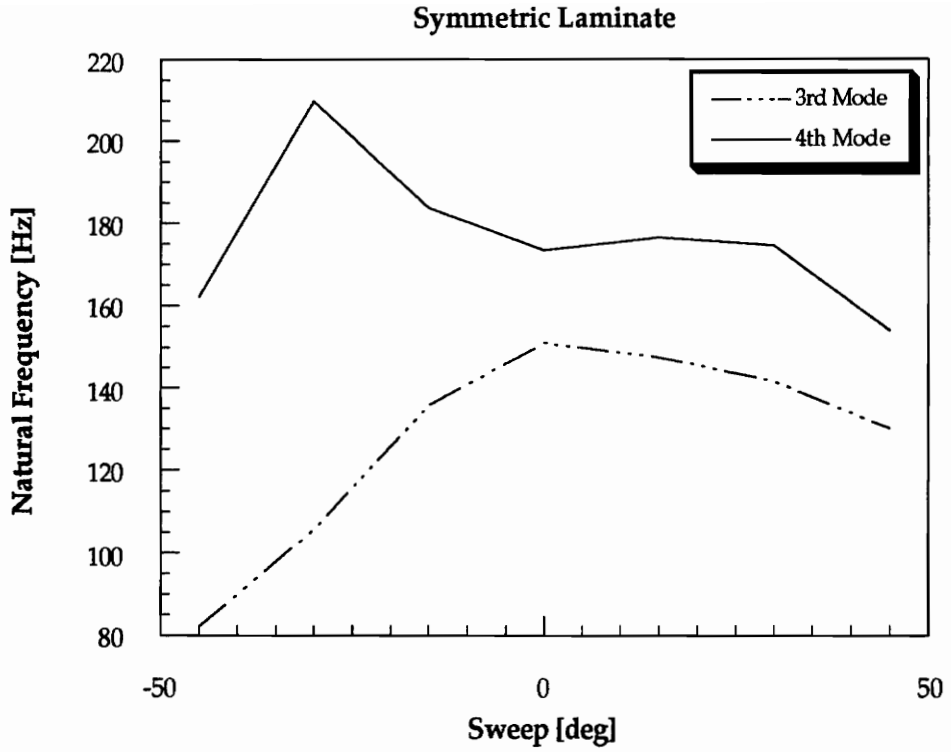

Fig. 4.15 Variation with Sweep of 3rd and 4th Vibration Frequencies for Aspect Ratio 1.

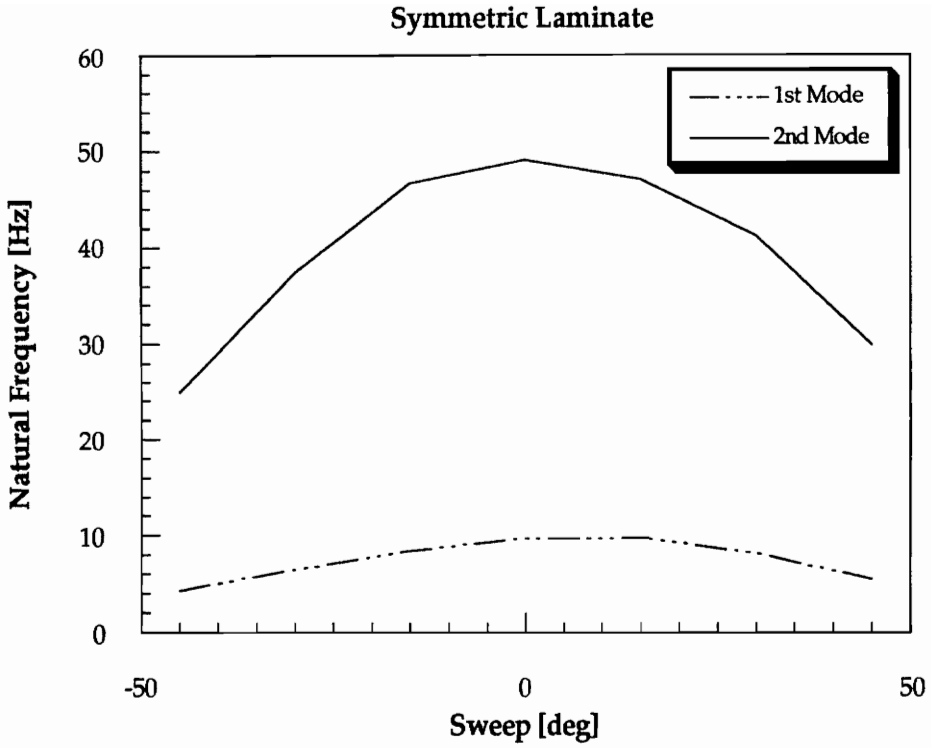

Fig. 4.16 Variation with Sweep of 1st and 2nd Vibration Frequencies for Aspect Ratio 3.

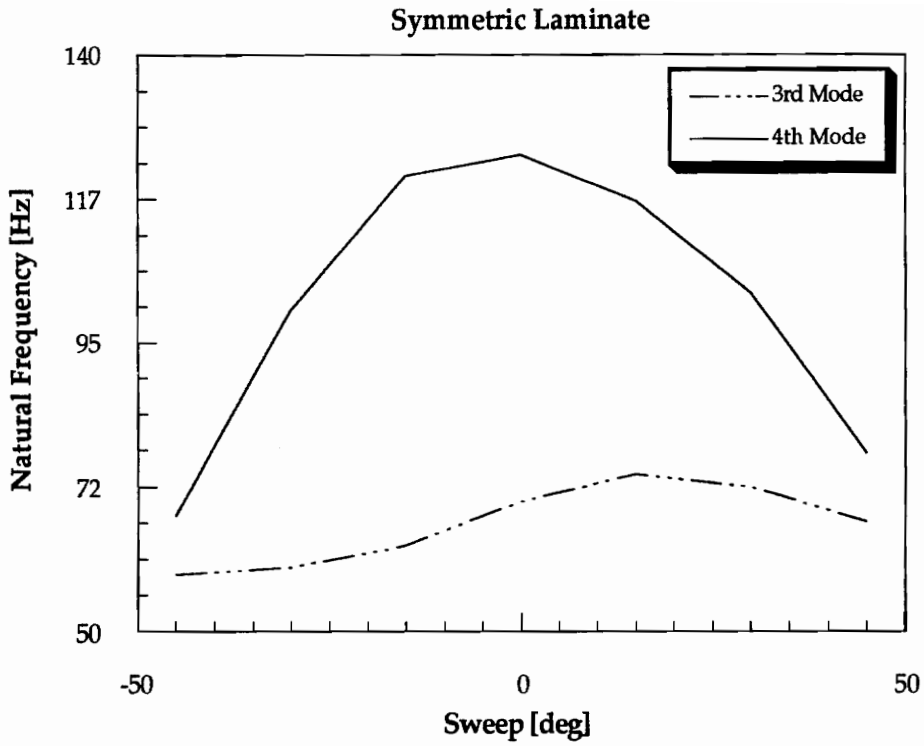

Fig. 4.17 Variation with Sweep of 3rd and 4th Vibration Frequencies for Aspect Ratio 3.

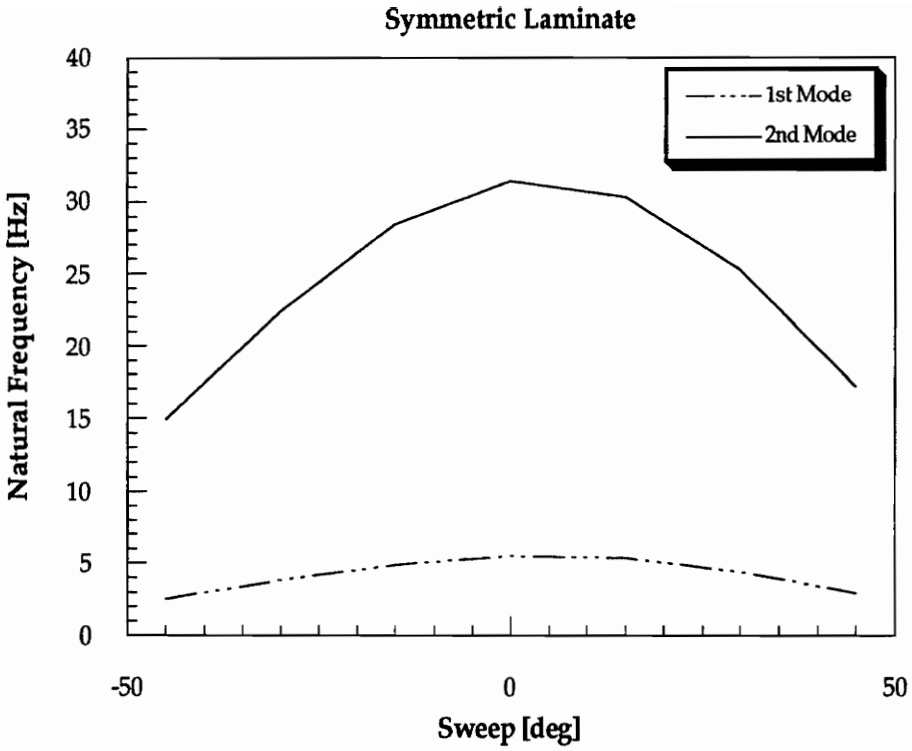

Fig. 4.18 Variation with Sweep of 1st and 2nd Vibration Frequencies for Aspect Ratio 5.

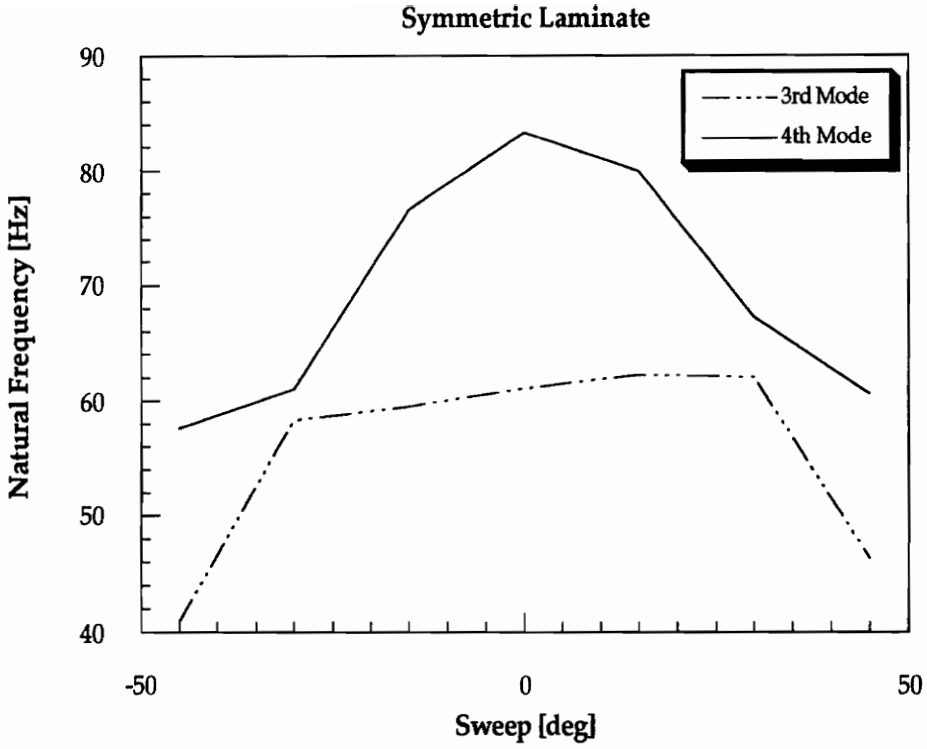

Fig. 4.19 Variation with Sweep of 3rd and 4th Vibration Frequencies for Aspect Ratio 5.

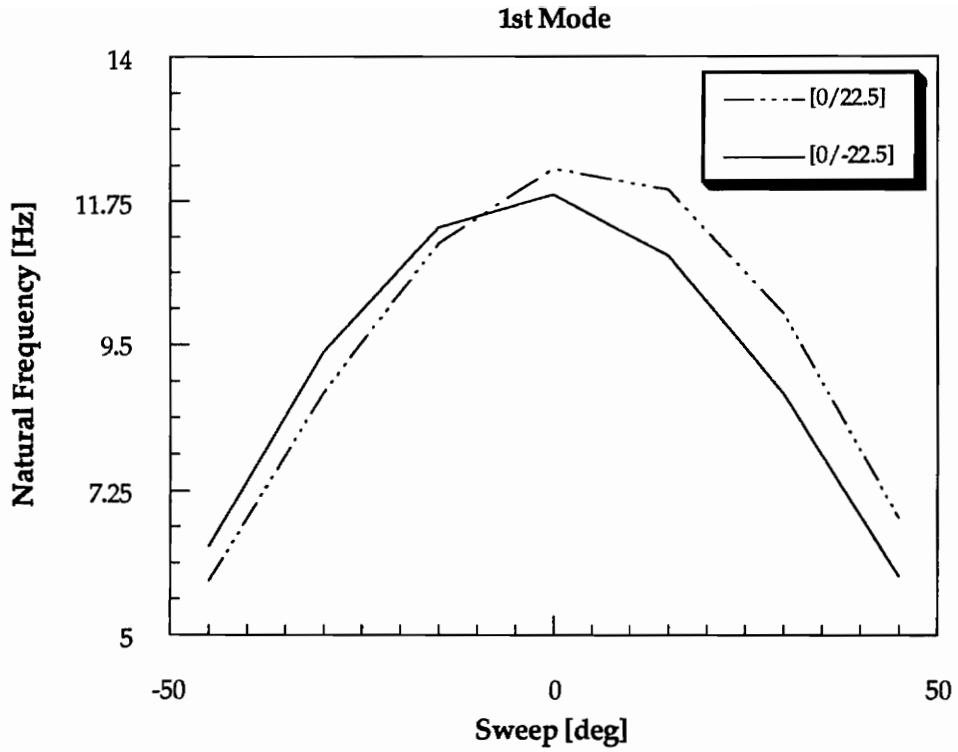

Fig. 4.20 Variation with Sweep of 1st Natural Frequency of an Unsymmetric Laminate.

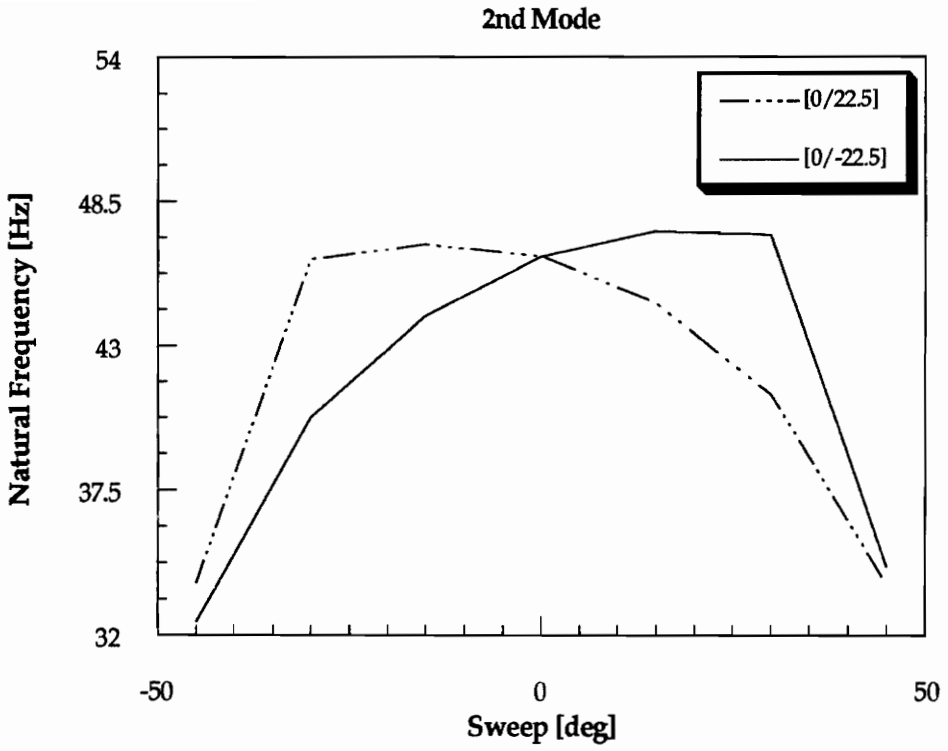

Fig. 4.21 Variation with Sweep of 2nd Natural Frequency of an Unsymmetric Laminate.

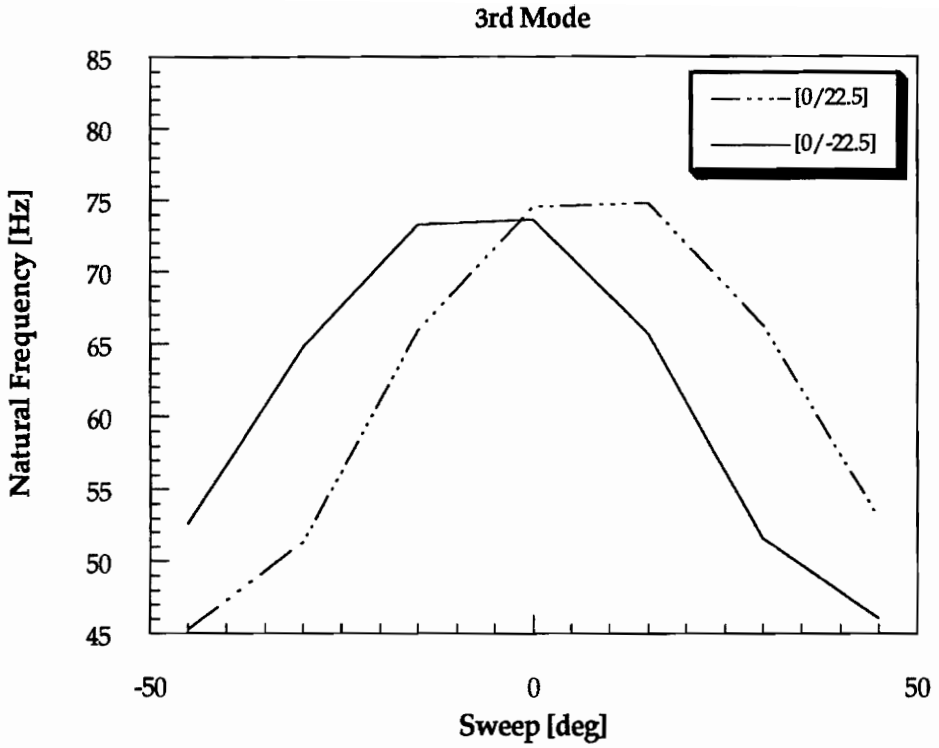

Fig. 4.22 Variation with Sweep of 3rd Natural Frequency of an Unsymmetric Laminate.

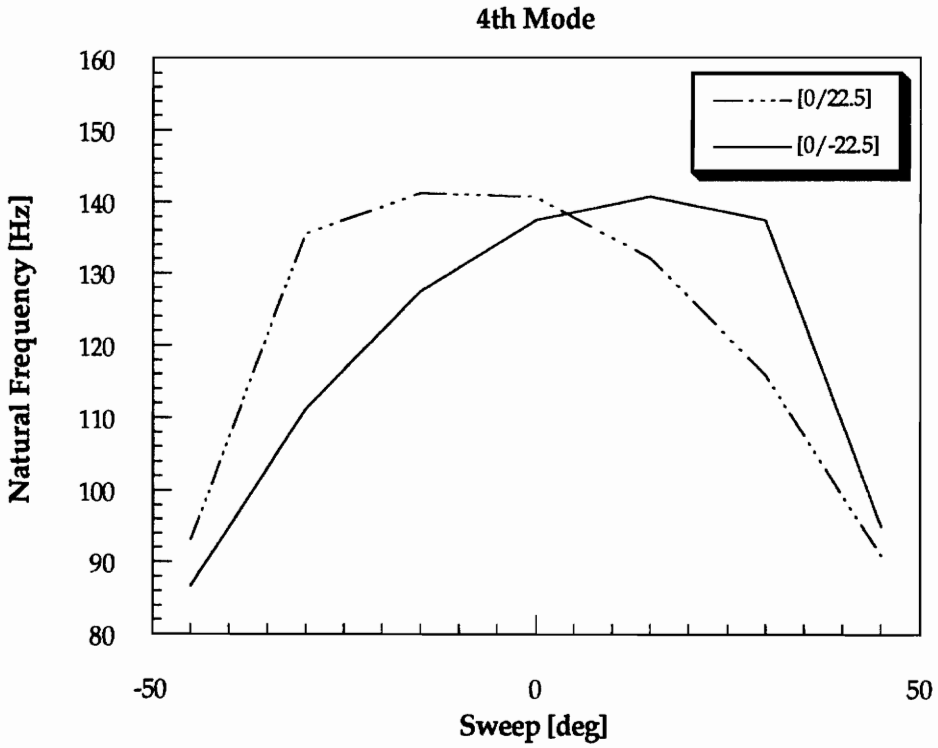

Fig. 4.23 Variation with Sweep of 4th Natural Frequency of an Unsymmetric Laminate.

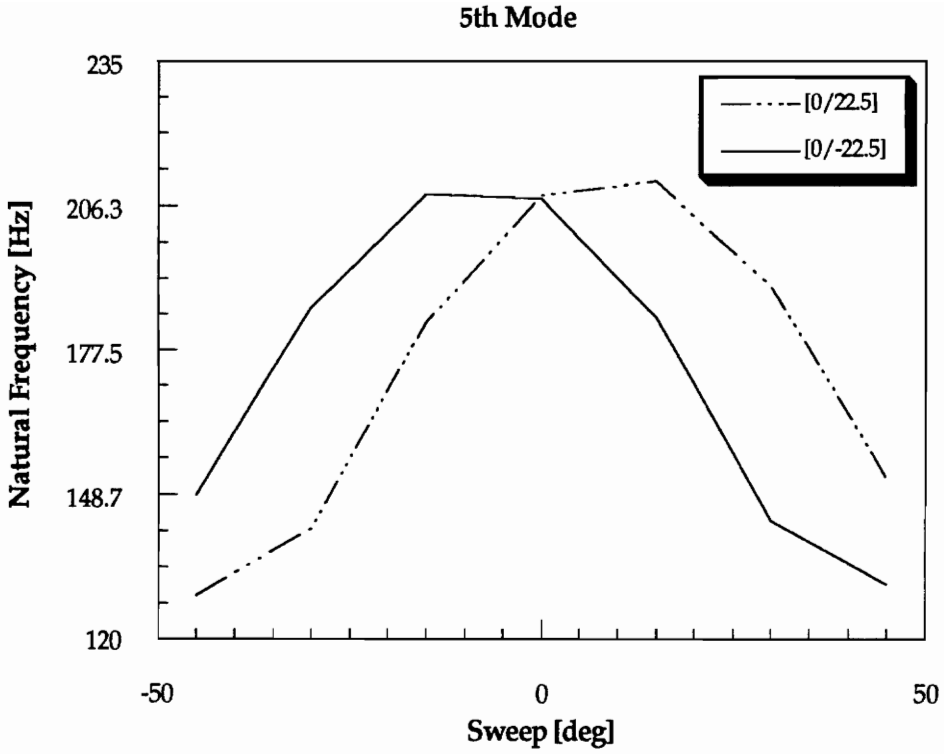

Fig. 4.24 Variation with Sweep of 5th Natural Frequency of an Unsymmetric Laminate.

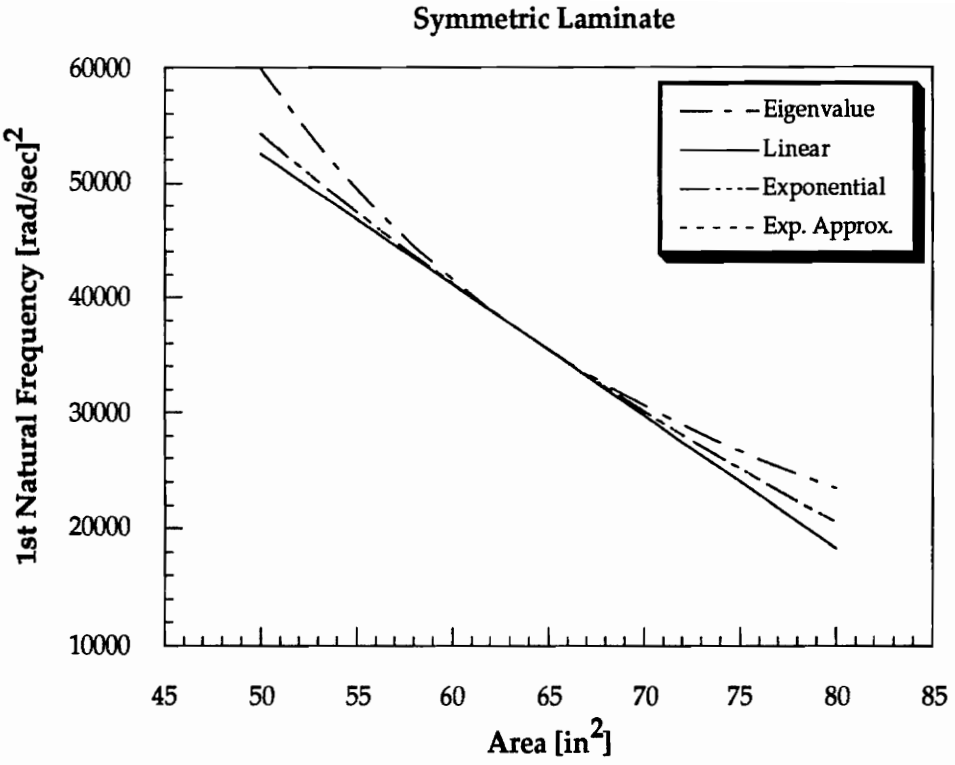

Fig. 4.25 Sensitivity of 1st Mode of Symmetric Laminate w.r.t. Area.

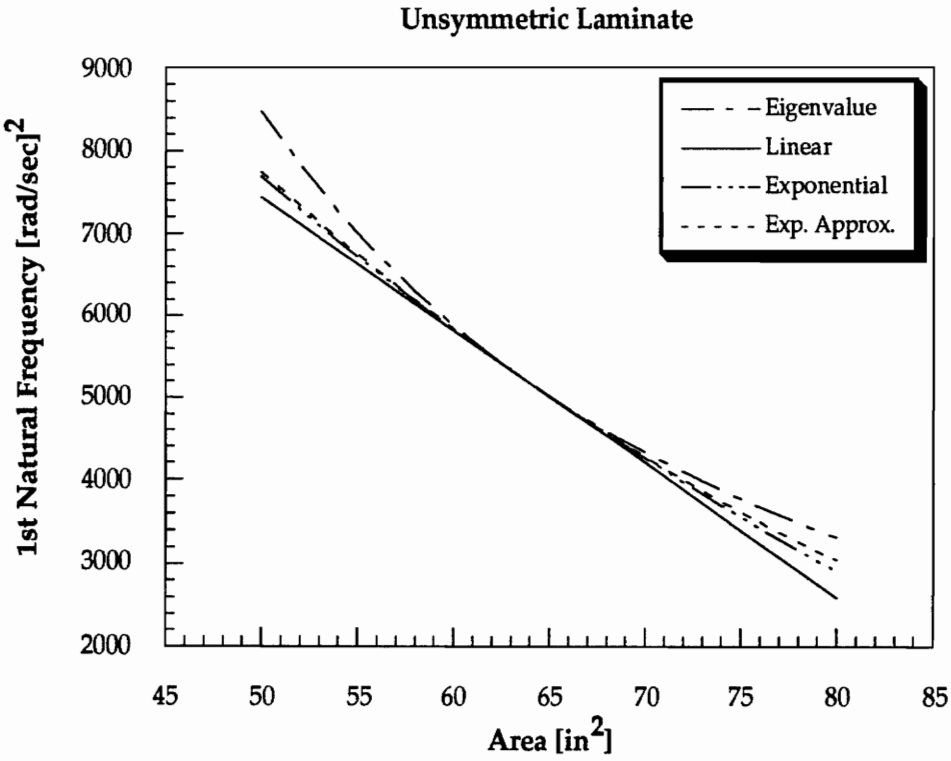

Fig. 4.26 Sensitivity of 1st Mode of Unsymmetric Laminate w.r.t. Area.

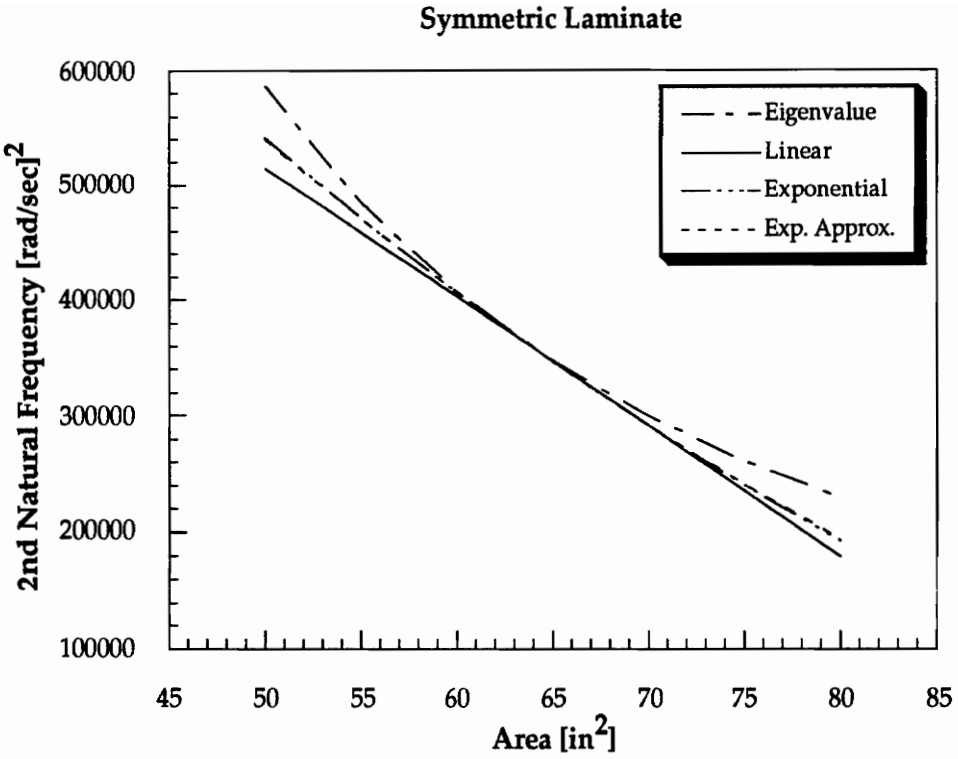

Fig. 4.27 Sensitivity of 2nd Mode of Symmetric Laminate w.r.t. Area.

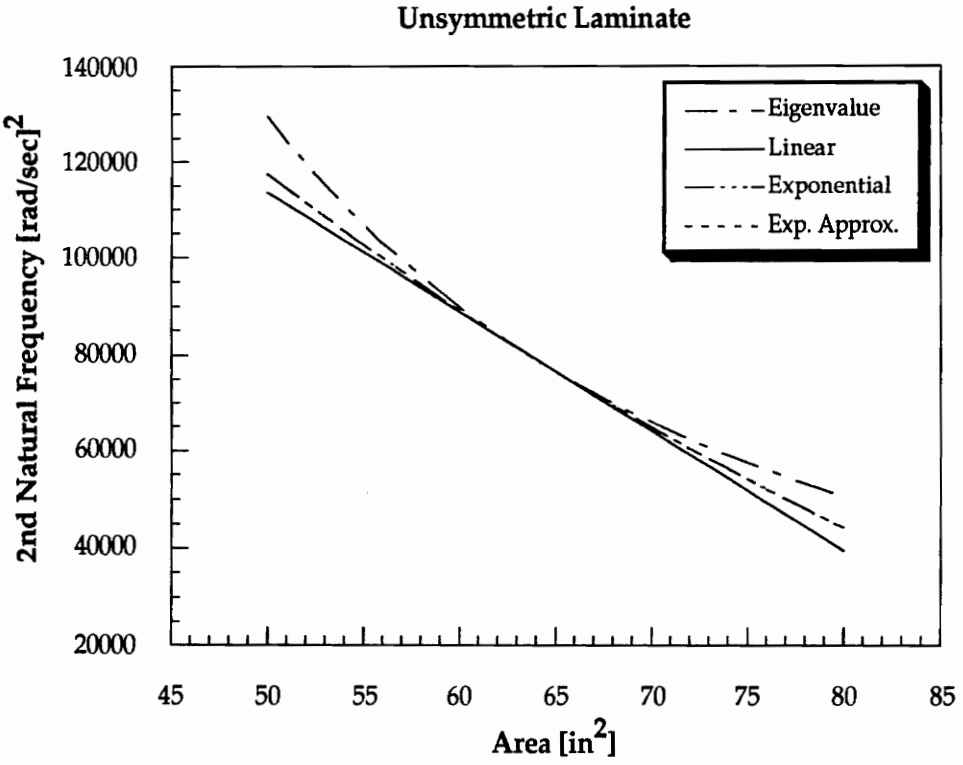

Fig. 4.28 Sensitivity of 2nd Mode of Unsymmetric Laminate w.r.t. Area.

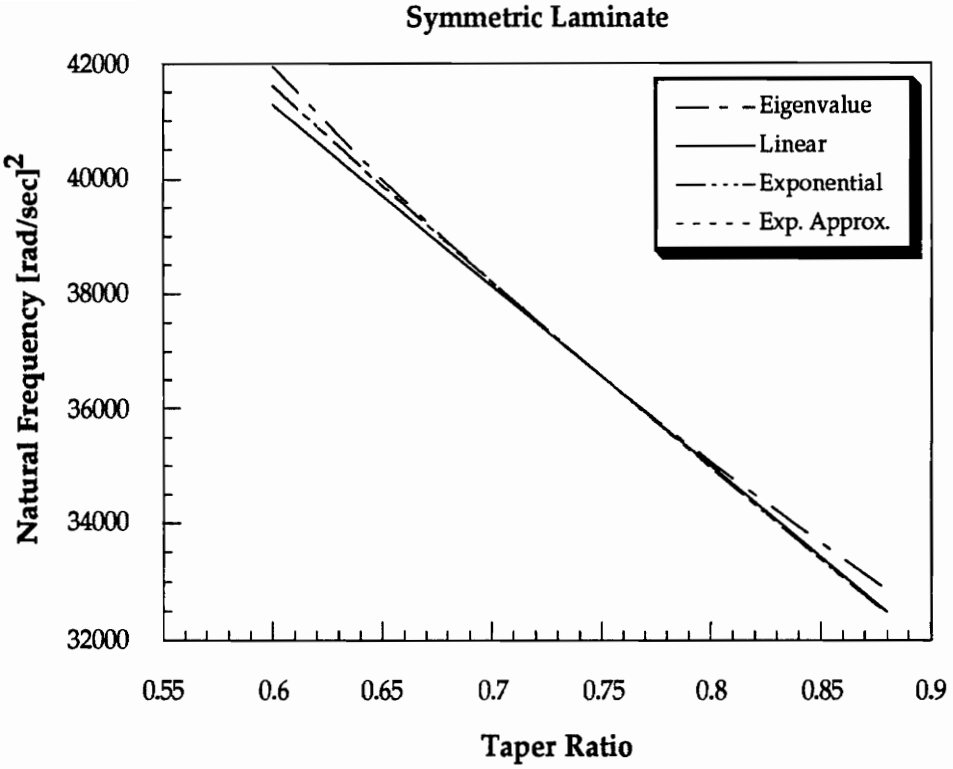

Fig. 4.29 Sensitivity of 1st Mode of Symmetric Laminate w.r.t. Taper Ratio.

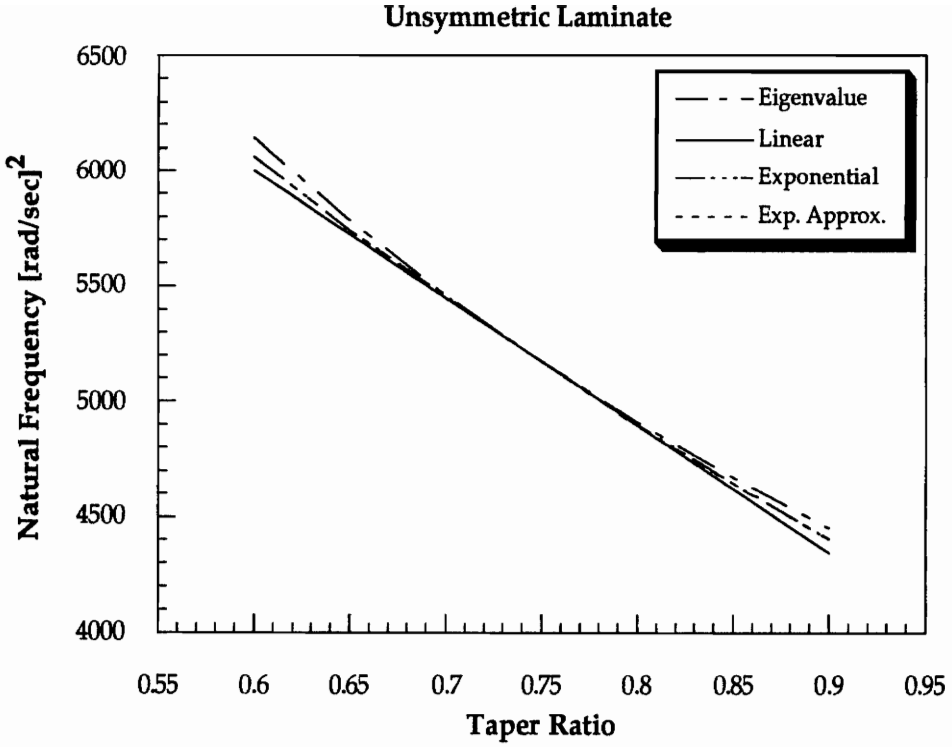

Fig. 4.30 Sensitivity of 1st Mode of Unsymmetric Laminate w.r.t. Taper Ratio.

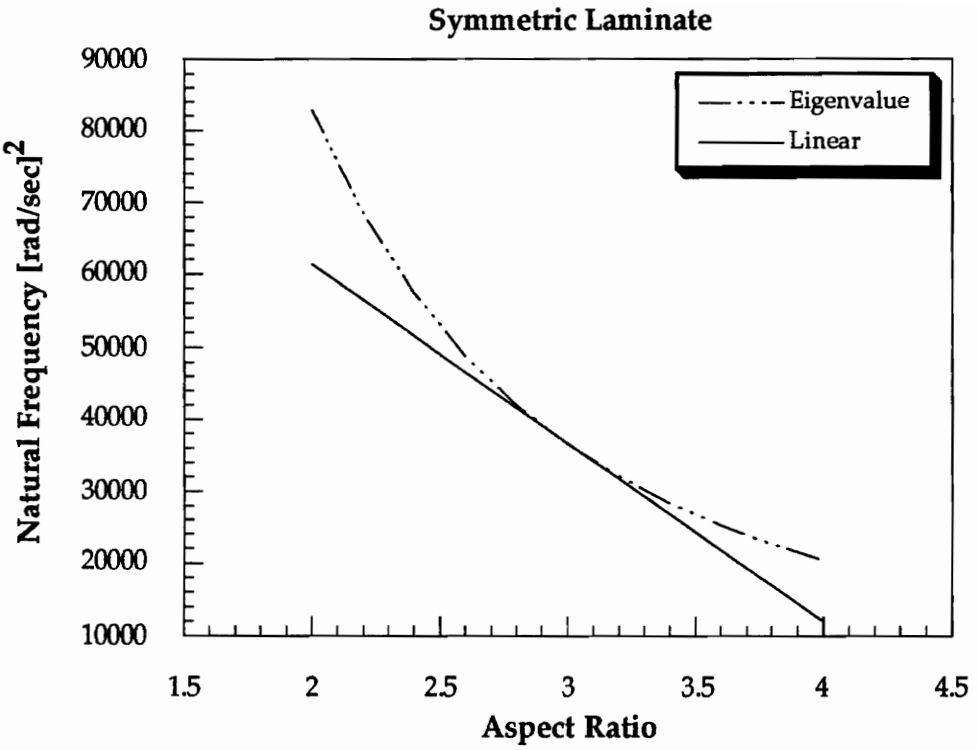

Fig. 4.31 Sensitivity of 1st Mode of Symmetric Laminate w.r.t. Aspect Ratio.

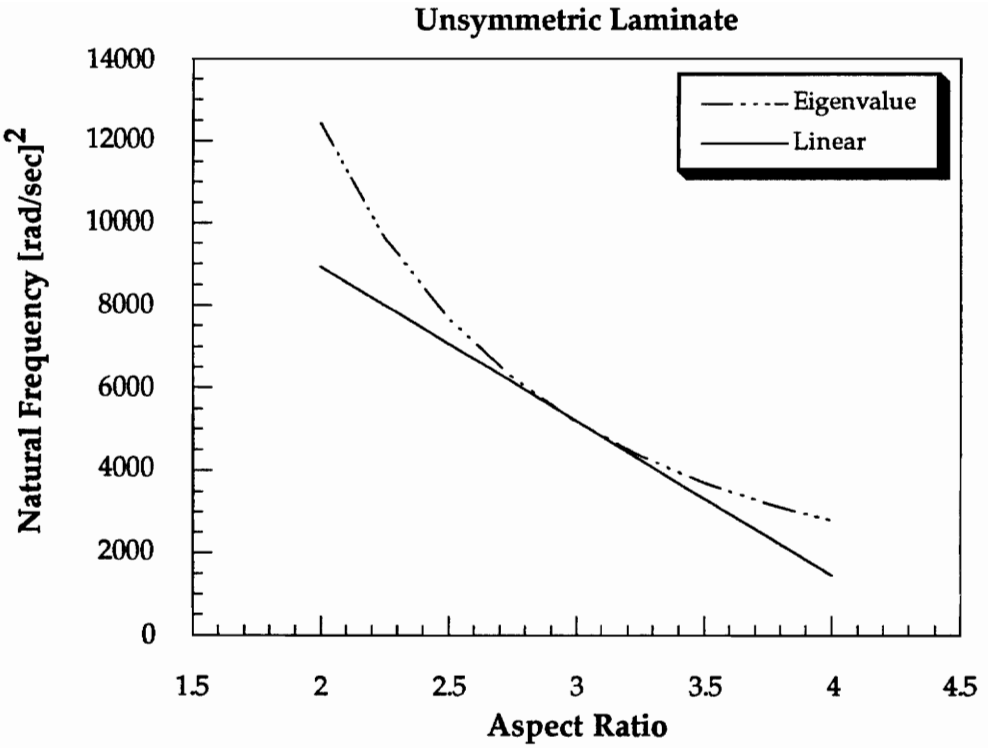

Fig. 4.32 Sensitivity of 1st Mode of Unsymmetric Laminate w.r.t. Aspect Ratio.

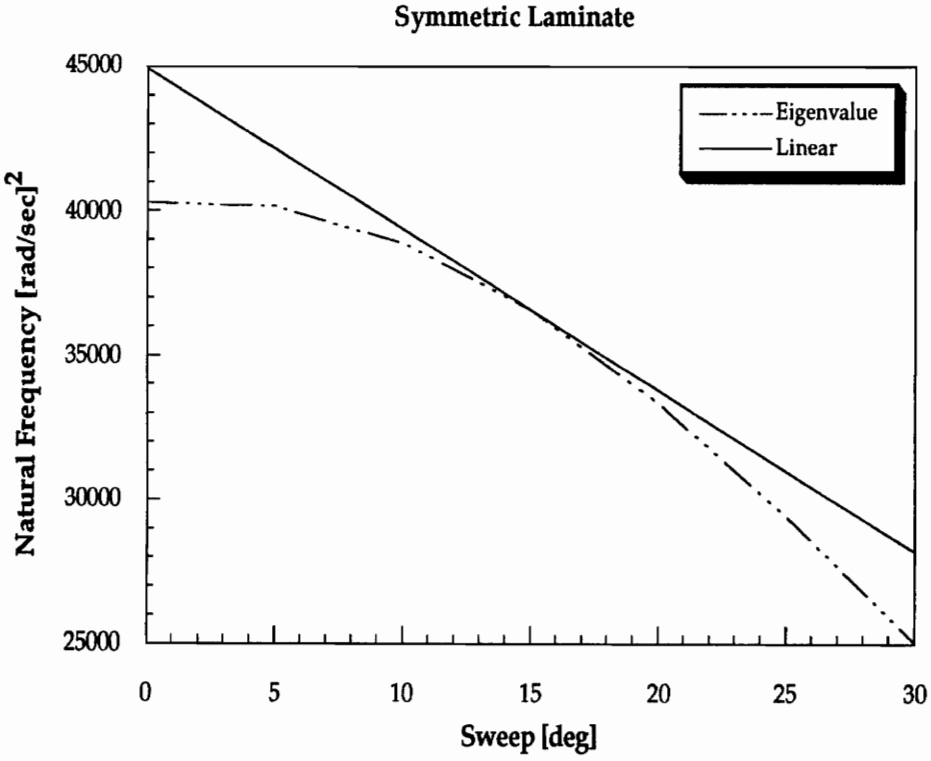

Fig. 4.33 Sensitivity of 1st Mode of Symmetric Laminate w.r.t. Sweep.

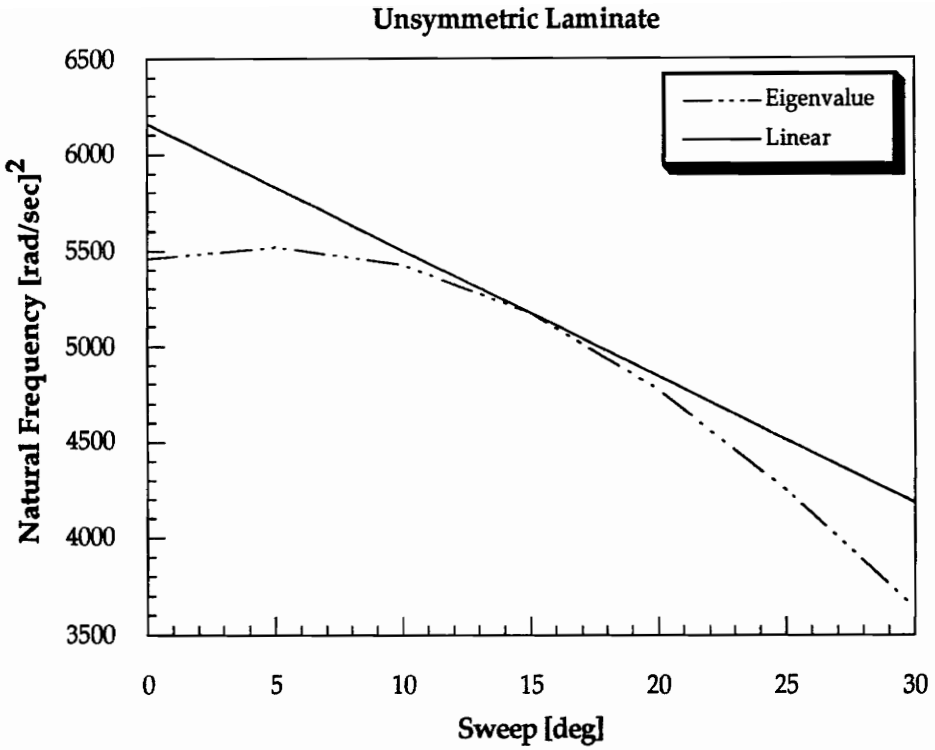

Fig. 4.34 Sensitivity of 1st Mode of Unsymmetric Laminate w.r.t. Sweep.

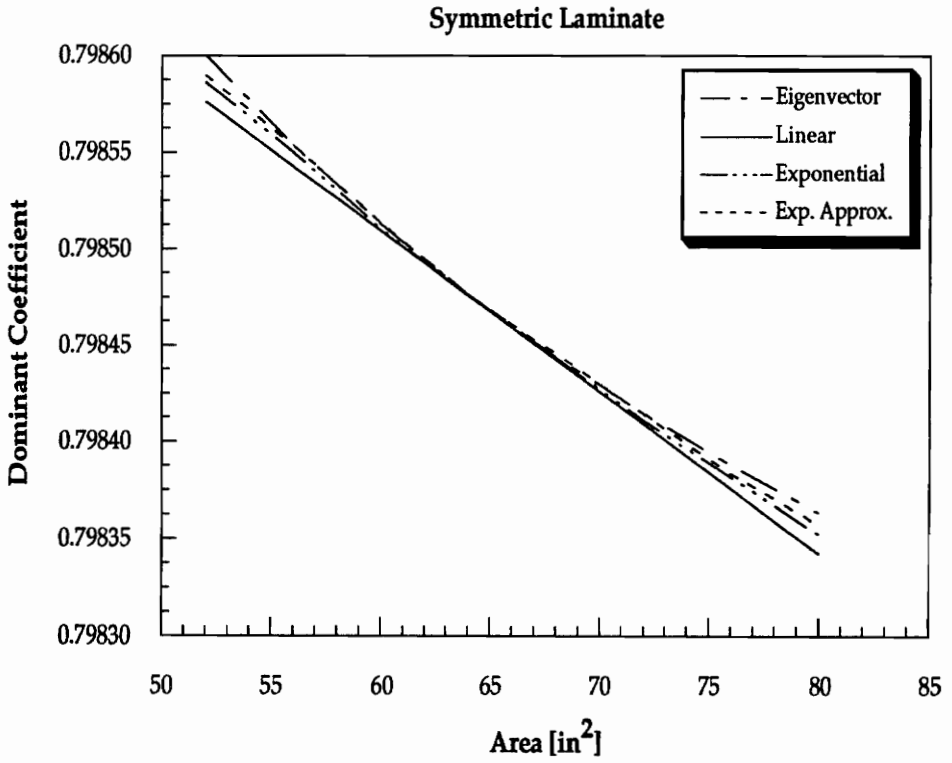

Fig. 4.35 Area Sensitivity of Dominant Coefficient of 1st Eigenvector.

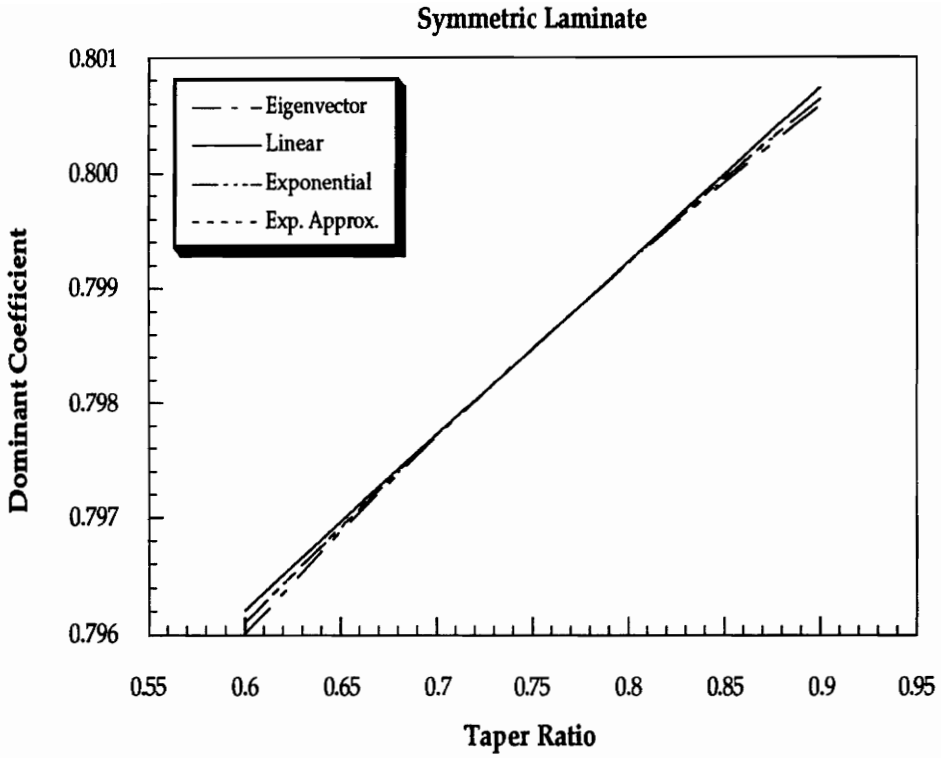

Fig. 4.36 Taper Ratio Sensitivity of Dominant Coefficient of 1st Eigenvector.

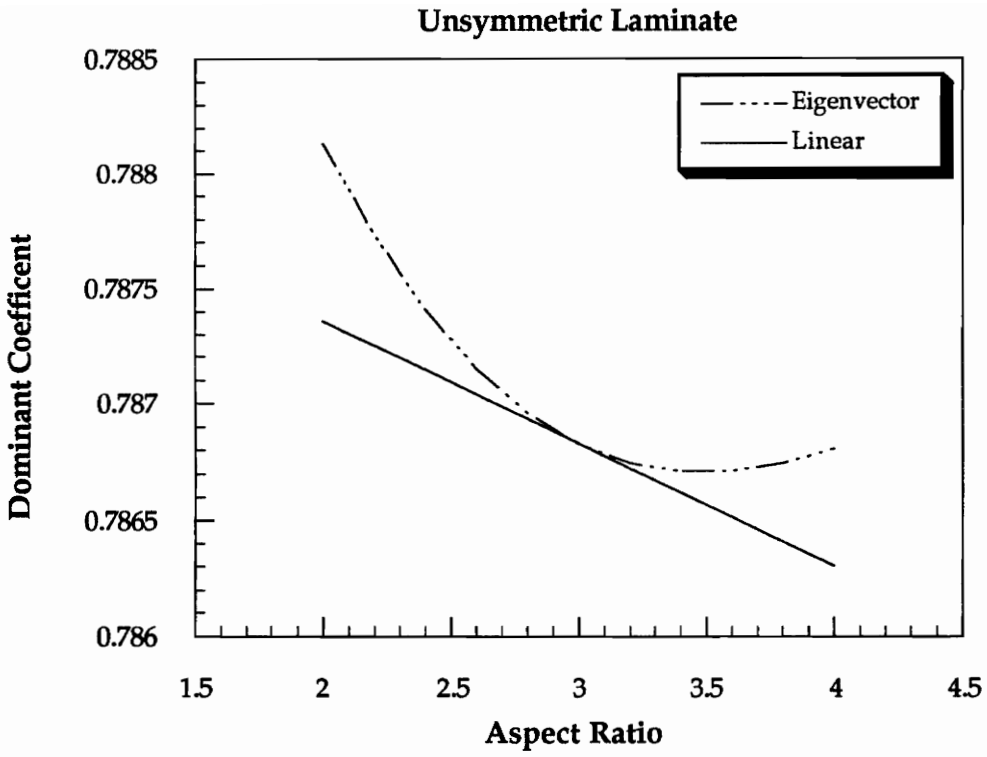

Fig. 4.37 Aspect Ratio Sensitivity of Dominant Coefficient of 1st Eigenvector.

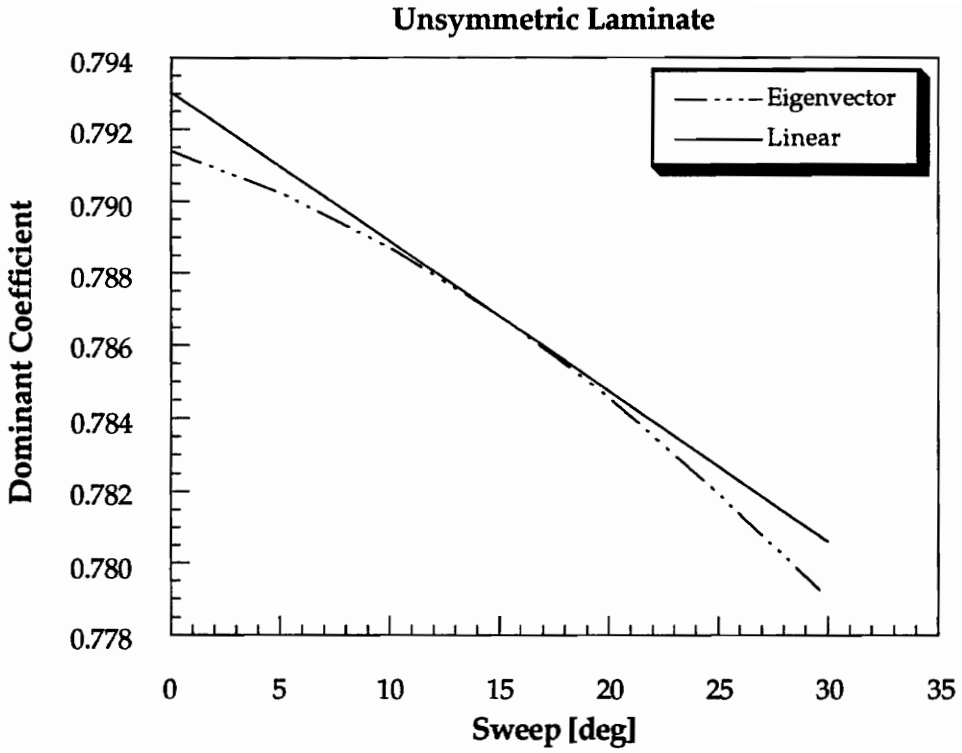

Fig. 4.38 Sweep Sensitivity of Dominant Coefficient of 1st Eigenvector.

5. Concluding Remarks and Future Research

A method has been developed which is capable of obtaining accurate static and free vibration results for skew tapered composite plates having arbitrary stacking sequences. It can also be used to perform static analysis of such plates. It is based on the Rayleigh-Ritz method in conjunction with Chebyshev polynomials. Springs of sufficiently high stiffness are used to simulate the essential boundary conditions. A sufficient number of terms in the deflection series has been used to ensure that convergence is reached. Whenever possible the present solutions are compared with those found in the literature and are found to be in good agreement. For the case of isotropic plates the frequency increases with increased skew angle. For composite plates the frequencies tend to decrease with an increase in the quarter chord sweep angle or the aspect ratio. Also, the frequencies increase with a decrease in the taper ratio. For unsymmetrically laminated plates it is seen that the vibration frequencies tend to decrease with increasing asymmetry. The sensitivity analysis of the frequencies and mode shapes with respect to taper ratio, wing sweep, aspect ratio and wing area is a logical extension to analyse these results. Such a study has also been presented.

The first order shape sensitivities of the free vibration response of symmetrically and unsymmetrically laminated tapered skew plates have been presented. Shape derivatives of the stiffness and mass matrices, eigenvalues and eigenvectors have been calculated using the central-difference method, with various step-sizes, as well as analytically. Approximations to the eigenvalues and eigenvectors have been obtained using three different methods and compared with the corresponding true values obtained by reanalysis. The eigenvalues demonstrated similar decreasing trends for changes in the area, aspect ratio and taper ratio whereas the sweep angle variation resulted in a different decreasing trend. The dominant coefficient of the

fundamental eigenvector decreased with an increase in the plate area, aspect ratio and sweep while it increased with a taper ratio increase. In general, the exponential schemes yielded good approximations whereas the linear method was not as accurate. Also, the finite difference derivatives may be too sensitive to very small step-sizes.

5.1 Future Work

As mentioned earlier, Wang [1991] presented two approximate methods to compute eigenvector derivatives. The first method was the explicit method, which was an improvement to the truncated modal summation representation of eigenvector derivatives. A mode-acceleration type approach was used to obtain a static solution to approximate the contribution due to unavailable higher modes. In the implicit method, which was based on the same data used by the explicit method, the eigenvector derivatives were assumed to be spanned by the truncated mode shapes together with a residual static mode. The unknown coefficients were computed by a Bubnov-Galerkin method from the governing equation for eigenvector derivatives. The implicit method is the optimum solution for the eigenvector derivatives when the residual static mode is introduced into the basis vector. At the time of writing of this thesis, the author is working on implementing these two methods to compute the eigenvector derivatives of generally laminated plates without having to use all the higher modes. This will significantly decrease the computational time required to compute the eigenvector derivarives.

References

1. Appala Satyam, A., 1974, "Torsional Vibrations and Stability of Thin-Walled Beams of Open Section Resting on an Elastic Foundation", M.E. Thesis, Department of Mechanical Engineering, Andhra University, Waltair, India.
2. Ashton, J. E. and Waddoups, M. E., 1969, "Analysis of Anisotropic Plates", *Journal of Composite Materials*, Vol. 3, pp. 470-479.
3. Baharlou, B. and Leissa, A. W., 1987, "Vibration and Buckling of Generally Laminated Composite Plates with Arbitrary Edge Conditions", *International Journal of Mechanical Science*, Vol. 29, No. 8, pp. 545-555.
4. Bergen, F. D. and Kapania, R. K., 1988, "Shape Sensitivity Analysis of Flutter Response of a Laminated Wing", *NASA Contractor Report 181725.*
5. Bert, C. W., 1982, "Research on Dynamics of Composite and Sandwich Plates", *Shock and Vibration Digest*, Vol. 14, No. 10, pp. 17-34.
6. Bert, C. W., 1985, "Research on Dynamic Behavior of Composite and Sandwich Plates", *Shock and Vibration Digest*, Vol. 17, pp. 3-15.
7. Bert, C. W. and Francis, P. H., 1974, "Composite Material Mechanics: Structural Mechanics", *AIAA J.*, Vol. 12, No. 9, pp. 1173-1186.
8. Bert, C. W. and Mayberry, B. L., 1969, "Free Vibrations of Unsymmetrically Laminated Anisotropic Plates with Clamped Edges", *Journal of Composite Materials*, Vol. 3, pp. 282-293.
9. Bhat, R. B., 1985, "Natural Frequencies of Rectangular Plates using Characteristic Orthogonal Polynomials in Rayleigh-Ritz Method", *Journal of Sound and Vibration*, Vol. 102, No. 4, pp. 493-499.
10. Bhat, R. B., 1987, "Flexural Vibration of Polygonal Plates using Characteristic Orthogonal Polynomials in Two Variables", *Journal of Sound and Vibration*, Vol. 114, No. 1, pp. 65-71.

11. Bonanni, D. L., Johnson, E. R., Starnes Jr., J. H., 1988, "Local Buckling and Crippling of Composite Stiffener Sections", CCMS-88-08, Virginia Polytechnic Institute and State University.

12. Brandon J. A., 1991, "Second-Order Design Sensitivities to Assess the Applicability of Sensitivity Analyses",*AIAA Jouurnal*, Vol. 29, No. 1, pp. 135-139.

13. Christiano, P. and Salmela, L., 1971, "Frequencies of Beams with Elastic Warping Restraint", *Journal of the Structures Division*, Vol. 97, pp. 1835-1840.

14. Crawley, E. F., 1979, "The Natural Modes of Graphite / Epoxy Cantilever Plates and Shells ", *Journal of Composite Materials*, Vol. 13, 195-205.

15. Crawley, E. F. and Dugundji, J., 1980, "Frequency Determination and Non-Dimensionalization for Composite Cantilever Plates", *Journal of Sound and Vibration*, Vol. 72, No. 1, pp. 1-10.

16. Dickinson, S. M. and Blasio, A. Di, 1986, "On the use of Orthogonal Polynomials in the Rayleigh-Ritz Method for the Study of the Flexural Vibration and Buckling of Isotropic and Orthotropic Rectangular Plates", *Journal of Sound and Vibration*, Vol. 108, No. 1, pp. 51-62.

17. Fletcher, C. A. J., 1984, *Computational Galerkin Methods*, Springer Verlag, New York.

18. Fox, R. L. and Kapoor, M. P., 1968, "Rate of Change of Eigenvalues and Eigenvectors", *AIAA Journal*, Vol. 6, No. 12, pp. 2426-2429.

    Giles, G. L., 1986, "Equivalent Plate Analysis of Aircraft Wing Box Structures with General Planform Geometry," *Journal of Aircraft*, Vol. 23, pp. 859-864.

19. Giles, G. L., 1989, "Further Generalization of an Equivalent Plate Representation for Aircraft Structural Analysis", *Journal of Aircraft*, Vol. 26, No. 1, pp. 67-74.

20. Haftka, R. T. and Kapania, R. K., 1986, "Sensitivity of Actively Damped Structures to Imperfections and Modeling Errors", *AIAA Journal*, Vol. 27, No. 10, pp. 1434-1440.

21. Jensen, D. W. and Crawley, E. F., 1984, "Frequency Determination Techniques for Cantilevered Plates with Bending-Torsion Coupling", *AIAA Journal*, Vol. 22, pp. 415-420.

22. Jones, R. M., 1973, "Buckling and Vibration of Unsymmetrically Laminated Cross-Ply Retangular Plates", *AIAA Journal*, Vol. 11, pp. 1626-1632.

23. Kamal, K. and Durvasula, S., 1986, "Some Studies on Free Vibration of Composite Laminates", *Composite Structures*, Vol. 5, pp. 177-202.

24. Kameswara Rao, C. and Appala Satyam, A., "Torsional Vibrations and Stability of Thin-walled Beams on Continuous Elastic Foundation", 1975, *AIAA Journal*, Vol. 13, pp. 232-234.

25. Kameswara Rao, C., Gupta, B. V. R. and Rao, D. L. N., 1974, "Torsional Vibrations of Thin-walled Beams on Continuous Elastic Foundation Using Finite Element Method", *Proceedings of International Conference on Finite Element Methods in Engineering*, Coimbatore, pp. 231-248.

26. Kameswara Rao, C. and Mirza, S., 1989, "Torsional Vibrations and Buckling of Thin-walled Beams on Elastic Foundation", *Thin-Walled Structures*, Vol. 7, pp. 73-82.

27. Kapania, R. K. and Byun, C., 1991, "Postprocessor for Prediction of Transverse Stresses in Laminated Plates Using Global Displacements Approximations", under preparation.

28. Kapania, R. K., Eldred, L. B. and Barthelemy, J.-F. M., 1991, "Sensitivity Analysis of a Wing Aeroelastic Response", *Proceedings of the AIAA/ASME/ASCE/AHS/ ASC 32nd Structures, Structural Dynamics and Materials Conference*, Baltimore, MD, Part 1, 497-505.

29. Kapania, R. K. and Raciti, S., 1989, "Recent Advances in the Analysis of Laminated Beams and Plates, Part II : Vibrations and Wave Propagation ", *AIAA Journal*, Vol. 27, No. 7., pp. 935-946.

30. Kapania, R. K. and Singhvi S., 1991, "Free Vibration Analyses of Generally Laminated Tapered Skew Plates", accepted for publication *Composites Engineering.*

31. Kapania, R. K. and Yang, T. Y., 1987 "Buckling, Postbuckling and Nonlinear Vibrations of Imperfect Plates", *AIAA Journal*, Vol. 25, No. 10, pp. 1338-1346.

32. Karpel, M., 1990, "Sensitivity Derivatives of Flutter Characteristics and Stability Margins for Aeroservoelastic Design", *Journal of Aircraft*, Vol. 27, No. 4, pp. 368-375.

33. Khdeir, A. A., 1988, "Free Vibration of Antisymmetrically Angle-Ply Laminated Plates Including Various Boundary Conditions", *Engineering Mechanics, Proceedings, 7th ASCE, EMD, Conference on Engineering Mechanics*, edited by R. A. Heller and M. P. Singh, American Society of Civil Engineers, New York, p. 284.

34. Lakshminarayana, H. V., Rajagopal, P., Ramamurthy, M. R. and Joshi, A., 1985, "Vibration Characteristics of a Swept Composite Wing Panel: Finite Element Analysis and Experimental Verification," *Journal of the Aeronautical Society of India*, Vol. 37, pp. 289-295.

35. Lam, K. Y., Liew, K. M. and Chow, S. T., 1989, "Two-Dimensional Orthogonal Polynomials for Vibration of Rectangular Composite Plates", *Composite Structures*, Vol. 13, pp. 239-250.

36. Laura, P. A. A. and Grossi, R. O., 1978, "Transverse Vibrations of Rectangular Homogeneous, Anisotropic Plates with Edges Elastically Restrained Against Rotation", Inst. Appl. Mech., Base Naval Puerto Belgrano, Argentina, Rept. IMA 78-18.

37. Lee, I. and Lee, J. J., 1990 "Vibration Analysis of Composite Plate Wing," *Computers and Structures*, Vol. 37, No. 6, pp. 1077-1085.

38. Leissa, A. W., 1981, "Advances in Vibration, Buckling, and Postbuckling Studies on Composite Plates", *Composite Structures*, edited by T. H. Marshall, Applied Science Publishers, London, pp. 312-334.

38. Leissa, A. W., 1981, "Advances in Vibration, Buckling, and Postbuckling Studies on Composite Plates", *Composite Structures*, edited by T. H. Marshall, Applied Science Publishers, London, pp. 312-334.

39. Leissa, A. W., 1969, *Vibration of Plates*, NASA SP-160.

40. Liew, K. M. and Lam, K. Y., 1990, "Application of Two Dimensional Orthogonal Plate Function to Flexural Vibration of Skew Plates", *Journal of Sound and Vibration*, Vol. 139, No. 2, pp. 241-252.

41. Lin, C. C. and King, W. W., 1974, "Free Transverse Vibrations of Rectangular Unsymmetrically Laminated Plates", *Journal of Sound and Vibration*, Vol. 36, No. 1, pp. 91-103.

42. McGee, O. G. and Leissa A. W., 1991, "Three-Dimensional Free Vibrations of Thick Skewed Cantilevered Plates", *Journal of Sound and Vibration*, Vol. 144, No. 2, pp. 305-322.

43. Minich, M. D. and Chamis, C. C., 1975, "Analytical Displacements and Vibrations of Cantilevered Unsymmetric Fiber Composite Laminates", NASA TMX-F1699.

44. Nair, P. S. and Durvasula, S., 1974, "Vibration of Generally Orthotropic Skew Plates", *Journal of Acoustical Society of America*, Vol. 55, No. 5, pp. 998-1002.

45. Pritchard, J. I. and Adelman H. M., 1991, "Differential Equation Based Method for Accurate Modal Approximations", *AIAA Journal*, Vol. 29, No. 3, pp. 484-486.

46. Rao, C. K. and Mirza, S., 1989, "Torsional Vibrations and Buckling of Thin-walled Beams on Elastic Foundation", *Thin-Walled Structures*, pp. 73-82.

47. Rao, C. K. and Satyam, A. A., 1975, "Torsional Vibrations and Stability of Thin-walled Beams on Continuous Elastic Foundation", *AIAA Journal*, Vol. 13, pp. 232-234.

48. Sheena, Z. and Karpel, M., 1985 "Static Aeroelastic Analysis Using Aircraft Vibration Modes", *Collected Papers of the Second International Symposium on Aeroelasticity and Structural Dynamics*, Aachen, W. Germany, April, pp. 229-232.

50. Thornton, E. A., 1977, "Free Vibrations of Unsymmetrically Laminated Cantilevered Composite Panels ", *Shock and Vibration Bulletin, U.S. Naval Research Laboratory, Proceedings*, No. 47, Pt. 2, pp. 79-88.

51. Wang, B. P., 1991, "Improved Approximate Methods for Computing Eigenvector Derivatives in Structural Dynamics", *AIAA Journal*, Vol. 29, No. 6, pp. 484-486.

52. Whitney, J. M. and Leissa, A. W., 1969, "Analysis of Heterogeneous Anisotropic Plates", *Transactions of the ASME, Journal of Applied Mechanics*, Vol. 36, pp. 261-266.

Appendix

A.1 The Jacobian of the Transformation

The original and the transformed coordinate systems are shown in Fig. 3.1. The η and ξ coordinates are so nondimensionalized that the four corner nodes have the coordinate values of ± 1. The geometric functions are as shown

$$\begin{aligned} x &= \sum_{i=1}^{4} N_i(\eta, \xi) x_i \\ y &= \sum_{i=1}^{4} N_i(\eta, \xi) y_i \end{aligned} \tag{a.1}$$

where

$$\begin{aligned} N_1(\eta, \xi) &= \frac{1}{4}(1+\eta)(1-\xi) \\ N_2(\eta, \xi) &= \frac{1}{4}(1+\eta)(1+\xi) \\ N_3(\eta, \xi) &= \frac{1}{4}(1-\eta)(1+\xi) \\ N_4(\eta, \xi) &= \frac{1}{4}(1-\eta)(1-\xi) \end{aligned} \tag{a.2}$$

The function $N_i(\eta, \xi)$ takes the value of unity at point i and zero elsewhere. The nodes are numbered as shown in Fig. 3.1. In order to change the derivatives from $\partial/\partial x$ and $\partial/\partial y$ to $\partial/\partial \eta$ and $\partial/\partial \xi$ we use the chain rule of partial differentiation

$$\begin{pmatrix} w_{,\eta} \\ w_{,\xi} \end{pmatrix} = \begin{bmatrix} x_{,\eta} & y_{,\eta} \\ x_{,\xi} & y_{,\xi} \end{bmatrix} \begin{pmatrix} w_{,x} \\ w_{,y} \end{pmatrix} = [J] \begin{pmatrix} w_{,x} \\ w_{,y} \end{pmatrix} \tag{a.3}$$

where the Jacobian matrix $[J]$ serves to transform the derivatives from (η, ξ) to (x, y) coordinates and, and vice versa

$$[J] = \begin{bmatrix} N_{1,\xi} & N_{2,\xi} & N_{3,\xi} & N_{4,\xi} \\ N_{1,\xi} & N_{2,\xi} & N_{3,\xi} & N_{4,\xi} \end{bmatrix} \begin{bmatrix} x_1 & y_1 \\ x_2 & y_2 \\ x_3 & y_3 \\ x_4 & y_4 \end{bmatrix} \tag{a.4}$$

The elements of the Jacobian matrix are denoted by J_{ij} and are shown below

$$\begin{aligned} J_{11} &= \frac{(crct - \xi\ rt)}{4} \\ J_{12} &= 0 \\ J_{21} &= \frac{(cc - \eta\ rt)}{4} \\ J_{22} &= \frac{L}{2} \end{aligned} \tag{a.5}$$

where

$$\begin{aligned} crct &= (x_1 - x_4) + (x_2 - x_3) \\ rt &= (x_1 - x_4) - (x_2 - x_3) \\ cc &= (x_2 + x_3) - (x_1 + x_4) \end{aligned} \tag{a.6}$$

Eq. $a.3$ can now be written in inverted form as

$$\begin{pmatrix} w_{,x} \\ w_{,y} \end{pmatrix} = [J]^{-1} \begin{pmatrix} w_{,\eta} \\ w_{,\xi} \end{pmatrix} \tag{a.7}$$

The elements of the inverse of the Jacobian matrix are denoted by J'_{ij} and are as follows

$$\begin{aligned} J'_{11} &= \frac{4}{(crct - \xi\ rt)} \\ J'_{12} &= 0 \\ J'_{21} &= \frac{2\ (\eta\ rt - cc)}{L\ (crct - \xi\ rt)} \\ J'_{22} &= \frac{2}{span} \end{aligned} \tag{a.8}$$

where L is the span of the plate. Using the theorem of transformation of double integrals, we have

$$dx\ dy = |J|\ d\eta\ d\xi \tag{a.9}$$

The determinant of the Jacobian matrix is referred to in mathematics as the Jacobian of x, y with respect to η, ξ and in this case would be

$$|J| = J_{11}\ J_{22} \tag{a.10}$$

It is obvious that if the plate is a rectangle, the Jacobian matrix is a diagonal matrix populated with constants only. If the distorted element is a parallelogram,$[J]$ is populated with constants only.

A.2 The Strain Transformation Matrix $[T]$

The elements of the 6 by 8 transformation matrix $[T]$ relating the strain and the curvature vectors in the (x,y) co-ordinate system to the pseudo strain and curvature vectors in the natural co-ordinate system are denoted by T_{ij} and are shown below

$$\begin{aligned}
T_{11} &= J'_{11} = T_{33} \\
T_{23} &= J'_{21} = T_{31} \\
T_{24} &= J'_{11} = T_{33} \\
T_{46} &= {J'_{11}}^2 \\
T_{55} &= \frac{J'_{21}\ J'_{11}\ rt}{L} \\
T_{56} &= {J'_{21}}^2 \\
T_{57} &= {J'_{22}}^2 \\
T_{58} &= 2\ J_{22}\ J_{21} \\
T_{65} &= \frac{{J'_{11}}^2\ rt}{L} \\
T_{66} &= 2\ J_{11}\ J_{21} \\
T_{68} &= 2\ J_{11}\ J_{22}
\end{aligned} \tag{a.11}$$

The remaining $T_{ij} = 0$.

A.3 The Chebyshev [B] Matrix

The $[B]$ matrix is the matrix whose elements consist of the partial derivatives of the Chebyshev plynomials with respect to η and ξ and is defined by

$$\begin{pmatrix} \epsilon' \\ \kappa' \end{pmatrix} = [B]\{q\} \qquad (a.12)$$

The details of the $[B]$ matrix are shown below

$$\begin{bmatrix}
T_{00,\eta} & T_{01,\eta} & \dots & T_{ij,\eta} & 0 & 0 & \dots & 0 & 0 & 0 & \dots & 0 \\
T_{00,\xi} & T_{01,\xi} & \dots & T_{ij,\xi} & 0 & 0 & \dots & 0 & 0 & 0 & \dots & 0 \\
0 & 0 & \dots & 0 & T_{00,\eta} & T_{01,\eta} & \dots & T_{kl,\eta} & 0 & 0 & \dots & 0 \\
0 & 0 & \dots & 0 & T_{00,\xi} & T_{01,\xi} & \dots & T_{kl,\xi} & 0 & 0 & \dots & 0 \\
0 & 0 & \dots & 0 & 0 & 0 & \dots & 0 & T_{00,\eta} & T_{01,\eta} & \dots & T_{mn,\eta} \\
0 & 0 & \dots & 0 & 0 & 0 & \dots & 0 & T_{00,\eta\eta} & T_{01,\eta\eta} & \dots & T_{mn,\eta\eta} \\
0 & 0 & \dots & 0 & 0 & 0 & \dots & 0 & T_{00,\xi\xi} & T_{01,\xi\xi} & \dots & T_{mn,\xi\xi} \\
0 & 0 & \dots & 0 & 0 & 0 & \dots & 0 & T_{00,\eta\xi} & T_{01,\eta\xi} & \dots & T_{mn,\eta\xi}
\end{bmatrix}$$

Vita

The author was born on January 31, 1968 in Jodhpur, India. After receiving his B.E. in Mechanical Engineering from K.R.E.C., University of Mangalore in May, 1989, he began work on his M.S. in Aerospace Engineering at Virginia Tech in August, 1989.